Institute of Thermoelectricity, Academy of Sciences and Ministry of Education and Science of Ukraine

Journal of THERMOELECTRICITY

International Research

Founded in December, 1993

published 6 times a year

No. 3 *2019*

Editorial Board

International Editorial Board

Founders – National Academy of Sciences, Ukraine
Institute of Thermoelectricity of National Academy of Sciences and Ministry of Education and Science of Ukraine

Certificate of state registration № КВ 15496-4068 ПР

Approved for printing by the Academic Council of Institute of Thermoelectricity of the National Academy of Sciences and Ministry of Education and Science, Ukraine

Address of editorial office:
Ukraine, 58002, Chernivtsi, General Post Office, P.O. Box 86.
Phone: +(380-372) 90 31 65.
Fax: +(380-3722) 4 19 17.
E-mail: jt@inst.cv.ua
http://www.jt.inst.cv.ua

Signed for publication 25.07.2019. Format 70×108/16. Offset paper №1. Offset printing.
Printer's sheet 11.5. Publisher's signature 9.2. Circulation 400 copies. Order 5.

Printed from the layout original made by "Journal of Thermoelectricity" editorial board
in the printing house of "Bukrek" publishers,
10, Radischev Str., Chernivtsi, 58000, Ukraine

CONTENTS

Rifert V.G., *doct. techn. sciences* [1]
Anatychuk L.I., *acad. National Academy of sciences of Ukraine*[2]
Barabash P.O., *cand. techn. sciences* [1]**,**
Usenko V.I., *doct. techn. sciences* [1]
Strikun A.P.[1]
Solomakha A.S., *cand. of techn. sciences* [1,2]
Petrenko V.G., *cand. of techn. sciences* [1]
Sereda V.V. *cand. techn. sciences* [1]**,**
Prybyla A.V., *cand. phys. – math. sciences* [2]

1NTUU KPI, 6 Politekhnicheskaya str, Kyiv, 03056, Ukraine;
[2]Institute of Thermoelectricity, 1 Nauky str., Chernivtsi, 58029, Ukraine
e–mail: anatych@gmail.com

EVOLUTION OF CENTRIFUGAL DISTILLATION SYSTEM WITH A THERMOELECTRIC HEAT PUMP FOR SPACE MISSIONS

Part 3. Analysis of local and integral characteristics of centrifugal distillation system with a thermoelectric heat pump

The paper describes a method for calculating the heat transfer coefficient and the efficiency of a centrifugal distiller, as well as determining the efficiency of a thermoelectric heat pump. For this, the results of theoretical and experimental studies of condensation and evaporation processes on a rotating surface and the study of processes in a liquid-liquid thermoelectric heat pump (THP) were used. A comparison was made of the calculated values of the average temperature difference ΔTav in THP and the temperature difference at the inlet to THP ΔTin with the experimental data obtained when testing the centrifugal distiller on water and urine. Bibl. 33, Fig. 3, Tabl. 2.
Key words: thermoelectricity, heat pump, distiller

Introduction

In the coming years, companies such as NASA, SpaceX, Boeing and others are planning long-term human missions to the Moon and the Mars. Obviously, manned space missions at the current level of cosmonautics development cannot be realized without the use of special systems for recovering water from various liquid vital products of the crew members. The development of reliable and efficient water recovery systems for manned space objects will dramatically reduce the cost of providing cosmonauts with water.

The absence of gravity significantly complicates the implementation of many traditional technological processes, including distillation. From this point of view, the use of centrifugal forces (centrifugal distillers) is a promising direction for use in life support systems of manned space missions. Systems based on this method can provide water regeneration from all known liquid vital products of astronauts (urine, sanitary water, atmospheric moisture condensate) to ensure high quality of the obtained distillate.

In [1-7], information is given on a 3-stage distiller with a thermoelectric heat pump. [8-11] show the

results of the development of a five-stage centrifugal distiller (CDS with THP) and its testing at the benches of the distiller manufacturer - Thermodistillation, Ukraine, and the Customer - Honeywell, USA. These results, as well as some methods for improving the performance of the CDS system, are given in [12, 13]. A more detailed review of works on a system with a centrifugal distiller is given in the first part of the paper [14], and a description of the research process - in [15]. The published results quite convincingly confirm the uniqueness of the system designed for the life support of manned spacecraft in long space missions and on the ISS.

Using the experimental data of a system with a centrifugal five-stage distiller and a thermoelectric heat pump (in terms of production, heat pump power, revolutions, degree of concentration, etc.), this paper substantiates the method of theoretical calculation of the temperature difference at the inlet to the THP $\Delta T_{in} = (T_{\text{in hot THP}} - T_{\text{in cold THP}})$ and the efficiency of THP (η_{THP}). An algorithm for calculating the temperature difference at the inlet to the THP is presented, the basis of which is the method for calculating the heat transfer coefficients in each stage of the distiller. The influence on the accuracy of calculating the temperature difference at the inlet to the THP and on the efficiency of the entire system of temperature depression and condensate supercooling in the cold circuit is shown. The calculation algorithm $\Delta T_{av} = (T_{\text{in hot}} + T_{\text{out hot}})/2 - (T_{\text{in cold}} + T_{\text{out cold}})/2$ in THP is analyzed.

Determination of the heat transfer coefficient in the distiller stage

Figure 1 shows a sketch of a rotating stage of a five-stage distiller. The stage consists of five parts: 1st central part, 2, 3 and 4 - disks at different angles with respect to the axis of rotation; Part 5 is a cylindrical ring. The total area of heat exchange is 0.07 m^2. There are five such steps in the apparatus.

The steam formed in the first stage, passing through the separation partitions, enters the condensation zone on the outer side of the disk, where, in contact with the heat exchange surface of the second stage, it condenses, transferring the heat of the initial liquid in the second stage. As a consequence, part of the liquid on the inner surface in the second stage evaporates, and the resulting steam condenses on the outside of the third stage and further, according to the same scheme, to the fifth stage. The steam in the last, fifth stage condenses on the film of technological distillate flowing down the surface of the rotating disk, which enters the apparatus from the cold circuit of THP.

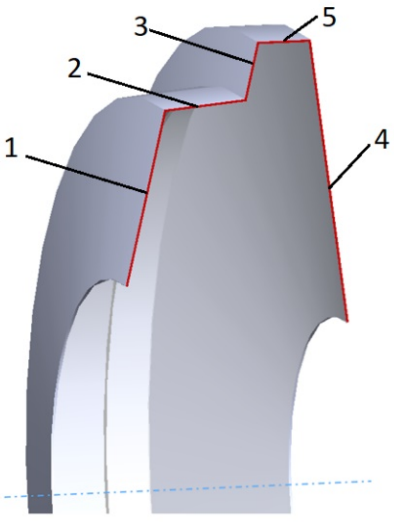

Fig. 1. Profile of heat exchange surface of one stage of a centrifugal distiller

The condensate formed in the condensation zones of each stage, under the action of centrifugal force, flows through the hydraulic shutters into the final condenser, where it is mixed with cooling technological

distillate.

After the system reaches steady-state operation, the concentration of the solution in all stages of the distiller, except the first, remains constant. The concentration of salts in the first stage will change during operation from the initial value to a certain limit, upon reaching which the power supply to the THP ceases.

The efficiency of the system depends on the flow of heat and mass transfer processes in the distiller, the scheme of movement of heat carriers, the efficiency of the battery, etc.

The total heat transfer coefficient of an individual stage is calculated by the formula:

$$k = 1/ (1/\alpha_c + 1/\alpha_e + \delta_w /\lambda_w), \quad (1)$$

where α_c is the coefficient of heat transfer during condensation of steam; α_e is the coefficient of heat transfer during evaporation of the liquid; δ_w and λ_w are the thickness and thermal conductivity of the heat exchange surface, respectively.

However, it is obvious that the value of the heat transfer coefficients depends on the nature of the liquid film flowing on a rotating surface.

Thus, to calculate the heat and mass transfer processes in the distiller requires knowledge of the hydrodynamic characteristics of the film and the coefficients of heat transfer during condensation and evaporation of the liquid on a rotating surface.

Heat exchange at condensation and evaporation in a rotating stage

The main hydrodynamic parameters of a liquid film flowing on a rotating surface are its average thickness and flow rate. A study of the flow of liquid film on a rotating surface was carried out in detail in [16]; as a result, it was possible to single out the characteristic modes of liquid film flow which affect the heat transfer process. The study of condensation on a rotating heat transfer surface was experimentally studied in [17 and 18]. In 19], a review is given of condensation on a rotating surface, and a method for calculating heat transfer is justified.

On surfaces 1–4 (see Fig. 1), when the distiller is operating, the evaporating liquid flows in the form of a thin film under the action of centrifugal acceleration $a \sim \omega 2R\sin\beta$, where ω is the angular velocity, 1 / sec; R is the radius of the rotating unit of the stage, m; β is the angle between the axis of rotation of the rotor and the heat exchange surface. In the annular (part 5, Fig. 1), evaporation occurs under the influence of forced centrifugal convection.

Condensation on the external surface of a rotating stage

At sites close to disk geometry (sections 1-4, except for part 5), the local coefficient of heat transfer during condensation (α_c) can be calculated by the formula

$$Nu = \alpha_c / \lambda (\nu^2/\omega^2 R\cos\beta)^{1/3} = 0.9Re^{-1/3} \quad (2)$$

where ω are revolutions, 1 / sec; R is the radius of the rotating unit of the stage, m; β is the angle between the axis of rotation and the heat transfer surface. Re is the local Reynolds number, which is calculated as $Re = Gd / 2\pi R\mu$, where Gd is the amount of steam condensed at the local surface section.

The average value of the heat transfer coefficient αc in each section of the stage is calculated taking into account the change in the area of the rotating surface from the radius of the disk.

Condensation of steam on a liquid film

In the annular condenser, steam condenses on a liquid film entering the condensation zone after cooling in the THP and an additional external heat exchanger [20].

The analysis of these data makes it possible to use the method proposed in [21] for the calculation of heat transfer for the case of condensation of steam on a liquid film under conditions of gravity. In this case, the heat transfer process is calculated by dependence

$$Nu = 0.018\ Re^{0.5}\ Pr^{0.7} \tag{3}$$

In this equation, the average film temperature is taken as the determining factor, and Re is determined from the initial water flow in the film.

The maximum steam temperature in the last stage is 30 ° C and the coolant temperature is 20 ° C. The calculation, taking into account the actual size of the disk on which steam condenses in the final capacitor, shows that *Re* can have a value in the range 60… 120, and *Pr* = 3… 6. Theoretically, the solution of heat transfer in a given region of change in the numbers *Re* and *Pr* for the determination of *Nu* was performed in [22, 23]. These calculations, as shown in [24, 25], give a good coincidence with the experiment, which allows us to use them in the future.

Evaporation on the internal surface of a rotating stage (sections 1-4, Fig.1)

The heat transfer coefficient during the evaporation of a liquid film on a rotating disk was first measured in [18]. In [19], an analysis of studies by other authors was made and an improved method for calculating α_{evap} was described taking into account the effect of turbulence in the film flow.

According to [19] at *Re* <25, the heat transfer coefficient must be calculated from the dependence:

$$Nu = 1.47\ Re^{-1/3} \tag{4}$$

If *Re*> 25, then it will be more accurate to use the graphs obtained in [22, 23] and which take into account the turbulization of the liquid film and the deviation of the heat transfer process from the Nusselt laminar theory.

Evaporation of liquid in the annular channel (section 5, Fig. 1)

In the annular channel (part 5, Fig. 1) there is a heat exchange under the influence on the process of evaporation of free convection, which occurs during microgravity due to the presence of centrifugal acceleration. Experimental studies of evaporation during free convection in the presence of centrifugal acceleration were performed in the 70s of the 20th century in [26–28]. In [26], the heat transfer coefficients were measured for water evaporation at $\omega 2R/g$ from 1 to 5250 and a heat flux $q = (2 \cdot 104 \ldots 2 \cdot 105)$ W / m^2. At low heat fluxes ($q < 2 \cdot 104$ W/m^2) that occur in CDS, there is no influence of heat flux on heat transfer even at $\omega 2R/g > 102$ and the heat transfer coefficient can be determined from the dependence [27]:

$$Nu = 0.75(Gr \cdot Pr)^{0.25}. \tag{5}$$

where $Nu = \alpha\delta_u/\lambda$, $Gr = \omega^2 R\delta_u 4/\nu^2$; δ_u is the thickness of liquid layer in the annular channel, *m*; *R* is radius on which the annular channel is located, m.

Calculation of the total temperature difference of steam in the distiller and the temperature difference at the inlet to THP

Tables 1 and 2 show the experimental data as a function of time τ: local temperatures, flow rate of the product (distillate) G_d, flow rate of the solution in the hot circuit, distillate flow in the cold circuit. Based on these data, the Reynolds number is calculated for the case of the flow of a liquid film on the inner and outer surfaces of the CDS working surface and, according to the corresponding formulas (1-5), heat

transfer coefficients for each part of the stage during evaporation and condensation (see Fig. 1).

Total heat transfer coefficient is calculated by formula (1).

Also, heat transfer coefficient is determined for each stage from the dependence:

$$k = Q_{cr}/F_{cr}\cdot\Delta T_{cr.}, \tag{6}$$

where F_{cr} is heat exchange surface, m^2; $\Delta T_{cr.}$ is temperature difference in the stage.

The total heat flow in the stage $Q_{st} = G\cdot r$, where G is the amount of steam condensed in the stage, r is phase transition heat of steam.

Knowing from the experiment the distillate production G_d of CDS, we determine $Q = \Sigma G_d \bullet r$ and then for water for the entire distiller $\Sigma\Delta T = (T_{in\ hot\ THP} - T_{in\ cold\ THP}) = Q/k\cdot F$

Following this, we compare the calculated $\Sigma\Delta T$ and $\Sigma\Delta T = (T_{in\ hot.THP} - T_{in.cold.\ THP})$ from the experimental data (Table 1).

For the experiments with urine one should take into account the presence of physicochemical temperature depression ΔT_{depr}. Its value is determined from the plot $\Delta T_{depr} = f(C)$, where urine concentration depends on the degree of water recovery. The concentration, in turn, is determined by the density of solution in the hot circuit (see Fig. 2).

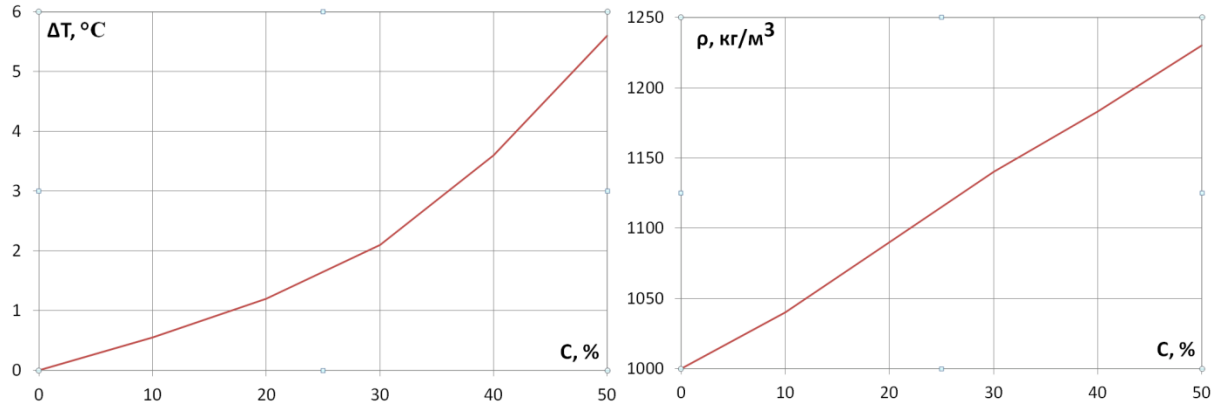

Fig.2 Dependence of physico-chemical temperature depression and solution density on the urine concentration (according to the research institute "KHIMMASH", Moscow)

Taking into account ΔT_{depr}, the temperature difference in the first stage $\Delta T_1 = T_{in} - \Delta T_{depr1}$. Further, according to the experimental data, we determine the thermal power supplied to the hot circuit $Q_h = c_p\cdot G_h\cdot(T_{in\ THP} - T_{out\ THP})$. From the heat balance of THP one can determine the thermal power from the cold side $Q_c = Q_h - W_{THP}$.

Theoretical value of temperature difference in the cold stage

$$\Delta T_c = Q_c/c_p\cdot G_c. \tag{7}$$

Calculation of the dependence of THP conversion coefficient on the temperature difference of heat carriers

The requirement is obvious that the design parameters and the supply current of the THP meet the condition for the maximum heating coefficient K defined by the formula

$$K = \frac{Q_h}{W} = \frac{Q_h}{Q_h - Q_c}, \tag{1}$$

where $W = Q_h - Q_c$ is electric power consumption; Q_c, Q_h are external heat flows on the cold and hot

surfaces of thermoelectric module, respectively. This will provide for heating of heat carrier in the working circuit of heat pump with minimum power consumption.

To optimize thermoelectric modules, the theory of optimal control is successfully used [28 – 33]. This method is also easily generalized to calculate the maximum heating coefficient, which characterizes the heat pump mode.

According to optimal control methods, the operating efficiency of thermoelectric module in heating mode can be assessed by the functional

$$J = \ln \frac{Q_h}{Q_c} = \ln \frac{q_h}{q_c} = \ln q_h - \ln q_c \quad , \tag{8}$$

where

$$q_h = \frac{Q_h}{n\,I}, \qquad q_c = \frac{Q_c}{n\,I} \tag{9}$$

- are specific (related to current strength I) heat flows on the hot and cold thermocouple junctions, respectively, n is the number of thermocouples in a thermopile. The minimum of functional J corresponds to maximum value of heating coefficient K.

To calculate the densities of heat flows q_c, q_h, we use the system of equations of non-equilibrium thermodynamics, which for the n- and p-type thermoelement legs is of the form

$$\left.\begin{aligned} \frac{dT}{dx} &= -\frac{\alpha j}{\kappa} T - \frac{q}{\kappa} \\ \frac{dq}{dx} &= \frac{\alpha^2 j^2}{\kappa} T + \frac{\alpha j}{\kappa} q + \frac{j^2}{\sigma} \end{aligned}\right\}_{n,p}, \tag{10}$$

where $j = \dfrac{I}{S}$ is specific current density in the legs, S is cross-section of legs, I is the value of supply current. The Seebeck coefficient, the electrical conductivity and thermal conductivity of leg materials are functions of temperature: $n,p = n,p(T)$ and can be assigned on the basis of approximation of the experimental data of measuring characteristics of thermoelectric materials.

Solution of system (10) for boundary conditions

$$T_n(0) = T_p(0) = T_h, \qquad T_n(l) = T_p(l) = T_c \tag{11}$$

will make it possible to calculate heat flows q_c, q_h using the relations

$$\begin{aligned} q_c &= -\sum_{n,p} \left[q(l) + j^2 r_0 \right], \\ q_h &= -\sum_{n,p} \left[q(0) - j^2 r_0 \right], \end{aligned} \tag{12}$$

where l is the height of thermoelement legs, r_0 is the value of contact resistance on thermoelement junctions.

From relations (12) it follows that q_c, q_h depend on the parameters of the current density in thermoelement legs j and on the magnitude of the contact resistance. In accordance with the optimal control theory, the values of $j_n, p,$, which ensure the minimum of the functional J (8), must satisfy the following optimum conditions

$$-\frac{\partial J}{\partial j}+\int_0^l \frac{\partial H\ (\psi,T,q,j)}{\partial j}dx=0\,, \tag{13}$$

where the Hamiltonian function H is given by

$$H=\sum_{n,p}(\psi_1 f_1\ +\psi_2 f_2\ )\,, \tag{14}$$

$(f_1\,,f_2\,)_{n,p}$ are right-hand sides of equations (4); $\psi=\left(\psi_1\,,\psi_2\right)_{n,p}$ is pulse vector the method of determination of which is described in [1, 2].

Relations (8) - (14) are the basis for computer design of optimal structures and calculation of optimal parameters of thermoelectric modules in heating mode for heat pumps.

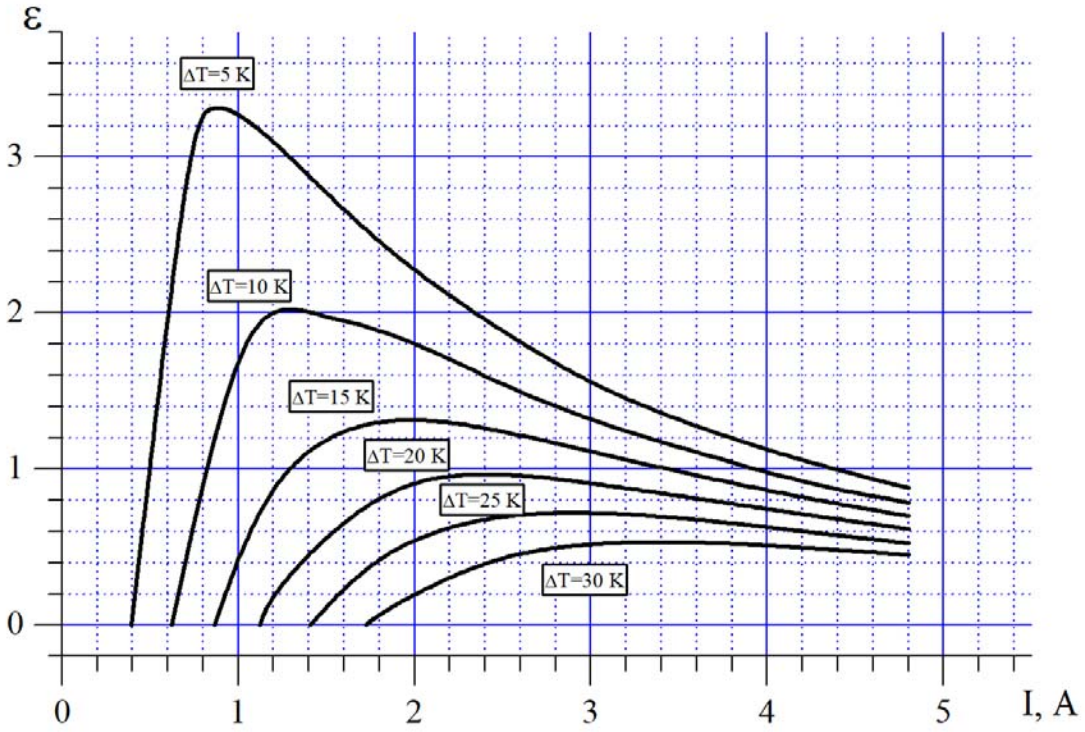

Fig.3 Dependence of the conversion coefficient of THP on supply current for different values of temperature difference between heat carriers

The algorithm for calculating the maximum heating coefficient is implemented numerically using computer modeling tools. In this case, the optimal current densities in the thermocouple legs j and their corresponding heat flows q_c, q_h are calculated, and the maximum value of the heating coefficient is determined.

Based on the above theory, the dependences of the THP conversion coefficient on the supply current were calculated for different values of the temperature difference between the heat carriers (Fig. 3).

As follows from Fig. 3, the conversion factor of THP strongly depends on the temperature difference between the heat carriers of the water distillation system. In addition, when designing a distiller, the THP mode of operation is important, namely, ensuring the optimal supply mode of thermoelectric power converters.

Results

Water evaporation

Table 1 shows the experimental data of studying the distiller operation on distilled water, the duration of operation was 50 minutes, the average power of the heat pump was 100 W, and the average production was 2.45 kg/h.

Table 1

Experimental data (water, n = 1100 rpm)

Time	Drive			THP	Weight		TDS	Flow		Product-ion	SPC	Temperature			
	U	*I*	*W*	*W*	In	Out		hot	cold			Hot in THP	Hot out THP	Cold in THP	Cold out THP
min	V	A	W	W	Γ		mg/l	l/h		l/h	W-h/kg	^{0}C			
10	20.6	3.3	68.0	101	224	152	5	90	88	2.18	77.5	25.5	29.6	22.6	19.5
30	20.6	3.3	68.0	99	1000	902	5	90	88	2.42	69.0	26.3	30.1	22.8	20.0
40	20.6	3.3	68.0	100	1438	1326	4	90	88	2.58	65.1	25.5	29.0	22.0	19.5
50	20.6	3.3	68.0	100	1838	1710	5	90	88	2.60	64.6	25.5	28.7	22.0	19.6
Average	20.6	3.3	68.0	100			5			2.45	69.1				
Total					1838	1710									

Here, production stands for distiller capacity, TDS is total number of dissolved solids.

In the calculation process, only the correction of the steam temperature in the last stage was performed:

1st step: according to the known inlet and outlet temperatures of the thermoelectric heat pump in the hot circuit and the flow rate, we determine the real thermal power, which is supplied in the hot circuit: $Q_h = c_p G_h\ (T_{\text{in hot THP}} - T_{\text{out hot THP}})$;

2nd step: from the heat pump balance we determine the thermal power on the cold side of the heat pump: $Q_c = Q_h - W_{\text{THP}}$;

3d step: we determine the calculated temperature difference in the cold circuit: $\Delta T_c = (T_{\text{in cold THP}} - T_{\text{out cold THP}}) = Q_c/c_p \cdot G_c$.

As a result of the calculation, the obtained deviation of ΔT_c from the experimental data does not exceed 0.1 °C.

In some individual cases, the theoretical calculation of the total temperature difference at the distiller $\Sigma\Delta T$ and $\Delta T_{\text{in}} = (T_{in\ hot\ \text{THP}} - T_{\text{in cold THP}})$ shows that there is a deviation of the value ΔT_{in}, which is several degrees higher than the calculated one. This was due to supercooling of the distillate in the cold circuit of the heat pump, which led to a significant increase in the total temperature difference $\Sigma\Delta T$ on the heat pump and, as a result, to a decrease in its efficiency. An additional experiment, where the degree of condensate cooling in the final condenser was specially controlled, showed that it is possible to significantly reduce the temperature difference at the inlet of the heat pump from the cold side in the calculation and in the experiment. At the same time, the efficiency of the heat pump η grows, which becomes the same as in the

theoretical calculation. This, in some cases, gives a reduction in specific energy consumption of SPC by 10-15 %.

Urine evaporation

Table 2 shows the experimental data of studying the distiller operation on urine, the duration of operation was 107 minutes, the average power of the heat pump was 203 W, and the average production was 3.35 kg / h.

Table 2

Experimental data (urine, n = 1100 rpm)

Time	Drive			THP	Weight		TDS	Flow		Product-ion	SPC	Temperature			
	U	*I*	*W*	*W*	in	Out		hot	Cold			Hot in THP	Hot out THP	Cold in THP	Cold out THP
min	V	A	W	W	G		mg/l	l/h		kg/h	W-h/kg	^{0}C			
5	20.8	3.35	69.7	202	-	-	-	-	-	-	-	-	-	-	-
13	20.8	3.35	69.7	202	680	710	37	89	90	3.50	77.6	33.1	38.2	25.5	22,.5
25	20.8	3.40	70.7	202	1366	1416	60	89	89	353	77.3	32.9	37.9	25.1	22.0
47	20.8	3.43	71.3	201	2024	2098	79	90	89	3.41	79.9	33.4	38.5	25.4	22.3
59	20.8	3.43	71.3	199	2674	2770	84	89	89	3.36	80.4	34.3	39.6	25.8	22.8
71	20.9	3.45	72.1	211	3324	3444	90	89	89	3.37	84.0	34.9	40.2	26.0	23.1
83	20.9	3.47	72.5	205	3360	4106	94	90	89	3.31	83.8	35.6	41.1	26.4	23.6
95	20.9	3.50	73.1	205	4572	4734	96	89	89	3.14	88.6	36.6	42.0	27.0	24.2
107	20.9	3.50	73.1	201	5170	5362	97	89	89	3.14	87.2	36.5	41.7	26.0	23.4
Average	20.8	3.44	71.7	203						3.35	115.1				
Total					5170	5362									

Table 2 shows that, over time, the temperature difference on the heat pump increases and, as a consequence, the system production decreases and the specific power consumption increases.

For the case of urine processing, when calculating the total temperature difference on a thermoelectric heat pump $\Sigma\Delta T = (T_{\text{in hot THP}} - T_{\text{in cold THP}})$, it is also necessary to take into account the effect of temperature depression, which increases with increasing urine concentration, i.e. with increasing operating time of the distiller.

During the experiments, the temperature of the water supplied to the additional heat exchanger to cool the cold circuit distillate of the heat pump was not monitored separately.

As a result, the main indicators of the system (production and power consumption) when working on a distillate, all other things being equal, are significantly better than when processing urine.

Conclusions

1. This paper shows that a multistage centrifugal distiller is a complex structure in which the individual stages of the distiller have a heat exchange surface assembled from elements whose angle of inclination with respect to the centrifugal acceleration vector varies from 00 to 900.
2. To perform an adequate thermal calculation of such an apparatus, dependences were selected and

substantiated for calculating heat transfer during evaporation and condensation, as well as the heat transfer coefficient on the individual components of the heat transfer surface.

3. The effect of physicochemical temperature depression and supercooling of a technical distillate in a cold circuit in a thermoelectric heat pump on the energy efficiency of a distillation system is shown.
4. The experimental and theoretical results obtained in this paper and in the previous parts [14-15] will be used to create a mathematical model of the water regeneration (distillation) system. A mathematical model is necessary to optimize the operating and geometric parameters of the system as applied to specific operating conditions.

References

1. Rifert V., Barabash P., Goliad N. (1990). Methods and processes of thermal distillation of water solutions for closed water supply systems. *SAE Paper 901249, 20th Intersociety Conference on Environmental Systems (Williamsburg, July 1990).*
2. Samsonov N, Bobe L., Novikov V., Rifert V., et al. (1994). Systems for water reclamation from humidity condensate and urine for space station. *SAE Paper 941536, 24th International society Conference on Environmental Systems (June, 1994).*
3. Samsonov N.M., Bobe L.S., Novikov V., Rifert V.G., Barabash P.A, et al.. (1995). Development of urine processor distillation hardware for space stations. (1995). *SAE Paper 951605, 25th International Conference on Environmental Systems (San Diego, July 1995).*
4. Samsonov N.M., Bobe L.S, Novikov V., Rifert V.G., et al.(1997). Updated systems for water recovery from humidity condensate and urine for the International space station. *SAE Paper 972559, 27th International Conference on Environmental Systems (Nevada, July 1997).*
5. Samsonov N.M., Bobe L.S, Novikov V., Rifert V.G., et al. (1999). Development and testing of a vacuum distillation subsystem for water reclamation from urine. *SAE Paper 1999-01-1993, 29th International Conference on Environmental Systems, 1999.*
6. Rifert V., Usenko V., Zolotukhin I., MacKnight A., Lubman A. (1999). Comparison of secondary water processors using distillation for space applications. *SAE Paper 99-70466, 29th International Conference on Environmental Systems (Denver, July 1999).*
7. Rifert V., Strikun A., Usenko V. (2000). Study of dynamic and extreme performances of multistage centrifugal distiller with the thermoelectric heat pump. *SAE Technical Papers 2000. 30th International Conference on Environmental Systems (Toulouse; France; 10-13 July 2000).*
8. Rifert V., Usenko V., Zolotukhin I., MacKnight A. and Lubman A. (2001). Design optimisation of cascade rotary distiller with the heat pump for water reclamation from urine. *SAE Paper 2001-01-2248, 31st International Conference on Environmental Systems (Orlando, July 2001).*
9. Rifert V. G., Usenko V.I., Zolotukhin I.V., MacKnight A.and Lubman A. (2003).Cascaded distillation technology for water processing in space. *SAE Paper 2003-01-2625. 34st International Conference on Environmental Systems (Orlando, July 2003).*
10. Lubman A., MacKnight A., Rifert V., Zolotukhin I. and Pickering K. (2006). Wastewater processing cascade distillation subsystem. design and evaluation. *SAE International, 2006-01-2273. July 2006.*
11. Lubman A., MacKnight A., Rifert V., and Barabash P. (2007). Cascade distillation subsystem hardware development for verification testing. *SAE International, 2007-01-3177, July 2007.*
12. Rifert V.G., Anatychuk L.I., Barabash P.A., Usenko V.I., Strikun A.P., Prybyla A.V. (2017). Improvement of the distillation methods by using centrifugal forces for water recovery in space flight applications. *J. Thermoelectricity*, 1, 71-83.
13. Rifert Vladimir G., Barabash Petr A., Usenko Vladimir, Solomakha Andrii S., Anatychuk Lukyan I., Prybyla.A.V. (2017). Improvement the cascade distillation system for long-term space flights. *68th*

International Astronautical Congress (IAC) (Adelaide, Australia, 25-29 September 2017). IAC-17-A1.IP.25.

14. Rifert V.G., Anatychuk L.I., Barabash P.O., Usenko V.I., Strikun A.P, Solomakha A.S., Petrenko V.G., Prybyla A.V. (2019). Evolution of centrifugal distillation system with a thermoelectric heat pump for space missions. Part 1. Review of publications on centrifugal distillation in the period of 1990 – 2017. J.Thermoelectricity, 1, стор.
15. Rifert V.G., Anatychuk L.I., Barabash P.O., Usenko V.I., Strikun A.P, Solomakha A.S., Petrenko V.G., Prybyla A.V. (2019). Evolution of centrifugal distillation system with a thermoelectric heat pump for space missions. Part 2. . Study of the variable characteristics of a multi-stage distillation system with a thermoelectric heat pump. J.Thermoelectricity, 2.
16. Muzhilko A.A., Rifert V.G., Barabash P.A. (1985) Flow of liquid film over the surface of a rotating disk. *Heat transfer. Soviet research.*
17. Butuzov A.I., Rifert V.G. (1972). An experimental study of heat transfer during condensation of steam at a rotating disk. *Heat Transfer-Soviet Research*, 4(6).
18. Butuzov A.I. and Rifert V.G. (1973). Heat transfer in evaporation of liquid from a film on a rotating disk. *Heat Transfer-Soviet Research, 5(1).*
19. Rifert V.G., Barabash P.A., Solomakha A.S., Usenko V., Sereda V.V., Petrenko V.G.(2018). Hydrodynamics and heat transfer in centrifugal film evaporator. *Bulgarian Chemical Communications, 50, Special Issue K, 49-57.*
20. Rifert V.G., Barabash P.A., Goliyad N.N. Condensation of steam on a water film falling down a rotating surface. *Heat transfer. Soviet research, 16 (3), 132-137.*
21. Gimbutis G. (1988). *Heat exchange with gravitational flow of liquid film*. Monograph. Vilnus.
22. Bae S., Maulbetsch J.S., Rohsenow W.M. (1969). *Refrigerant forced-convection condensation inside horizontal tubes. Report No. DSR-79760-64.* Massachusetts Institute of Technology (Cambridge, MA).
23. Traviss D.P., Baron A.N., Rohsenow W.M..(1971). Forced-convection condensation inside tubes. *Report No. DSR-72591-74. Massachusetts Institute of Technology.(Cambridge, MA)*
24. Rifert V.G., Sereda V.V., Gorin V.V., Barabash P.A., Solomakha A.S. (2018). Restoration of correctness and improvement of a model for film condensation inside tubes. *Bulgarian Chemical Communications, 50, Special Issue K, 58-69.*
25. Rifert V., Sereda V., Solomakha A. (2019). Heat transfer during film condensation inside plain tubes. Review of theoretical research. *Heat and Mass Transfer/Waerme- und Stoffuebertragung*, 2019.
26. Usenko V.I., Fainzilberg S.N. (1974). Effect of acceleration on the critical heat load with the boiling of freons on elements having small transverse dimensions. *High Temperature*.
27. Usenko V.I., Podgoretskiy V.M., Kudelya P.P. (1985). Nucleate boiling heat transfer from freon-11 and 12 at very high «g». *Heat transfer. Soviet research*.
28.Anatychuk L.I.., Prybyla A.V. (2015). Optimization of thermal connections in thermoelectric liquid-liquid heat pumps for water purification systems of space application. *J.Thermoelectricity*, 4, 45 – 51.
29. Anatychuk L.I., Prybyla A.V. (2015). Optimization of power supply system of thermoelectric liquid-liquid heat pump. *J.Thermoelectricity*, 6, 53 – 58.
30. Anatychuk L.I., Rozver Yu.Yu., Prybyla A.V. (2017). Experimental study of thermoelectric liquid-liquid heat pump. *J.Thermoelectricity*, 3, C. 33 – 39.
31Anatychuk L.I., Prybyla A.V. (2017). Limiting possibilities of thermoelectric liquid-liquid heat pump. *J.Thermoelectricity*, 4, 33 – 39.
32. Anatychuk L.I., Prybyla A.V. (2017). The influence of quality of heat exchangers on the properties of thermoelectric liquid-liquid heat pumps. *J.Thermoelectricity*, 5, 33 – 39.

33. Anatychuk L.I., Prybyla A.V. (2017). On the coefficient of performance of thermoelectric liquid-liquid heat pumps with regard to energy loss for heat carrier transfer. *J.Thermoelectricity*, 6, 33 – 39.

Submitted 05.06.2019

Риферт В.Г., *док. техн. наук* [1]
Анатичук Л.І., *акад. НАН України*[2]
Барабаш П.О., *канд. техн. наук*[1]
Усенко В.І., *док. техн. наук*[1]
Стрикун А.П.[1]
Соломаха А.С., *канд. техн. наук*[1,2]
Петренко В.Г., *канд. техн. наук*[1]
Середа В.В. *канд. техн. наук*[1]
Прибула А.В., *канд. фіз.– мат. наук* [1]

[1]НТУ «КПИ», вул. Політехнічна, 6, Київ, 03056, Україна;
[2]Інститут термоелектрики, вул. Науки, 1,
Чернівці, 58029, Україна; *e–mail:* anatych@gmail.com;
[3]Чернівецький національний університет
ім. Юрія Федьковича, вул. Коцюбинського 2,
Чернівці, 58000, Україна

ЕВОЛЮЦІЯ СИСТЕМИ ВІДЦЕНТРОВОЇ ДИСТИЛЯЦІЇ З ТЕРМОЕЛЕКТРИЧНИМ ТЕПЛОВИМ НАСОСОМ ДЛЯ КОСМІЧНИХ МІСІЙ

Частина 3. Аналіз локальних і інтегральних характеристик системи відцентрової дистиляції з термоелектричним тепловим насосом

У роботі описана методика розрахунків коефіцієнта теплопередачі й ефективності відцентрового дистилятора, а також визначення ефективності термоелектричного теплового насоса. Для цього використані результати теоретичних і експериментальних досліджень процесів конденсації й випару на обертовій поверхні й дослідження процесів у рідинно-рідинному термоелектричному тепловому насосі (ТНР). Зроблене порівняння розрахункових значень середнього температурного перепаду ΔT_{cp} у ТНР і різниці температур на вході в ТНР ΔT_{in} з експериментальними даними, отриманими при випробуванні відцентрового дистилятора на воді й урині. Бібл. 33, рис. 3, табл. 2.

Ключові слова: термоелектрика, тепловий насос, дистилятор

Риферт В.Г., *док. техн. наук* [1]
Анатычук Л.И., *акад. НАН Украины*[2,3]
Барабаш П.О. *канд. техн. наук*[1]
Усенко В.И. *док. техн. наук*[1]
Стрикун А.П.[1]
Соломаха А. С., *канд. техн. наук*[1,2]
Петренко В. Г., *канд. техн. наук*[1]
Середа В.В. *канд. техн. наук*[1]
Прибила А. В. *канд. физ.-мат. наук* [2,3]

[1]НТУ «КПИ», вул. Политехническая, 6,
Киев, 03056, Украина;
[2]Институт термоэлектричества НАН и МОН Украины,
ул. Науки, 1, Черновцы, 58029, Украина,
e–mail: anatych@gmail.com
[3]Черновицкий национальный университет
им. Юрия Федьковича, ул. Коцюбинского, 2,
Черновцы, 58012, Украина

ЭВОЛЮЦИЯ СИСТЕМЫ ЦЕНТРОБЕЖНОЙ ДИСТИЛЛЯЦИИ С ТЕРМОЭЛЕКТРИЧЕСКИМ ТЕПЛОВЫМ НАСОСОМ ДЛЯ КОСМИЧЕСКИХ МИССИЙ

Часть 3. Анализ локальных и интегральных характеристик системы центробежной дистилляции с термоэлектрическим тепловым насосом

В работе описана методика расчета коэффициента теплопередачи и эффективности центробежного дистиллятора, а также определение эффективности термоэлектрического теплового насоса. Для этого использованы результаты теоретических и экспериментальных исследований процессов конденсации и испарения на вращающейся поверхности и исследование процессов в жидкостно-жидкостном термоэлектрическом тепловом насосе (ТНР). Сделано сравнение расчетных значений среднего температурного перепада ΔT_{cp} в ТНР и разницы температур на входе в ТНР ΔT_{in} с экспериментальными данными, полученными при испытании центробежного дистиллятора на воде и урине. Библ. 33, рис. 3, табл. 2.
Ключевые слова: термоэлектричество, тепловой насос, дистиллятор.

References

1. Rifert V., Barabash P., Goliad N. (1990). Methods and processes of thermal distillation of water solutions for closed water supply systems. *SAE Paper 901249, 20th Intersociety Conference on Environmental Systems (Williamsburg, July 1990).*
2. Samsonov N, Bobe L., Novikov V., Rifert V., et al. (1994). Systems for water reclamation from humidity condensate and urine for space station. *SAE Paper 941536, 24th International society*

Conference on Environmental Systems (June, 1994).

3. Samsonov N.M., Bobe L.S., Novikov V., Rifert V.G., Barabash P.A, et al.. (1995). Development of urine processor distillation hardware for space stations. (1995). *SAE Paper 951605, 25th International Conference on Environmental Systems (San Diego, July 1995).*
4. Samsonov N.M., Bobe L.S, Novikov V., Rifert V.G., et al.(1997). Updated systems for water recovery from humidity condensate and urine for the International space station. *SAE Paper 972559, 27th International Conference on Environmental Systems (Nevada, July 1997).*
5. Samsonov N.M., Bobe L.S, Novikov V., Rifert V.G., et al. (1999). Development and testing of a vacuum distillation subsystem for water reclamation from urine. *SAE Paper 1999-01-1993, 29th International Conference on Environmental Systems, 1999.*
6. Rifert V., Usenko V., Zolotukhin I., MacKnight A., Lubman A. (1999). Comparison of secondary water processors using distillation for space applications. *SAE Paper 99-70466, 29th International Conference on Environmental Systems (Denver, July 1999).*
7. Rifert V., Strikun A., Usenko V. (2000). Study of dynamic and extreme performances of multistage centrifugal distiller with the thermoelectric heat pump. *SAE Technical Papers 2000. 30th International Conference on Environmental Systems (Toulouse; France; 10-13 July 2000).*
8. Rifert V., Usenko V., Zolotukhin I., MacKnight A. and Lubman A. (2001). Design optimisation of cascade rotary distiller with the heat pump for water reclamation from urine. *SAE Paper 2001-01-2248, 31st International Conference on Environmental Systems (Orlando, July 2001).*
9. Rifert V. G., Usenko V.I., Zolotukhin I.V., MacKnight A.and Lubman A. (2003).Cascaded distillation technology for water processing in space. *SAE Paper 2003-01-2625. 34st International Conference on Environmental Systems (Orlando, July 2003).*
10. Lubman A., MacKnight A., Rifert V., Zolotukhin I. and Pickering K. (2006). Wastewater processing cascade distillation subsystem. design and evaluation. *SAE International, 2006-01-2273. July 2006.*
11. Lubman A., MacKnight A., Rifert V., and Barabash P. (2007). Cascade distillation subsystem hardware development for verification testing. *SAE International, 2007-01-3177, July 2007.*
12. Rifert V.G., Anatychuk L.I., Barabash P.A., Usenko V.I., Strikun A.P., Prybyla A.V. (2017). Improvement of the distillation methods by using centrifugal forces for water recovery in space flight applications. *J. Thermoelectricity*, 1, 71-83.
13. Rifert Vladimir G., Barabash Petr A., Usenko Vladimir, Solomakha Andrii S., Anatychuk Lukyan I., Prybyla.A.V. (2017). Improvement the cascade distillation system for long-term space flights. *68th International Astronautical Congress (IAC) (Adelaide, Australia, 25-29 September 2017). IAC-17-A1.IP.25.*
14. Rifert V.G., Anatychuk L.I., Barabash P.O., Usenko V.I., Strikun A.P, Solomakha A.S., Petrenko V.G., Prybyla A.V. (2019). Evolution of centrifugal distillation system with a thermoelectric heat pump for space missions. Part 1. Review of publications on centrifugal distillation in the period of 1990 – 2017. J.Thermoelectricity, 1.
15. Rifert V.G., Anatychuk L.I., Barabash P.O., Usenko V.I., Strikun A.P, Solomakha A.S., Petrenko V.G., Prybyla A.V. (2019). Evolution of centrifugal distillation system with a thermoelectric heat pump for space missions. Part 2. . Study of the variable characteristics of a multi-stage distillation system with a thermoelectric heat pump. J.Thermoelectricity, 2.
16. Muzhilko A.A., Rifert V.G., Barabash P.A. (1985) Flow of liquid film over the surface of a rotating disk. *Heat transfer. Soviet research.*
17. Butuzov A.I., Rifert V.G. (1972). An experimental study of heat transfer during condensation of steam at a rotating disk. *Heat Transfer-Soviet Research*, 4(6).
18. Butuzov A.I. and Rifert V.G. (1973). Heat transfer in evaporation of liquid from a film on a rotating disk. *Heat Transfer-Soviet Research, 5(1).*

19. Rifert V.G., Barabash P.A., Solomakha A.S., Usenko V., Sereda V.V., Petrenko V.G.(2018). Hydrodynamics and heat transfer in centrifugal film evaporator. *Bulgarian Chemical Communications, 50, Special Issue K, 49-57.*
20. Rifert V.G., Barabash P.A., Goliyad N.N. Condensation of steam on a water film falling down a rotating surface. *Heat transfer. Soviet research, 16 (3), 132-137.*
21. Gimbutis G. (1988). *Heat exchange with gravitational flow of liquid film*. Monograph. Vilnus.
22. Bae S., Maulbetsch J.S., Rohsenow W.M. (1969). *Refrigerant forced-convection condensation inside horizontal tubes. Report No. DSR-79760-64.* Massachusetts Institute of Technology (Cambridge, MA).
23. Traviss D.P., Baron A.N., Rohsenow W.M..(1971). Forced-convection condensation inside tubes. *Report No. DSR-72591-74. Massachusetts Institute of Technology.(Cambridge, MA)*
24. Rifert V.G., Sereda V.V., Gorin V.V., Barabash P.A., Solomakha A.S. (2018). Restoration of correctness and improvement of a model for film condensation inside tubes. *Bulgarian Chemical Communications, 50, Special Issue K, 58-69.*
25. Rifert V., Sereda V., Solomakha A. (2019). Heat transfer during film condensation inside plain tubes. Review of theoretical research. *Heat and Mass Transfer/Waerme- und Stoffuebertragung*, 2019.
26. Usenko V.I., Fainzilberg S.N. (1974). Effect of acceleration on the critical heat load with the boiling of freons on elements having small transverse dimensions. *High Temperature*.
27. Usenko V.I., Podgoretskiy V.M., Kudelya P.P. (1985). Nucleate boiling heat transfer from freon-11 and 12 at very high «g». *Heat transfer. Soviet research*.
28.Anatychuk L.I.., Prybyla A.V. (2015). Optimization of thermal connections in thermoelectric liquid-liquid heat pumps for water purification systems of space application. *J.Thermoelectricity*, 4, 45 – 51.
29. Anatychuk L.I., Prybyla A.V. (2015). Optimization of power supply system of thermoelectric liquid-liquid heat pump. *J.Thermoelectricity*, 6, 53 – 58.
30. Anatychuk L.I., Rozver Yu.Yu., Prybyla A.V. (2017). Experimental study of thermoelectric liquid-liquid heat pump. *J.Thermoelectricity*, 3, C. 33 – 39.
31Anatychuk L.I., Prybyla A.V. (2017). Limiting possibilities of thermoelectric liquid-liquid heat pump. *J.Thermoelectricity*, 4, 33 – 39.
32. Anatychuk L.I., Prybyla A.V. (2017). The influence of quality of heat exchangers on the properties of thermoelectric liquid-liquid heat pumps. *J.Thermoelectricity*, 5, 33 – 39.
33. Anatychuk L.I., Prybyla A.V. (2017). On the coefficient of performance of thermoelectric liquid-liquid heat pumps with regard to energy loss for heat carrier transfer. *J.Thermoelectricity*, 6, 33 – 39.

Submitted 05.06.2019

P.V. Gorskiy

P.V. Gorskiy *doc. phys.– math. science*[1,2],
Mytskaniuk N.V.[1,2]

[1]Institute of Thermoelectricity of the NAS and MES of Ukraine, 1, Nauky str, Chernivtsi, 58029, Ukraine;
e-mail: anatych@gmail.com
[2]Yu.Fedkovych Chernivtsi National University,
2, Kotsiubynskyi str., Chernivtsi, 58000, Ukraine

Mytskaniuk N.V.

ON THE TEMPERATURE DEPENDENCES OF THERMOELECTRIC CHARACTERISTICS OF BISMUTH TELLURIDE-METAL TRANSIENT LAYER WITH DUE REGARD FOR PERCOLATION EFFECT

The basic relationships are obtained by calculation, which determine the temperature dependences of thermoelectric characteristics of thermoelectric material-metal transient contact layers with due regard for percolation theory. Specific quantitative results and plots of the temperature dependences of the electrical and thermal contact resistances, the thermoEMF, the power factor, and the dimensionless thermoelectric figure of merit are given for bismuth telluride – nickel contact pair. It has been established that in the temperature range of 200-400 K on retention of uneven distribution of metal particles in transient layer and its thickness in the range of 20-150 μm, the electrical contact resistance varies from $7 \cdot 10^{-7}$ to $1.9 \cdot 10^{-5}$ Ohm·cm^2, the thermal contact resistance – from 0.052 to 0.98 K·cm^2/W, the thermoEMF– from 155 to 235 μV/K, the power factor – from $4.2 \cdot 10^{-5}$ to $6.8 \cdot 10^{-5}$ W/(m·K^2), the dimensionless thermoelectric figure of merit – from 0.35 to 1.08. After levelling the concentration, the electrical contact resistance decreases by a factor of 1.12 – 3.6, the thermal contact resistance decreases by a factor of 1.15 – 2.08, the thermoEMF is practically unvaried, the power factor increases by a factor of 1.19 – 2.79, the dimensionless thermoelectric figure of merit increases maximum 1.2 times. Bibl. 14, Fig. 22.

Key words: thermoelectric material-metal contact, near-contact transient layer, electrical contact resistance, thermal contact resistance, thermoEMF, percolation theory.

Introduction

The efficiency of thermoelectric modules of sufficiently large sizes is mainly determined by the figure of merit of thermoelectric materials of thermoelement legs. However, as the size of thermoelectric legs decreases in the direction of temperature gradient, this efficiency becomes increasingly dependent on the electrical and thermal contact resistances of thermoelectric material – metal layer, in particular, due to the Joule heat release on the contact resistances. These resistances should be essentially lower than those of thermoelectric legs [1-3]. This fact put a limit on the miniaturization of thermoelectric power converters – generators and coolers.

Indeed, let, for instance, r_{ce} – specific, that is related to unit contact area, electrical contact resistance. Then, if ρ_s – specific electrical resistance of TEM, and l_s – the length of thermoelectric leg in the direction of temperature gradient, then the condition of small influence of contact resistance on the efficiency of thermoelectric power converter is given by:

$$l_s >> r_{ce} / \rho_s , \qquad (1)$$

whence it is seen that the lower specific contact resistance, the shorter (in the direction of temperature gradient) thermoelectric legs can be made. Moreover, it has been found that in the manufacture of thermoelectric legs it is desirable to maintain an optimal ratio l_s/S_s, where S_s – cross-sectional area of the leg, owing to which a decrease in specific electric contact resistance by a factor of K all other things being equal, leads to a reduction in TEM consumption by a factor of K^2. And TEM is known to be most scarce and expensive part of thermoelectric power converter. But an even more important factor that determines the urgency of the miniaturization of thermoelectric energy converters is the need to use them in order to create favorable temperature conditions for the operation of microelectronic components of various-purpose electronic equipment.

However, for the design of thermoelectric energy converters and the correct assessment of their effectiveness, it is of fundamental importance to know the temperature dependences of the thermoelectric characteristics of transient contact layers, and up to now they have only partially been considered in the theory of thermoelectric energy conversion, and in the design of thermoelectric energy converters they have not been fully taken into account, although experimental data on the temperature dependences, for example, of TEM-metal electric contact resistances do exist [4 – 7].

Therefore, *the purpose of this work* is to develop a model of TEM-metal transient contact layer structure with regard to percolation theory and to calculate on its basis the temperature dependences of thermoelectric characteristics of transient contact layers.

Physical model of TEM-metal transient layer with due regard for percolation effect and its mathematical description

The electrical resistance of transient layer in the case when contact metal or solder does not form intermetallides with TEM and is not a doping impurity for it, which, for instance, is valid for contact structures with anti-diffusion layers [8], can be considered such that consists of three parts: 1) due to diffusion of metal particles in TEM without change in chemical composition and macroscopic characteristics of metal and TEM; 2) due to deviation of TEM surface from the ideal plane; 3) due to the interface between metal and TEM, in particular the potential barrier on this interface. In this paper, we consider only the first part. In our consideration we will take into account the percolation effect [9, 10].

First we consider a physical model which illustrates the necessity of taking into account percolation effect on examination of electrical conductivity and thermal conductivity of transient layer which is a thermoelectric material with metal particles diffused thereto. This model is shown in Fig.1.

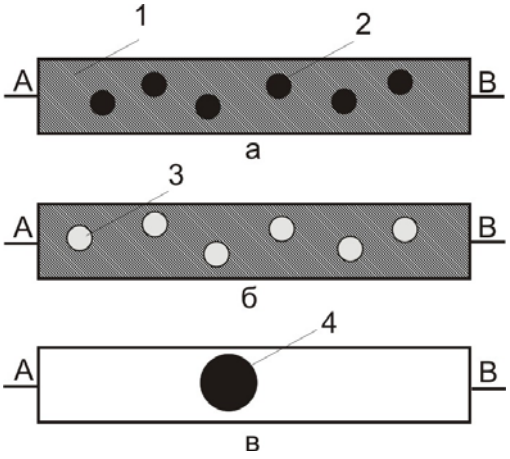

Fig.1. Physical model that illustrates the need to use percolation theory: a) TEM bar with metal particles; b) TEM bar with vacuum cavities (pores); c) hypothetical evacuated or perfectly dielectric volume comprising a single conducting particle, A,B – electrical contacts,1-TEM, 2-metal particles, 3-vacuum cavities, 4-single conducting particle

Before considering, incidentally, we note that prior to creation of percolation theory the electrical conductivity and thermal conductivity of the two-phase TEM-metal system shown in Fig. 1a were calculated through the volumetric fraction v_m of metal in it according to the so-called "mixing formulae", which for this case have the form [11]:

$$\sigma(v_m) = \sigma_s(1 - v_m) + \sigma_m v_m . \tag{2}$$

$$\kappa(v_m) = \kappa_s(1 - v_m) + \kappa_m v_m \tag{3}$$

The limited applicability of this formula can be seen from the following physical considerations.

Imagine that at first our system consists of TEM, and part of the material in it is gradually replaced by vacuum cavities (pores) (Fig.1b). From traditional formulae of the type (2) and (3) it follows that the electrical conductivity and (or) thermal conductivity of this system will become zero only when all TEM or other electrically conducting (and, therefore, heat-conducting) material is replaced by vacuum or another ideally non-conducting for electricity and (or) heat phase. But on the other hand, it is clear that the electrical conductivity and (or) thermal conductivity of the "hypothetical" system shown in Fig.1c, in which, a single conducting particle in the volume of the non-conducting phase, that does not touch the electrodes, is also equal to zero (for electrical conductivity this is true, if we do not consider the phenomenon of breakdown of a dielectric or current in vacuum, and for thermal conductivity – if we do not consider the transfer of heat by radiation). From this it is clear that if the leading phase does not form end-to-end connected regions, there must exist a critical volume fraction of vacuum pores, or another non-conducting phase, provided that the conductivity and thermal conductivity of the system exceed zero. This phenomenon is called the percolation phenomenon. It is taken into account by the so-called percolation theory. In accordance with it, the electrical conductivity and thermal conductivity of the two-phase three-dimensional system "TEM-metal" is determined by the following formulae [9,10]:

$$\sigma = 0.25\left\{\sigma_s(2 - 3v_m) + \sigma_m(3v_m - 1) + \sqrt{[\sigma_s(2 - 3v_m) + \sigma_m(3v_m - 1)]^2 + 8\sigma_m\sigma_s}\right\}, \tag{4}$$

$$\kappa = 0.25\left\{\kappa_s(2 - 3v_m) + \kappa_m(3v_m - 1) + \sqrt{[\kappa_s(2 - 3v_m) + \kappa_m(3v_m - 1)]^2 + 8\kappa_m\kappa_s}\right\}, \tag{5}$$

where v_m – the volumetric part of metal in transient layer.

Indeed, suppose that one of the phases does not conduct electricity and heat at all, that is, we assume that $\sigma_s = 0$ and $\kappa_s = 0$. Then formulae (4) and (5) will acquire the form:

$$\sigma = 0.5\sigma_m(3v_m - 1), \tag{6}$$

$$\kappa = 0.5\kappa_m(3v_m - 1). \tag{7}$$

The characteristic feature of formulae (6), (7) is that in conformity with them not only $\sigma = \sigma_m$ and $\kappa = \kappa_m$ at $v_m = 1$, which obviously should be done, but also, unlike traditional formulae (2) and (3), $\sigma = 0$ and $\kappa = 0$ at $0 < v_m \le 1/3$. So, critical volumetric fraction of an absolutely non-conducting phase equal to 2/3 and upon reaching or exceeding which the electrical conductivity and thermal conductivity of a two-phase system with this phase vanish, really exists, as mentioned above.

Therefore, it is clear that, as a result of the percolation phenomenon, the theoretically predicted values of the electrical and thermal contact resistances should be greater than according to the traditional theory of

composites. Note that the limiting values of the electrical conductivity and thermal conductivity of a two-phase system according to formulae (4), (5) are the same as according to formulae (2), (3).

The volumetric metal part $v_m(y)$, which, generally speaking, depends on the normalized to layer thickness d_0 of dimensionless coordinate $0 \le y \le 1$ and satisfies the boundary conditions $v_m(0) = 1$, $v_m(1) = 0$, is determined from the diffusion equation of the type [12] with a constant intensity of the source of metal particles as follows:

$$v_m(y) = \frac{(A_m/\gamma_m)\left[1-(1-A)y-Ay^2\right]}{(A_m/\gamma_m)\left[1-(1-A)y-Ay^2\right]+(A_s/\gamma_s)\left[(1-A)y+Ay^2\right]}, \tag{8}$$

where $A_m, A_s, \gamma_m, \gamma_s$ – atomic (molecular) masses of metal and TEM and their densities, respectively. The dimensionless parameter A depends on the mode of contact creation and is determined in this way:

$$A = Qd_0^2/2Dn_0, \tag{9}$$

where Q – the intensity of metal particles entering transient layer, D – coefficient of diffusion of metal particles in TEM, n_0 – atomic concentration of metal.

If the uneven distribution of metal particles in the transient layer is preserved, then the electrical conductivity $\sigma_l(y)$ and thermal conductivity $\kappa_l(y)$ of such a layer in accordance with relations (4), (5), (8) depend on the normalized coordinate y, and, therefore, the magnitude of the electrical and thermal contact resistances of such a layer can be evaluated by the formulae:

$$r_{ce} = d_0 \int_0^1 \frac{dy}{\sigma_l(y)}, \tag{10}$$

$$r_{ct} = d_0 \int_0^1 \frac{dy}{\kappa_l(y)}, \tag{11}$$

and the value of thermoEMF by the formula:

$$\alpha = \frac{\int_0^1 \{(\alpha_m/\kappa_m)v_m(y)+(\alpha_s/\kappa_s)[1-v_m(y)]\}dy}{\int_0^1 \{\kappa_m^{-1}v_m(y)+\kappa_s^{-1}[1-v_m(y)]\}dy}. \tag{12}$$

If, however, the distribution of the metal particles in transient layer has been levelled, then the electrical conductivity $\sigma_l(y)$ and thermal conductivity $\kappa_l(y)$ dependent on the normalized coordinate should in this case be replaced by their established values σ_{la} and κ_{la} obtained by formulae (4) and (5) after substitution in them instead of the coordinate dependent volumetric metal fraction $v_m(y)$ of its established value v_{ma} which is defined as:

$$v_{ma} = \int_0^1 \frac{(A_m/\gamma_m)\left[1-(1-A)y-Ay^2\right]}{(A_m/\gamma_m)\left[1-(1-A)y-Ay^2\right]+(A_s/\gamma_s)\left[(1-A)y+Ay^2\right]}dy. \tag{13}$$

Thus, formulae (10) – (12) will be given by:

$$r_{ce} = \frac{d_0}{\sigma_{la}}, \tag{14}$$

$$r_{ct} = \frac{d_0}{\kappa_{la}}, \tag{15}$$

$$\alpha = \frac{(\alpha_m/\kappa_m)v_{ma} + (\alpha_s/\kappa_s)(1-v_{ma})}{\kappa_m^{-1}v_{ma} + \kappa_s^{-1}(1-v_{ma})}. \tag{16}$$

Procedure for calculating characteristics of transient contact layer

The calculation starts with theoretical approximation of the temperature dependences of the kinetic coefficients of TEM and metal.

We approximate the kinetic coefficients of TEM. Let at some temperature T_0 we know its thermoelectric parameters, namely the thermoEMF α_{s0}, the electrical conductivity σ_{s0} and the thermal conductivity κ_{s0}. To construct their temperature dependences, using this data we make the following model assumptions:

1) zone spectrum of carriers in TEM is parabolic and isotropic with temperature independent effective mass;
2) quasi-elastic scattering of carriers in the relevant temperature region occurs on the deformation potential of acoustic phonons with energy independent cross section and mean free path inversely proportional to temperature;
3) lattice thermal conductivity of semiconductor is determined by phonon-phonon scattering with umklapp and is inversely proportional to temperature.

Provided that these assumptions are valid, the carrier scattering index r = –0.5. Taking into account its value, the construction of the necessary temperature dependences on the basis of known general relations [13] is carried out in the following order.

From the relation for the thermoEMF

$$\alpha_{s0} = \frac{k}{e}\left[\frac{2F_1(\eta_0)}{F_0(\eta_0)} - \eta_0\right] \tag{17}$$

we find a reduced chemical potential η_0 of carrier gas at temperature T_0.

Using the condition of constant carrier concentration and their effective mass, from the equation

$$\frac{T^{1.5}F_{0.5}(\eta)}{T_0^{1.5}F_{0.5}(\eta_0)} = 1 \tag{18}$$

we determine the temperature dependence of reduced chemical potential η of carrier gas on temperature T in given temperature range.

From the relation

$$\alpha_s = \frac{k}{e}\left[\frac{2F_1(\eta)}{F_0(\eta)} - \eta\right] \tag{19}$$

we determine the temperature dependence of the thermoEMF of TEM.

From the relation

$$L_s(\eta)=\left(\frac{k}{e}\right)^2\left[\frac{3F_2(\eta)}{F_0(\eta)}-\frac{4F_1^2(\eta)}{F_0^2(\eta)}\right] \tag{20}$$

we determine the temperature dependence of the Lorentz number of TEM.

The temperature dependence of the electrical conductivity of TEM for the above model assumptions is determined as:

$$\sigma_s=\sigma_{s0}\left(\frac{T_0}{T}\right)^{1.5}\frac{F_0(\eta)F_{0.5}(\eta_0)}{F_{0.5}(\eta)F_0(\eta_0)}\,. \tag{21}$$

The temperature dependence of the thermal conductivity of TEM with regard to everything said above is determined as:

$$\kappa_s=\sigma_s L_s(\eta)T+\left[\kappa_{s0}-\sigma_{s0}L_s(\eta_0)T_0\right]\frac{T_0}{T}\,. \tag{22}$$

In formulae (17) – (21), $F_m(\eta)$ denote the Fermi integrals that are determined by the following relation:

$$F_m(\eta)=\int_0^\infty x^m\left[\exp(x-\eta)+1\right]^{-1}dx\,. \tag{23}$$

Relations (17) - (22) completely determine the temperature dependences of the thermoEMF, the electrical conductivity and the thermal conductivity of TEM.

Approximation of the temperature dependences of the electrical conductivity, the thermal conductivity and the thermoEMF of metal is done as follows. We assume that in metal, just as in TEM, scattering of free carriers takes place on the deformation potential of acoustic phonons, and in the real temperature region the mean free path of carriers is inversely proportional to temperature. Then, taking into account strong degeneracy of carriers in metal, the temperature dependence of its electrical conductivity will be determined as [14]:

$$\sigma_m=\sigma_{m0}\cdot(T_0/T)\,, \tag{24}$$

and, therefore, taking into account the Wiedemann-Franz relation, the thermal conductivity of the metal κ_m will be considered to be temperature independent. We will also consider the thermoEMF of the metal α_m to be independent of temperature. Then, knowing the above mentioned temperature dependences, from relations (8) – (16) we find the temperature dependences of the characteristics of transient contact layer.

Results of calculation and their discussion

The temperature dependences of the electrical and thermal contact resistances, the thermoEMF and the dimensionless thermoelectric figure of merit of the TEM-metal transient contact layer for bismuth telluride-nickel pair obtained in the framework of the calculation procedure described above, provided that the uneven distribution of the metal atoms in the layer is preserved, are shown in Figs. 2 – 8.

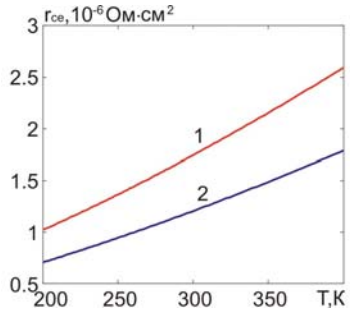

Fig.2. Temperature dependences of electrical contact resistance with due regard for percolation effect at transient layer thickness of 20 μm: 1 – A=0; 2 – A=1.

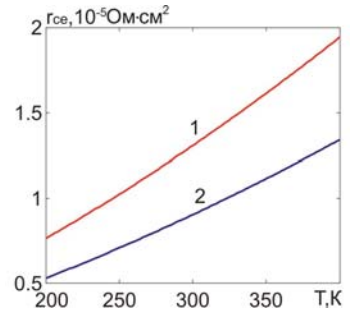

Fig.3. Temperature dependences of electrical contact resistance with due regard for percolation effect with due regard for percolation effect at transient layer thickness of 150 μm: 1 – A=0; 2 – A=1.

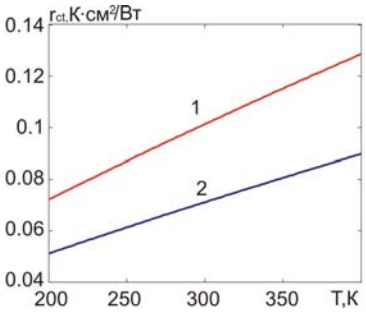

Fig.4. Temperature dependences of thermal contact resistance with due regard for percolation effect at transient layer thickness of 20 μm: 1 – A=0; 2 – A=1.

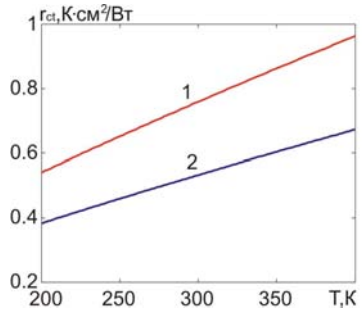

Fig.5. Temperature dependences of thermal contact resistance with due regard for percolation effect at transient layer thickness of 150 μm: 1 – A=0; 2 – A=1.

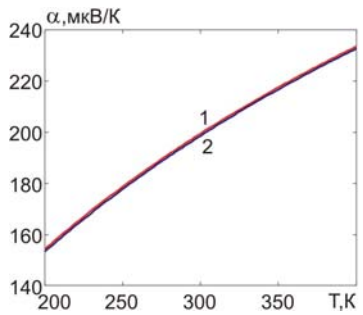

Fig.6. Temperature dependences of transient layer thermoEMF: 1 – A=0; 2 – A=1.

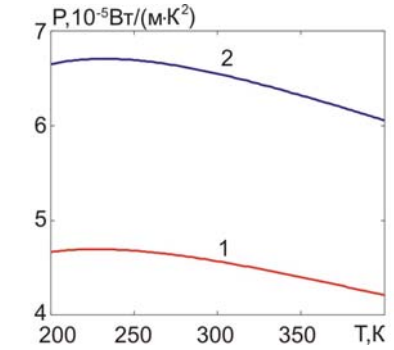

Fig.7. Temperature dependences of transient layer power factor with due regard for percolation effect: 1 – A=0; 2 – A=1.

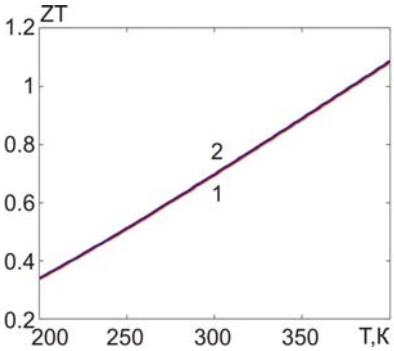

Fig.8. Temperature dependences of transient layer thermoelectric figure of merit with due regard for percolation effect
1 – A=0; 2 – A=1.

Similar temperature dependences after levelling metal concentration in transient layer are shown in Figs. 9 – 15.

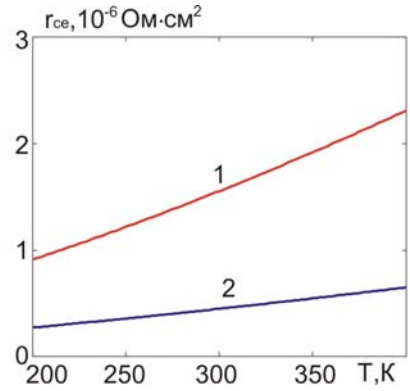

Fig.9. Temperature dependences of electrical contact resistance with due regard for percolation effect after levelling metal concentration at transient layer thickness of 20 μm:
1 – A=0; 2 – A=1.

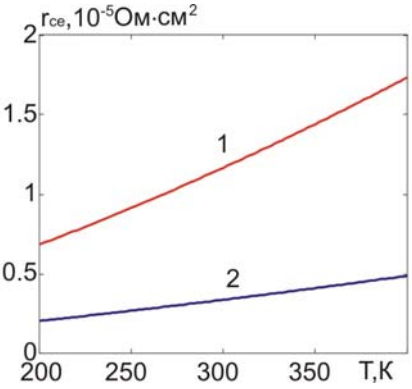

Fig.10. Temperature dependences of electrical contact resistance with due regard for percolation effect after levelling metal concentration at transient layer thickness of 150 μm:
1 – A=0; 2 – A=1.

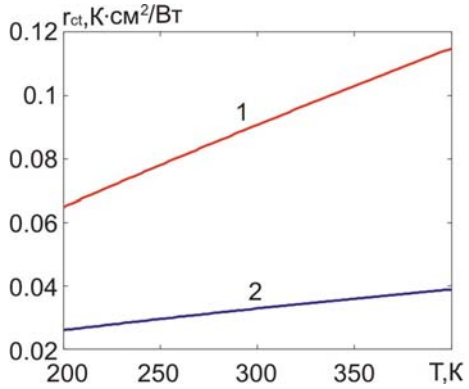

Fig.11. Temperature dependences of thermal contact resistance with due regard for percolation effect after levelling metal concentration at transient layer thickness of 20 μm:
1 – A=0; 2 – A=1.

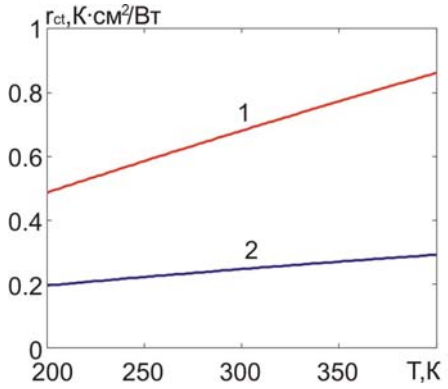

Fig.12. Temperature dependences of thermal contact resistance with due regard for percolation effect after levelling metal concentration at transient layer thickness of 150 μm:
1 – A=0; 2 – A=1.

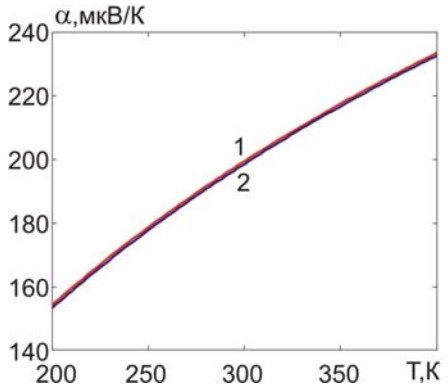

Fig.13. Temperature dependences of transient layer thermoEMF after levelling metal concentration: 1 – A=0; 2 – A=1.

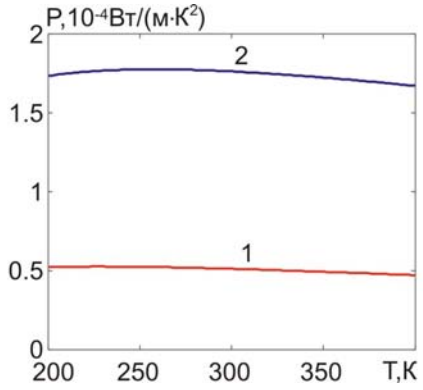

Fig.14. Temperature dependences of transient layer power factor with due regard for percolation effect after levelling metal concentration: 1 – A=0; 2 – A=1.

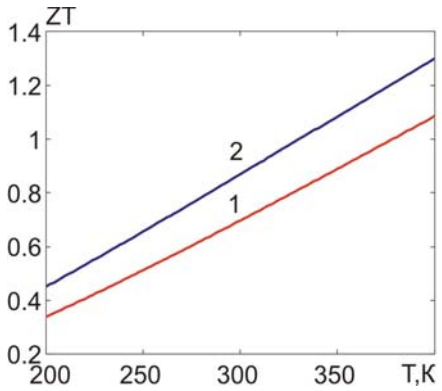

Fig.15. Temperature dependences of transient layer dimensionless thermoelectric figure of merit with due regard for percolation theory after levelling metal concentration:
1 – A=0; 2 – A=1.

When plotting, the following material parameters for 300K were taken: σ_m=1.25·10^5 S/cm, σ_s=800 S/cm, κ_m=92 W /(m·K), κ_s=1.4 W /(m·K), α_m= – 23 μV/K, α_s= 200 μV/K, and, besides, A_m=58.5, A_s=801, ρ_m=9100 kg/m^3, ρ_s=7700 kg/m^3. It can be seen from the figures that in the temperature range studied, the electrical and thermal contact resistances, the thermoEMF, and the dimensionless thermoelectric figure of merit of transient layer increase, and the power factor has a maximum in the range of 200 - 250 K. Such temperature dependences can be explained by an increase in the resistivities of metal and semiconductor, a decrease in their thermal conductivity, and an increase in the thermoEMF of semiconductor with a rise in temperature. With an increase in the thickness of transient layer, the electrical and thermal contact resistances increase in proportion to this thickness. The presence of a maximum in the temperature dependence of power factor is explained by two competing processes: an increase in the thermoEMF and a decrease in TEM electrical conductivity with a rise in temperature. It should be noted that the thermoEMF of transient layer is mainly determined by the semiconductor due to the fact that thermal conductivity of metal is significantly greater than thermal conductivity of semiconductor.

In addition, it can be seen from the figures that with increasing parameter A, that is, the intensity of metal atoms entering transient layer, the thermal and electrical contact resistances, as well as the thermoEMF decrease, and the power factor and the dimensionless thermoelectric figure of merit increase. On the whole, in the studied ranges of temperature, the intensity of metal entering transient layer, and the transient layer thickness, the electrical contact resistance varies from 7·10^{-7} to 1.9·10^{-5} Ohm·cm^2, the thermal contact resistance – from 0.052 to 0.98 K·cm^2/W, the thermoEMF – from 155 to 235 μV/K, the power factor – from 4.2·10^{-5} to 6.8·10^{-5} W/(m·K^2), the dimensionless thermoelectric figure of merit – from 0.35 to 1.08. Thus, the electrical and thermal contact resistances, predicted with due regard for percolation theory, are, as expected, essentially higher, and the power factor and the dimensional thermoelectric figure of merit – essentially lower than without regard to this theory. Taking into account the percolation theory does not affect the predicted temperature dependence of the thermoEMF of transient contact layer.

It is also seen from the figures that after levelling metal concentration in the bulk of transient layer, the anticipated values of the electrical and thermal contact resistances at all temperatures decrease, the thermoEMF is practically unvaried, and the power factor and the dimensionless thermoelectric figure of merit increase as compared to the case of uneven distribution, but not so essentially as without regard to percolation theory.

As regards the effect of parameter *A*, that is, the intensity of metal entering transient layer, on the predicted thermoelectric properties of transient layer, both in the case of uneven and uniform distribution, with due regard for percolation theory the same tendency is preserved as without regard to this theory. The sole exception is power factor. Unlike the case of uneven distribution of concentration, when it has a maximum both at *A*=0 and at *A*=1, after its levelling in the temperature range under study the power factor

has a maximum only at A=1.

In general, in the studied ranges of temperature, the intensity of metal entering transient layer and the thickness of transient layer after levelling metal concentration the electrical contact resistance varies from $2.5\cdot10^{-7}$ to $1.75\cdot10^{-5}$ Ohm·cm^2, the thermal contact resistance – from 0.025 to 0.85 K·cm^2/W, the thermoEMF – from 155 to 235 V/K, the power factor – from $5\cdot10^{-5}$ to $1.9\cdot10^{-4}$ W/(m·K^2), the dimensionless thermoelectric figure of merit – from 0.35 to 1.3. Thus, after the concentration is levelled, the electrical contact resistance drops by a factor of 1.12 – 3.6, the thermal contact resistance decreases by a factor of 1.15 – 2.08, the thermoEMF is practically unvaried, the power factor grows by a factor of 1.19 – 2.79, the dimensionless thermoelectric figure of merit grows maximum 1.2 times. Note that though for thermoelectric contact structures such characteristics thereof as power factor and dimensionless thermoelectric figure of merit do not have self-importance in terms of designing thermoelectric power converters, they are useful for the integral quality evaluation of these structures.

Effect of contact resistance on the efficiency of thermoelectric generator module

The above temperature dependences of the electrical and thermal contact resistances were used to calculate the efficiency of thermoelectric generator modules with the height of thermoelectric legs 3 and 1.5 mm, respectively. The calculations were performed by methods of object-oriented simulation in Comsol Multiphysics software environment.

For this purpose, a physical model shown in Fig.16 was considered.

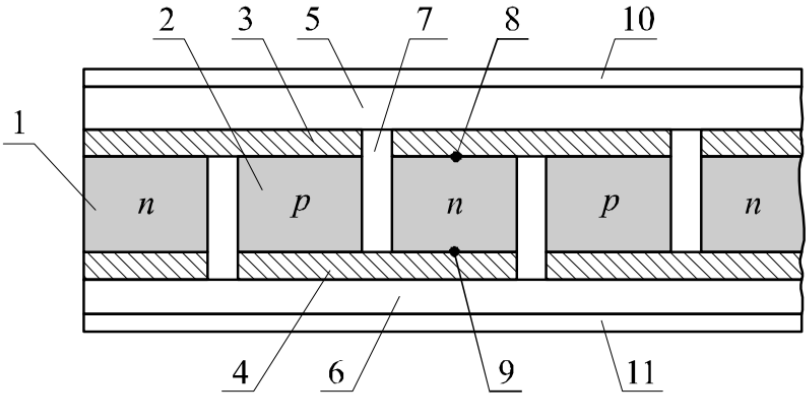

Fig. 16. Physical model of thermoelectric generator module.
1 – n-type leg; 2 – p-type leg; 3, 4 – electrical interconnects;
5, 6 – ceramic plates; 7 – gas; 8, 9 – electrical contacts between legs and interconnect plates;
10 – thermal contact between ceramic plate and hot thermostat;
11 – thermal contact between ceramic plate and cold thermostat.

The distribution of temperature and electrical potential in the module was found from the system of differential equations with respect to temperature T and electrochemical potential U. These equations were obtained on the basis of the law of conservation of energy which is given by the following two equations:

$$\nabla\vec{w} = 0\,, \tag{25}$$

$$\vec{w} = \vec{q} + U\vec{j}\,. \tag{26}$$

In formulae (25) and (26), $\vec{j}$ – electric current density, $\vec{q}$ – heat flux density:

$$\vec{q} = -\kappa\nabla T + \Pi\vec{j}\,, \tag{27}$$

where Π is the Peltier coefficient; κ is thermal conductivity.

$$\Pi = \alpha T, \tag{28}$$

where α is the Seebeck coefficient, T is temperature.

The electric current density is found from the equation

$$\vec{j} = -\sigma\nabla U - \sigma\alpha\nabla T \quad \vec{j} = -\sigma\nabla U - \sigma\alpha\nabla T, \tag{29}$$

where σ is electrical conductivity.

Substituting (26), (27) into (25), we obtain

$$-\nabla(\kappa\nabla T) + (\nabla\Pi + \nabla U)\vec{j} = 0 \quad -\nabla(\kappa\nabla T) + (\nabla\Pi + \nabla U)\vec{j} = 0. \tag{30}$$

From expression (30), using (28) and (29), we obtain the following equation to find the distributions of temperature and potential:

$$-\nabla\left[\left(\sigma\alpha^2 T + \kappa\right)\nabla T\right] - \nabla(\sigma\alpha T\nabla U) - \sigma\left[(\nabla U)^2 + \alpha\nabla T\nabla U\right] = 0\,. \tag{31}$$

To obtain the second equation, we will use the law of conservation of electrical charge:

$$\nabla\vec{j} = 0 \quad div\,\vec{j} = 0. \tag{32}$$

Substituting (29) into (32), we obtain the following equation:

$$\nabla(\sigma\alpha\nabla T) + \nabla(\sigma\nabla U) = 0 \quad -\nabla(\sigma\alpha\nabla T) - \nabla(\sigma\nabla U) = 0. \tag{33}$$

System (31), (33) is a system of differential equations with variable second-order partial differential coefficients, which describes the distribution of temperature and potential in an inhomogeneous thermoelectric medium. A feature of the system of equations (31), (33) is that the parameters α, σ, κ depend on the spatial coordinates *x, y, z* both directly and implicitly through the temperature *T* (*x, y, z*). This leads to the fact that it becomes inevitable to use numerous computer methods to solve equations of this kind.

In a computer model, the thermoelectric field is described by a two-element column matrix in the functional space of twice differentiable functions, namely, the coordinate dependences of temperature and potential:

$$M = \begin{pmatrix} T(x,y,z) \\ U(x,y,z) \end{pmatrix}. \tag{34}$$

Matrix M satisfies one matrix differential equation

$$\nabla(c\nabla M) = f \quad -\nabla(-c\nabla M) = f, \tag{35}$$

whose components are equations (31) and (33) if the matrix nonlinear coefficients of equation (35) have the

form

$$c = \begin{pmatrix} \sigma\alpha^2 T + \kappa & \sigma\alpha T \\ \alpha\sigma & \sigma \end{pmatrix}, f = \begin{pmatrix} \sigma\left[(\nabla U)^2 + \nabla T \nabla U\right] \\ 0 \end{pmatrix}. \quad (36)$$

A system of equations of the form (35) with allowance for (36) is solved for each of the layers that make up the thermoelectric module. For this, we additionally introduce the boundary conditions for the continuity of temperature, electric potential, heat flux, and electric current density at the boundaries of the layers. In addition, for reasons of optimality of the conditions under which the thermoelement operates, and which are determined from the requirement to achieve the maximum value of the efficiency, the potentials on the switching electrodes and the temperatures of the "hot" and "cold" thermostats are set. Therefore, the potentials on the switching electrodes of one of the legs are 0 and 0.0573 V, on the second - 0.0573 and 0.1146 V, and the temperatures of the "cold" and "hot" thermostats are 273 and 573 K, respectively.

The impact of the electrical and thermal contact resistances is taken into account in the physical model in the framework of two approaches. The first is that the contact layer is not explicitly introduced into the physical model, but its electrical conductivity and thermal conductivity are considered to be known from experiment or, in this case, temperature functions preliminarily calculated by calculation. Then, the proportionality of the electrical and thermal contact resistances to the layer thickness is taken into account. The second approach is that a contact layer with temperature-dependent thermal conductivity and electrical conductivity, taking into account its thickness, is explicitly introduced into the physical model. The thermoEMF of the contact layer at this stage of research is not taken into account.

Such mathematical description allows solving the above described system of equations for temperature and potential in Comsol Multiphysics simulation environment. The results of solving Eq.(11) are three-dimensional temperature and electrical fields in given geometry of thermoelectric module. Their examples for one thermoelement which is part of the module with the height of leg 3 mm are shown in Figs. 16, 17. Knowing these fields, it is easy to calculate the basic energy characteristics of the module.

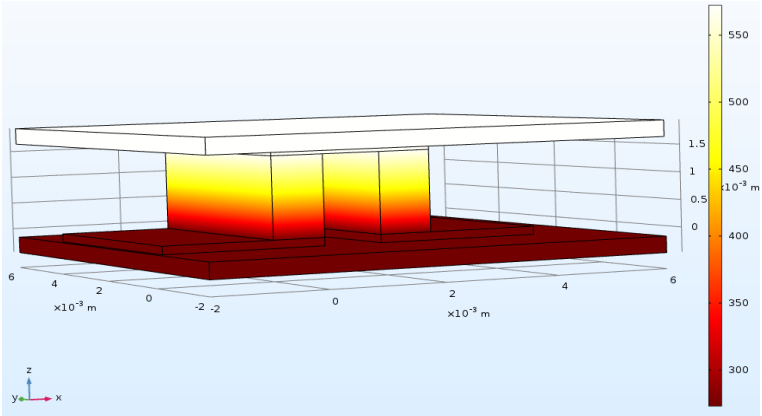

Fig.17. Temperature field in thermoelement

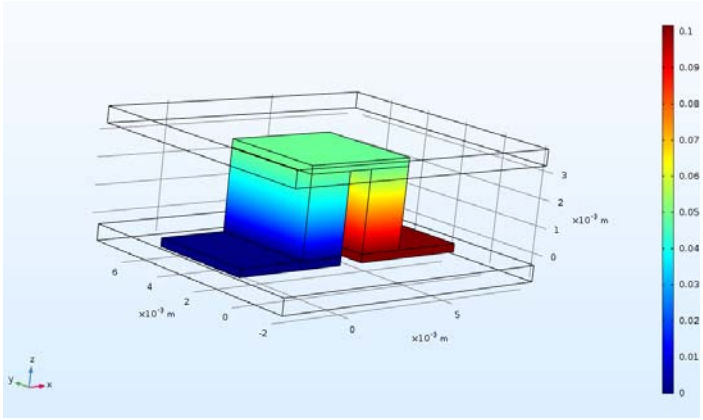

Fig.18.Electric potential distribution in thermoelement

The results of these calculations are presented in Figs.19 – 22.

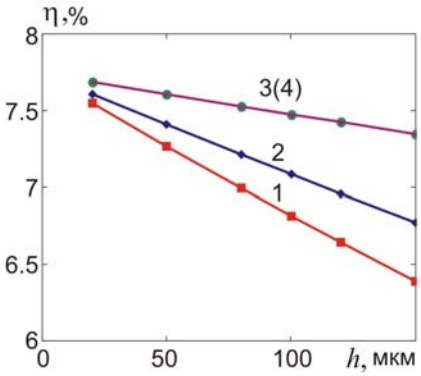

Fig.19. Dependence of generator module efficiency with the height of leg 3 mm on transient layer thickness for the case when contact resistance is considered to be a lumped parameter:1 – A=0, the distribution of metal atoms in transient layer is uneven; 2 – A=1, the distribution of metal atoms in transient layer is uneven; 3 – A=0, the distribution of metal atoms in transient layer is uniform;4 – A=1, the distribution of metal atoms in transient layer is uniform

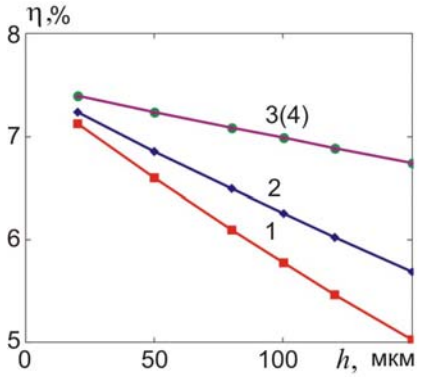

Fig.20. Dependence of generator module efficiency with the height of leg 1.5 mm on transient layer thickness for the case when contact resistance is considered to be a lumped parameter:1 – A=0, the distribution of atoms in transient layer is uneven; 2 – A=1, the distribution of metal atoms in transient layer is uneven; 3 – A=0, the distribution of metal atoms in transient layer is uniform;4 – A=1, the distribution of metal atoms in transient layer is uniform

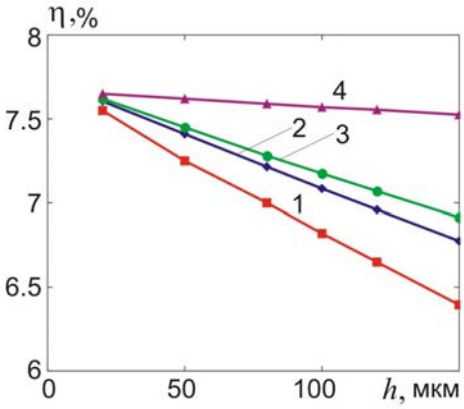

Fig.21. Dependence of generator module efficiency with the height of leg 3 mm on transient layer thickness for the case when transient layer is explicitly introduced into model:1 – A=0, the distribution of metal atoms in transient layer is uneven; 2 – A=1, the distribution of metal atoms in transient layer is uneven; 3 – A=0, the distribution of metal atoms in transient layer is uniform;4 – A=1, the distribution of metal atoms in transient layer is uniform

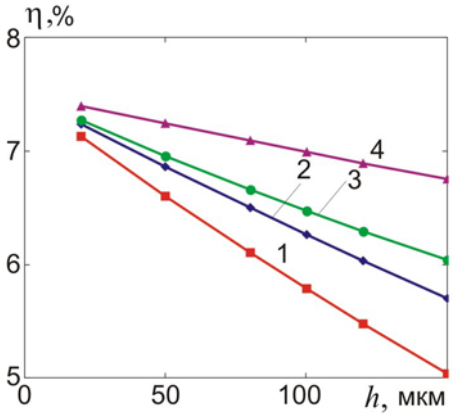

Fig.22. Dependence of generator module efficiency with the height of leg 1.5 mm on transient layer thickness for the case when transient layer is explicitly introduced into model:1 – A=0, the distribution of metal atoms in transient layer is uneven; 2 – A=1, the distribution of metal atoms in transient layer is uneven; 3 – A=0, the distribution of metal atoms in transient layer is uniform;4 – A=1, the distribution of metal atoms in transient layer is uniform

Note that in this case, just as in the absence of clusters in transient layer, its thermoEMF was considered to be zero.

It can be seen from the figures that in this case, just as in the absence of clusters, the efficiency of the thermoelement in the mode of electric energy generation is maximum when the distribution of metal atoms in transient layer is uniform. In addition, other things being equal, it is the greater, the greater the intensity of the source from which the metal enters transient layer. In the case of uneven distribution of metal atoms in transient layer, the efficiency decreases with increasing transient layer thickness the more, the smaller the height of the thermoelectric leg. However, the efficiency value is somewhat reduced as compared to the case when there are no clusters in transient layer. In general, in the considered range of thermoelectric leg heights and layer thicknesses, the efficiency changes from 5% to 7.5% when the contact layer is explicitly introduced into the model, and from 5 to 7.4% when the contact resistance is considered to be a lumped parameter. In the case when transient layer is introduced into model, the efficiency after levelling the distribution of metal atoms in transient layer essentially depends on the intensity of the source from which a steady-state diffusion of metal to TEM occurs.

Conclusions

1. With due regard for percolation effect, the temperature dependences of the electrical and thermal contact resistances, the thermoEMF, the power factor and the thermoelectric figure of merit of bismuth telluride-nickel transient contact layers were calculated on the assumption that carrier scattering in semiconductor and metal occurs on the deformation potential of acoustic phonons, the thermal conductivity of metal is determined by electron gas, and the lattice thermal conductivity of semiconductor – by phonon-phonon scattering with umklapp. In this case it was believed that nickel does not form new phases with bismuth telluride.
2. It is shown that both with uneven and uniform distribution of metal atoms in transient layer, the electrical and thermal contact resistances, the thermoEMF and the dimensionless thermoelectric figure of merit of transient layer are growing functions of temperature and the intensity of metal atoms entering transient layer during contact creation.
3. Power factor in the temperature range under study is a growing function of the intensity of metal atoms entering transient layer, and at the same time has a maximum on the temperature dependence in case of uneven distribution of metal atoms in transient layer. However, at low intensities of metal atoms entering transient layer it becomes a monotonically decreasing function of temperature in case of levelling the distribution of the concentration of metal atoms in transient layer.

4. In the case of uneven distribution of metal atoms in the temperature range of 200 – 400 K, the intensity of metal atoms entering transient layer, which corresponds to a change in parameter *A* from 0 to 1 and the thickness range of transient layer from 20 to 150 μm, the electrical contact resistance changes from $7 \cdot 10^{-7}$ to $1.9 \cdot 10^{-5}$ Ohm·cm^2, the thermal contact resistance – from 0.052 до 0.98 K·cm^2/W, the thermoEMF – from 155 to 235 μV/K, the power factor – from $4.2 \cdot 10^{-5}$ до $6.8 \cdot 10^{-5}$ W/(m·K^2), the dimensionless thermoelectric figure of merit – from 0.35 до 1.08.
5. After levelling the distribution of the concentration of metal atoms in transient layer, the electrical contact resistance decreases by a factor of 1.12 – 3.6, the thermal contact resistance decreases by a factor of 1.15 – 2.08, the thermoEMF is practically unvaried, the power factor increases by a factor of 1.19 – 2.79, the thermoelectric figure of merit grows maximum by a factor of 1.2 as compared to the case of uneven distribution.
6. Studies of the effect of transient contact layer with clusters on the efficiency of thermoelement in generation mode have shown that, all other things being equal, if the influence of the thermoEMF of transient layer is ignored, in the considered range of thermoelectric leg heights and layer thicknesses in the case when a contact layer is explicitly introduced into the model, the efficiency varies from 5 to 7.5%. However, if contact resistance is considered to be a lumped parameter, the efficiency changes from 5 to 7.4%. In the case when transient layer is introduced into the model, the efficiency after levelling the distribution of metal atoms in transient layer essentially depends on the intensity of the source from which steady diffusion of metal into TEM occurs, whereas in the case when contact resistance is considered to be a lumped parameter, this dependence is weak.

References

1. Anatychuk L.I. (2003). *Termoelektrichestvo. Tom 2. Termoelektricheskiie preobrazovateli energii [Thermoelectricity. Vol.2. Thermoelectric power converters]*. Chernivtsi: Institute of Thermoelectricity [in Russian].
2. Aswal D.K., Basu R., Singh A. (2016). Key issues in development of thermoelectric power generators: high figure-of-merit materials and their highly conducting interfaces with metallic interconnects. *Energy Convers. Manag*., 114, 50-67. http://refhub.elsevier.com/S2468-6069(18)30133-3/sref1
3. Anatychuk L.I., Kuz R.V. (2012). The energy and economic parameters of *Bi-Te* based thermoelectric generator modules for waste heat recovery. *J.Thermoelectricity*, 4, 7 5-82.
4. Drabkin I.A., Osvensky V.B., Sorokin A.I., Panchenko V.P., Narozhnaia O.E. (2017). Kontaktnoie soprotivleniie v sostavnykh termoelektricheskikh vetviakh [Contact resistance in composite thermoelectric legs]. *Fizika i Tekhnika Poluprovodnikov – Semiconductors,* 51(8), 1038-1040 [in Russian].
5. Alieva T.D., Barkhalov B.Sh., Abdinov D.Sh. (1995).). Struktura i elektricheskiie svoistva granits razdela kristallov $Bi_{0.5}Sb_{1.5}Te_3$ i $Bi_2Te_{2.7}Se_3$ s nekotorymi splavami [Structure and electrical properties of interfaces between $Bi_{0.5}Sb_{1.5}Te_3$ and $Bi_2Te_{2.7}Se_3$ crystals with certain alloys]. *Neorganicheskiie Materialy – Inorganic Materials*, 31 (2), 194-198.
6. Gupta Rahul P., Xiong K., White J.B., Cho Kyeongjae, Alshareef H.N., Gnade B.E. (2010). Low resistance ohmic contacts to Bi_2Te_3 using Ni and Co metallization. *Journal of the Electrochemical Society,* **157** (6), H666-H670. DOI: 10.1149/1.3385154
7. Gupta R.P., McCarty R., Sharp J. (2014). Practical contact resistance measurement method for bulk Bi_2Te_3 based thermoelectric devices. *J. El. Mat*., 43(6), 1608-1612.
8. Bublik V.T., Voronin A.I., Ponomarev V.F., Tabachkova N.Yu. (2012). Izmeneniie struktury prikontaknoi oblasti termoelektricheskikh materialov na osnove telluride vismuta pri povyshennykh temperaturakh

[Change in the structure of near-contact area of thermoelectric materials based on bismuth telluride at elevated temperatures]. *Izvestiia vysshykh uchebnykh zavedenii.* Materaily Elektronnoi Tekhniki - *News of Higher Educational Institutions.* Materials of Electronic Technique, 2, 17-20 [in Russian].

9. Zaiman G. (1982). *Models of disorder*. Moscow: Mir [Russian transl.]
10. Snarskii A.O., Zhenirovskii M.I., Bezsudnov I.V. (2006). The law of Wiedemann-Franz in thermoelectric composites. *J.Thermoelectricity*, 3, 59-65.
11. Klemens P.G. (1958). Lattice thermal conductivity. *Solid State Physics. Advances in Research and Applications. Vol.7.* New York: Academic Press Inc. Publishers.
12. Tikhonov A.N., Samarskiy A.A. (1972). *Uravneniia matematicheskoi fiziki [Mathematical physics equations]*. Moscow: Nauka [in Russian].
13. Goltsman B.M., Kudinov I.A., Smirnov I.A. (1972). *Poluprovodnikovyie termoelektricheskiie materaily na osnove Bi_2Te_3 [Semiconductor thermoelectric materials based on Bi_2Te_3]*. Moscow: Nauka [in Russian].
14. Lifshits E.M., Pitaevskii L.P. (1979). *Fizicheskaia kinetika [Physical kinetics]*. Moscow: Nauka [in Russian].

Submitted 11.06.2019

Горський П.В. *док. фіз.– мат. наук*[1,2]
Мицканюк Н.В.[1,2]

[1]Інститут термоелектрики НАН і МОН України,
вул. Науки, 1, Чернівці, 58029, Україна;
e-mail: anatych@gmail.com;
[2]Чернівецький національний університет
ім. Юрія Федьковича, вул. Коцюбинського 2,
Чернівці, 58000, Україна

ПРО ТЕМПЕРАТУРНІ ЗАЛЕЖНОСТІ ТЕРМОЕЛЕКТРИЧНИХ ХАРАКТЕРИСТИК ПЕРЕХІДНОГО ШАРУ ТЕЛУРИД ВІСМУТУ МЕТАЛ З УРАХУВАННЯМ ЯВИЩА ПЕРКОЛЯЦІЇ

Розрахунковим шляхом отримано основні співвідношення, які визначають температурні залежності термоелектричних характеристик перехідних контактних шарів термоелектричний матеріал-метал з урахуванням явища перколяції. Конкретні кількісні результати та графіки температурних залежностей електричного та теплового контактних опорів, термоЕРС, фактору потужності та безрозмірної термоелектричної ефективності перехідного контактного шару наведено для контактної пари телурид вісмуту – нікель. Встановлено, що у температурному інтервалі 200-400 К за умови збереження нерівномірного розподілу частинок металу у перехідному шарі і його товщини в діапазоні 20-150 мкм електричний контактний опір змінюється від $7\cdot10^{-7}$ до $1.9\cdot10^{-5}$ Ом·см^2, тепловий контактний опір – від 0.052 до 0.98 К·см^2/Вт, термоЕРС – від 155 до 235 мкВ/К, фактор потужності – від $4.2\cdot10^{-5}$ до $6.8\cdot10^{-5}$ Вт/(м·К^2), безрозмірна термоелектрична ефективність – від 0.35 до 1.08. Після вирівнювання концентрації електричний контактний опір спадає у 1.12 – 3.6 рази, тепловий контактний опір спадає у 1.15 – 2.08 рази, термоЕРС практично не змінюється, фактор потужності зростає у 1.19 – 2.79 рази, безрозмірна термоелектрична ефективність зростає максимально у 1.2 рази. Бібл. 14, рис. 22.

Ключові слова: контакт термоелектричний матеріал – метал, приконтактний перехідний шар, електричний контактний опір, тепловий контактний опір, термоЕРС, теорія протікання.

Горский П.В., *док. физ-мат. наук*[1,2]
Мыцканюк Н.В.[1,2]

[1]Институт термоэлектричества НАН и МОН Украины, ул. Науки, 1,
Черновцы, 58029, Украина, *e–mail: anatych@gmail.com;*
[2]Черновицкий национальный университет
им. Юрия Федьковича, ул. Коцюбинского, 2,
Черновцы, 58012, Украина

О ТЕМПЕРАТУРНОЙ ЗАВИСИМОСТИ ТЕРМОЭЛЕКТРИЧЕСКИХ ХАРАКТЕРИСТИК ПЕРЕХОДНОГО СЛОЯ ТЕЛЛУРИДА ВИСМУТА МЕТАЛЛ С УЧЕТОМ ЯВЛЕНИЯ ПЕРКОЛЯЦИИ

Расчетным путем получены основные соотношения, определяющие температурные зависимости термоэлектрических характеристик переходных контактных слоев термоэлектрический материал-металл с учетом явления перколяции. Конкретные количественные результаты и графики температурных зависимостей электрического и теплового контактных сопротивлений, термоЭДС, фактора мощности и безразмерной термоэлектрической эффективности переходного контактного слоя приведены для контактной пары теллурид висмута - никель. Установлено, что в температурном интервале 200-400 К при условии сохранения неравномерного распределения частиц металла в переходном слое и его толщины в диапазоне 20-150 мкм электрический контактное сопротивление меняется от $7 \cdot 10^{-7}$ до $1.9 \cdot 10^{-5}$ Ом · см2, тепловое контактное сопротивление - от 0.052 до 0.98 к·см^2/Вт, термоЭДС - от 155 до 235 мкВ/К, фактор мощности - от $4.2 \cdot 10^{-5}$ до $6.8 \cdot 10^{-5}$Вт/(м·К^2), безразмерная термоэлектрическая эффективность - от 0.35 до 1.08. После выравнивания концентрации электрический контактное сопротивление приходит в 1.12 - 3.6 раза, тепловой контактное сопротивление приходит в 1.15 - 2.08 раза, термоЭДС практически не меняется, фактор мощности возрастает в 1.19 - 2.79 раза, безразмерная термоэлектрическая эффективность возрастает максимально в 1.2 раза. Библ. 14, рис. 22.

Ключевые слова: контакт термоэлектрический материал – металл, приконтактный переходной слой, электрический контактное сопротивление, тепловой контактное сопротивление, термоЭДС, теория протекания.

References

1. Anatychuk L.I. (2003). *Termoelektrichestvo. Tom 2. Termoelektricheskiie preobrazovateli energii [Thermoelectricity. Vol.2. Thermoelectric power converters]*. Chernivtsi: Institute of Thermoelectricity [in Russian].
2. Aswal D.K., Basu R., Singh A. (2016). Key issues in development of thermoelectric power generators: high figure-of-merit materials and their highly conducting interfaces with metallic interconnects. *Energy Convers. Manag*., 114, 50-67. http://refhub.elsevier.com/S2468-6069(18)30133-3/sref1
3. Anatychuk L.I., Kuz R.V. (2012). The energy and economic parameters of *Bi-Te* based thermoelectric generator modules for waste heat recovery. *J.Thermoelectricity*, 4, 7 5-82.

4. Drabkin I.A., Osvensky V.B., Sorokin A.I., Panchenko V.P., Narozhnaia O.E. (2017). Kontaktnoie soprotivleniie v sostavnykh termoelektricheskikh vetviakh [Contact resistance in composite thermoelectric legs]. *Fizika i Tekhnika Poluprovodnikov – Semiconductors,* 51(8), 1038-1040 [in Russian].
5. Alieva T.D., Barkhalov B.Sh., Abdinov D.Sh. (1995).). Struktura i elektricheskiie svoistva granits razdela kristallov $Bi_{0.5}Sb_{1.5}Te_3$ i $Bi_2Te_{2.7}Se_3$ s nekotorymi splavami [Structure and electrical properties of interfaces between $Bi_{0.5}Sb_{1.5}Te_3$ and $Bi_2Te_{2.7}Se_3$ crystals with certain alloys]. *Neorganicheskiie Materialy – Inorganic Materials*, 31 (2), 194-198.
6. Gupta Rahul P., Xiong K., White J.B., Cho Kyeongjae, Alshareef H.N., Gnade B.E. (2010). Low resistance ohmic contacts to Bi_2Te_3 using Ni and Co metallization. *Journal of the Electrochemical Society,* **157** (6), H666-H670. DOI: 10.1149/1.3385154
7. Gupta R.P., McCarty R., Sharp J. (2014). Practical contact resistance measurement method for bulk Bi_2Te_3 based thermoelectric devices. *J. El. Mat*., 43(6), 1608-1612.
8. Bublik V.T., Voronin A.I., Ponomarev V.F., Tabachkova N.Yu. (2012). Izmeneniie struktury prikontaknoi oblasti termoelektricheskikh materialov na osnove telluride vismuta pri povyshennykh temperaturakh [Change in the structure of near-contact area of thermoelectric materials based on bismuth telluride at elevated temperatures]. *Izvestiia vysshykh uchebnykh zavedenii.* Materaily Elektronnoi Tekhniki - *News of Higher Educational Institutions.* Materials of Electronic Technique, 2, 17-20 [in Russian].
9. Zaiman G. (1982). *Models of disorder*. Moscow: Mir [Russian transl.]
10. Snarskii A.O., Zhenirovskii M.I., Bezsudnov I.V. (2006). The law of Wiedemann-Franz in thermoelectric composites. *J.Thermoelectricity*, 3, 59-65.
11. Klemens P.G. (1958). Lattice thermal conductivity. *Solid State Physics. Advances in Research and Applications. Vol.7.* New York: Academic Press Inc. Publishers.
12. Tikhonov A.N., Samarskiy A.A. (1972). *Uravneniia matematicheskoi fiziki [Mathematical physics equations]*. Moscow: Nauka [in Russian].
13. Goltsman B.M., Kudinov I.A., Smirnov I.A. (1972). *Poluprovodnikovyie termoelektricheskiie materaily na osnove Bi_2Te_3 [Semiconductor thermoelectric materials based on Bi_2Te_3]*. Moscow: Nauka [in Russian].
14. Lifshits E.M., Pitaevskii L.P. (1979). *Fizicheskaia kinetika [Physical kinetics]*. Moscow: Nauka [in Russian].

Submitted 11.06.2019

A. Snarskii *doc. phys.– math. science, professor*[1,2]**,**
P. Yuskevich[1]

A. Snarskii

[1]National Technical University of Ukraine "Igor Sikorsky Kyiv Polytechnic Institute", 37 Peremohy Ave., Kyiv, 03056 Ukraine *asnarskii@gmail.com*
[2]Institute of Information Registration Problems of the NAS of Ukraine, 2 Shpaka Str., 03113 Kyiv, Ukraine

P. Yuskevich

EFFECTIVE MEDIUM THEORY FOR THE THERMOELECTRIC PROPERTIES OF COMPOSITE MATERIALS WITH VARIOUS PERCOLATION THRESHOLDS

In the work, a modified effective medium theory is constructed for calculating the effective properties of thermoelectric composites with different values of percolation thresholds. It is shown that even at concentrations beyond the critical region, the threshold value is essential for determining the effective properties. Two fundamentally different cases of a set of local properties of the composite are considered. In one of these cases, the conductivity and thermal conductivity of one of the phases is simultaneously greater than the conductivity and thermal conductivity of the other phase. The second, anomalous case, when the electrical conductivity of the first phase (σ_1) is greater than that of the second, but the thermal conductivity of the first phase is less than that of the second, shows unusual concentration behavior of effective conductivity, i.e. with an increase in the well-conducting phase, the effective conductivity σ_e shows a decrease (rather than growth as in the standard case, see Fig. 1a), which at $p \approx \tilde{p}_c$ goes over to growth. Bibl. 5, Fig. 5.

Key words: thermoelectricity, percolation theory, percolation thresholds, composites, effective properties

Introduction

The calculation of effective values for composite materials is a complex problem that cannot be solved in the general case. Solutions are also possible as an exceptional case, for one-dimensional inhomogeneity, or for strictly periodic structures, for example, for spherical inclusions of one phase in the matrix of the other. Even in the case of simple-shaped inclusions, the solutions are rather bulky expressions of infinite series that are difficult to analyze [1 – 7].

To describe randomly inhomogeneous environment with randomly located inclusions of one phase in the other, there are approximate methods that allow one to approximately describe the concentration behavior of effective coefficients with different accuracy. For example, the Maxwell approximation [8] allows describing the concentration behavior of effective coefficients accurate to the first degree of concentration.

For the entire range of concentrations, a good approximation is the Bruggeman – Landauer approximation [9, 10], which is a self-consistency method (effective medium approximation).

The lack of the Bruggeman-Landauer approximation is the percolation threshold fixed in this approximation. With a large difference in the physical properties of the phases, for example, when the conductivity of the first phase σ_1 is much larger than that of the second $\sigma_2 \cdot (\sigma_1/\sigma_2) >> 1$, a sharp change in

the behavior of the effective conductivity σ_e with a change in the concentration of phases occurs when the concentration of the first phase σ_1 is equal to p_c=1/3. At the same time, the value of the percolation threshold p_c of real composites can be different depending on their structure, which is related to their fabrication technique.

In [11], a modification of the Bruggeman – Landauer approximation was presented, which allows one to specify any percolation threshold $\tilde{p}_c$ for the problem of calculating the effective conductivity.

The objective of this work is to modify the self-consistent approximation for calculating the effective thermoelectric properties of composites (Bruggeman-Landauer approximation for thermoelectric phenomena) and to show the influence of the assigned percolation threshold on the effective properties of two-phase thermoelectric composites.

The article is organized as follows: in the first section, we consider the Bruggeman-Landauer approximation and its modification based on [11]. In the second section, the system of thermoelectric equations is rewritten in a convenient form for constructing the Bruggeman-Landauer approximation and a modification of the approximation is proposed. From the obtained results it follows that the thermoelectric figure of merit, depending on the percolation threshold, has a maximum, which is an interesting consequence for experimental verification. In the third section, we present the calculation of effective properties in the "anomalous" case, where an unusual behavior of the effective conductivity is observed.

Modification of the Bruggeman-Landauer approximation in the effective conductivity problem

The Bruggeman-Landauer approximation can be written as

$$\frac{\sigma_e-\sigma_1}{2\sigma_e+\sigma_1}p+\frac{\sigma_e-\sigma_2}{2\sigma_e+\sigma_2}(1-\mathrm{p})=0\,, \tag{1}$$

where σ_1 is the first phase conductivity, σ_2 is the second phase conductivity.

The effective conductivity obtained from solution (1) describes well the entire concentration range. With greater inhomogeneity, at $\sigma_1/\sigma_2>>1$ close to concentration $p=p_c$=1/3 there is a sharp change in the concentration behavior of σ_e, which qualitatively describes the percolation behaviour (an analogue of the second-order phase transition). Naturally, such a "simple" approximation as (1) cannot completely describe percolation laws. For example, the critical indices σ_e close to p_c obtained from (1) [1, 11]. Their numerical value $t=q=1$ differs from the percolation (t=2 and q=0.73).

According to modification [11], the Bruggeman-Landauer approximation (1) is replaced by

$$\frac{\dfrac{\sigma_e-\sigma_1}{2\sigma_e+\sigma_1}}{1+c(p,\tilde{p}_c)\dfrac{\sigma_e-\sigma_1}{2\sigma_e+\sigma_1}}p+\frac{\dfrac{\sigma_e-\sigma_2}{2\sigma_e+\sigma_2}}{1+c(p,\tilde{p}_c)\dfrac{\sigma_e-\sigma_2}{2\sigma_e+\sigma_2}}(1-p)=0\,, \tag{2}$$

where $c(p,\tilde{p}_c)$, the Sarychev-Vinogradov term, is of the form

$$c(p,\tilde{p}_c)=(1-3\tilde{p}_c)\left(\frac{p}{\tilde{p}_c}\right)^{\tilde{p}_c}\left(\frac{1-p}{1-\tilde{p}_c}\right)^{1-\tilde{p}_c}\,, \tag{3}$$

and $\tilde{p}_c$ is the preassigned percolation threshold.

According to (2), $\sigma_e\ (p)$ at $h=\sigma_1/\sigma_2 \to 0$ close to $\tilde{p}_c$ has the same exponential behavior, as in the standard Bruggeman-Landauer approximation (1)

$$\sigma_e(p) \sim \sigma_1 \left(p - \tilde{p}_c\right)^t,\ \sigma_2 = 0,\ p > p_c,$$

$$\sigma_e(p) \sim \sigma_2 \left(\tilde{p}_c - p\right)^{-q},\ \sigma_1 = \infty,\ p < p_c, \tag{4}$$

where critical indices $t=1$ and $q=1$.

Modification of the Bruggeman-Landauer approximation for thermoelectric phenomena

In the case of thermoelectric phenomena we write the local relation between the electric current j, heat flux density q, temperature gradient $\nabla \mathrm{T}$ and electric field strength E in the form [8, 12]

$$\mathbf{j} = \sigma \mathbf{E} + \sigma\alpha(-\nabla T),$$

$$\frac{\mathbf{q}}{T} = \sigma\alpha \mathbf{E} + \kappa \frac{1+ZT}{T}(-\nabla T), \tag{5}$$

where σ,κ are electric conductivity and thermal conductivity, α is differential thermoEMF, and

$$ZT = \frac{\sigma\alpha^2}{\kappa} T, \tag{6}$$

thermoelectric figure of merit (the Ioffe number) Z multiplied by temperature.

Local kinetic coefficients σ, κ, α are coordinate-dependent and in the case of a two-phase composite take on the values σ_1, κ_1, α_1 in the first phase and σ_2, κ_2, α_2 - in the second.

The properties of composite as a whole are assigned by the effective kinetic coefficients relating by definition the volume average "currents" – electric $\mathbf{j}$ and thermal $\mathbf{q}$ to "forces" – electric field $\mathbf{E}$ and temperature gradient ∇T

$$\langle \mathbf{j} \rangle = \sigma_e \langle \mathbf{E} \rangle + \sigma_e \alpha_e \langle -\nabla \mathrm{T} \rangle,$$

$$\frac{\langle \mathbf{q} \rangle}{T} = \sigma_e \alpha_e \langle \mathbf{E} \rangle + \kappa_e \frac{1+Z_eT}{T} \langle -\nabla T \rangle, \tag{7}$$

where

$$Z_e = \frac{\sigma_e \alpha_e^{\,2}}{\kappa_e}.$$

Systems (5) and (7) can be written in matrix form, convenient for further consideration

$$\begin{pmatrix} \mathbf{j} \\ \langle \mathbf{q} \rangle / T \end{pmatrix} = \begin{pmatrix} \sigma & \sigma\alpha \\ \sigma\alpha & \kappa \dfrac{1+ZT}{T} \end{pmatrix} \begin{pmatrix} \langle \mathbf{E} \rangle \\ \langle -\nabla \mathrm{T} \rangle \end{pmatrix}. \tag{8}$$

Note that in this record, as it must be according to Onsager's principle [12, 13], the matrix of kinetic coefficients is symmetric. Similarly, for the effective values

$$\begin{pmatrix} \mathbf{j} \\ \dfrac{\langle \mathbf{q} \rangle}{T} \end{pmatrix} = \begin{pmatrix} \sigma_e & \sigma_e \alpha_e \\ \sigma_e \alpha_e & \kappa_e \dfrac{1+Z_e T}{T} \end{pmatrix} \begin{pmatrix} \langle \mathbf{E} \rangle \\ \langle -\nabla \mathrm{T} \rangle \end{pmatrix}. \tag{9}$$

Introduce a generalized current $\mathbf{i}$ and a generalized force $\mathbf{e}$

$$\mathbf{i} = \begin{pmatrix} \mathbf{j} \\ \langle \mathbf{q} \rangle / T \end{pmatrix}, \quad \mathbf{e} = \begin{pmatrix} \langle \mathbf{E} \rangle \\ \langle -\nabla \mathrm{T} \rangle \end{pmatrix}, \tag{10}$$

which are interrelated by the matrix of local kinetic coefficients $\hat{\Omega}$

$$\mathbf{i} = \hat{\Omega}\mathbf{e}, \qquad \hat{\Omega} = \begin{pmatrix} \sigma & \sigma\alpha \\ \sigma\alpha & \kappa \dfrac{1+ZT}{T} \end{pmatrix}, \tag{11}$$

and similarly for volume average currents and forces

$$\langle \mathbf{i} \rangle = \hat{\Omega}_e \langle \mathbf{e} \rangle. \tag{12}$$

In matrix notation, a self-consistent approximation of thermoelectric problem (analogue of the Bruggeman-Landauer equation) can be written as [2]

$$\frac{\hat{\Omega}_e - \hat{\Omega}_1}{2\hat{\Omega}_e + \hat{\Omega}_1} p + \frac{\hat{\Omega}_e - \hat{\Omega}_2}{2\hat{\Omega}_e + \hat{\Omega}_2}(1-p) = 0, \tag{13}$$

where expressions of the type $1/\left(2\hat{\Omega}_e + \hat{\Omega}_1\right)$ are understood as multiplying on the right by the inverse matrix.

Here, we (similarly to [11]) propose the following modification of a self-consistent approximation (13) for thermoelectric problem

$$\frac{\dfrac{\hat{\Omega}_e - \hat{\Omega}_1}{2\hat{\Omega}_e + \hat{\Omega}_1}}{1 + c(p, \tilde{p}_c)\dfrac{\hat{\Omega}_e - \hat{\Omega}_1}{2\hat{\Omega}_e + \hat{\Omega}_1}} p + \frac{\dfrac{\hat{\Omega}_e - \hat{\Omega}_2}{2\hat{\Omega}_e + \hat{\Omega}_2}}{1 + c(p, \tilde{p}_c)\dfrac{\hat{\Omega}_e - \hat{\Omega}_2}{2\hat{\Omega}_e + \hat{\Omega}_2}}(1-p) = 0. \tag{14}$$

Note at once that at $\tilde{p}_c = 1/3$ Eq.(14) goes over to standard approximation (13).

Fig.1 shows the concentration dependences of σ_e, κ_e, α_e, Z_eT for various $\tilde{p}_c$.

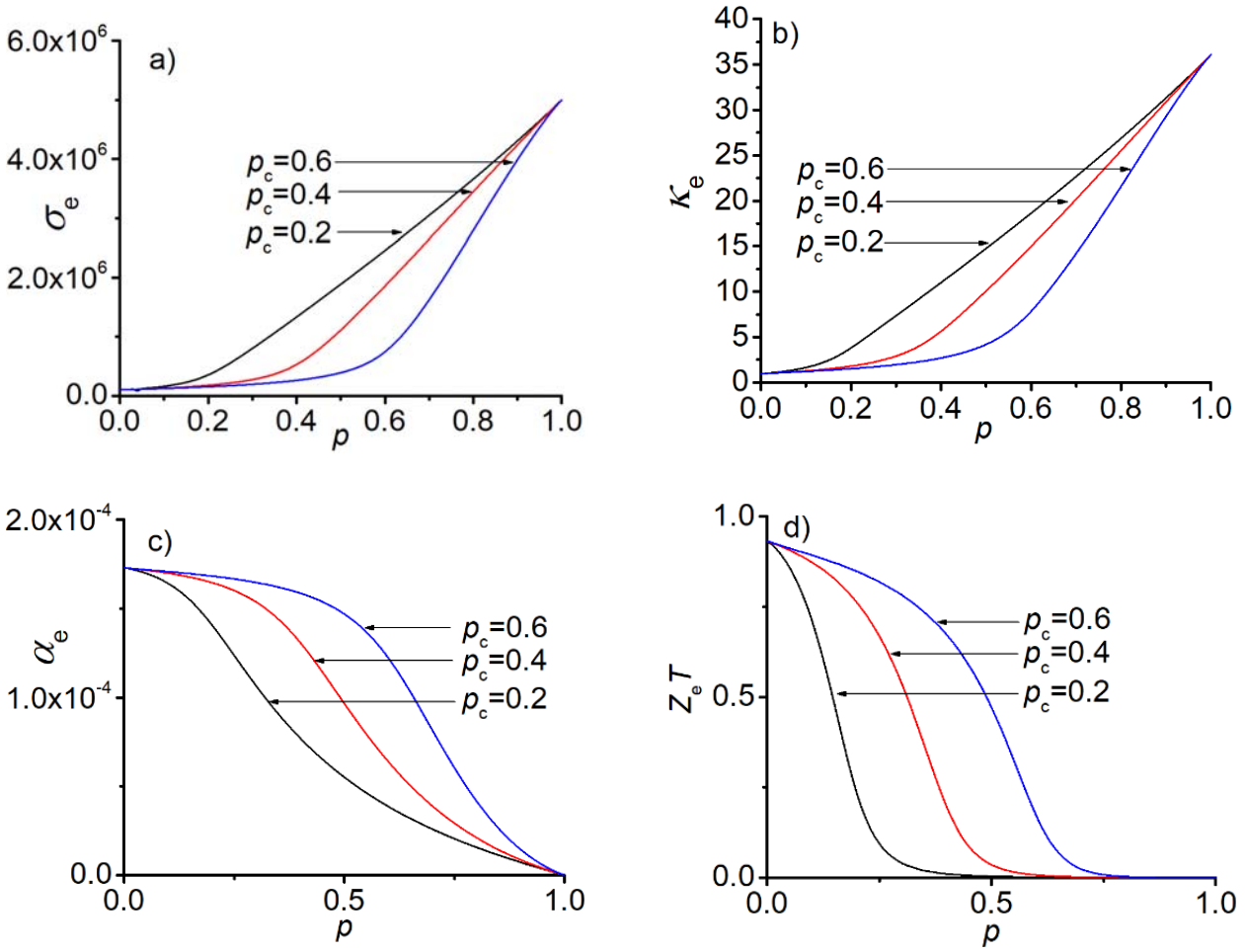

Fig. 1 Concentration dependences of effective conductivity, thermal conductivity, thermoEMF and figure of merit. The values of coefficients in the phases were selected [15]: for the first phase – $\sigma_1=5\cdot10^6$ *Ohm*$^{-1}$*m*$^{-1}$, $\kappa_1=36.1$ *W/(m·K)*, $\alpha_1=0$ *V/K*
for the second phase – $\sigma_2=10^5$ *Ohm*$^{-1}$*m*$^{-1}$, $\kappa_2=0.963$ *W/(m·K)*, $\alpha_2=173\cdot10^6$

As can be seen from Fig. 1, the effective conductivity increases with the addition of a better conductive phase, as it must be. Effective thermal conductivity behaves similarly. Accordingly, the effective thermoEMF decreases when a phase with a lower thermoEMF is added. It can also be seen from Fig. 1 that, for example, for effective conductivity, all lines behave identically, however, the region is shifted in which there is a sharp increase in conductivity, or, in other words, the percolation threshold is shifted. The thermoelectric figure of merit (the Ioffe number) decreases monotonically, as it must be, when the first phase with a lower thermoelectric figure of merit is added.

It can be strictly shown that in the case of $h_\sigma=\sigma_1/\sigma_2\to0$ and $h_\kappa=\kappa_1/\kappa_1\to0$, σ_e and κ_e either become equal to zero at $\sigma_2=0$ and $\kappa_2=0$ and $p\to\tilde{p}_c$, or diverge at $\sigma_1=\infty$ and $\kappa_1=\infty$ and $p\to\tilde{p}_c$.

As follows from (14), the values of effective coefficients at a given concentration p of the first phase depend on the percolation threshold of composite $\tilde{p}_c$. The closer concentration p to $\tilde{p}_c$, the more significant is this dependence, but even at lower concentrations, the difference occurs.

Fig. 2 shows the dependences of effective coefficients σ_e, κ_e, α_e, Z_eT on the value of $\tilde{p}_c$ for different values of p-concentration of the first phase.

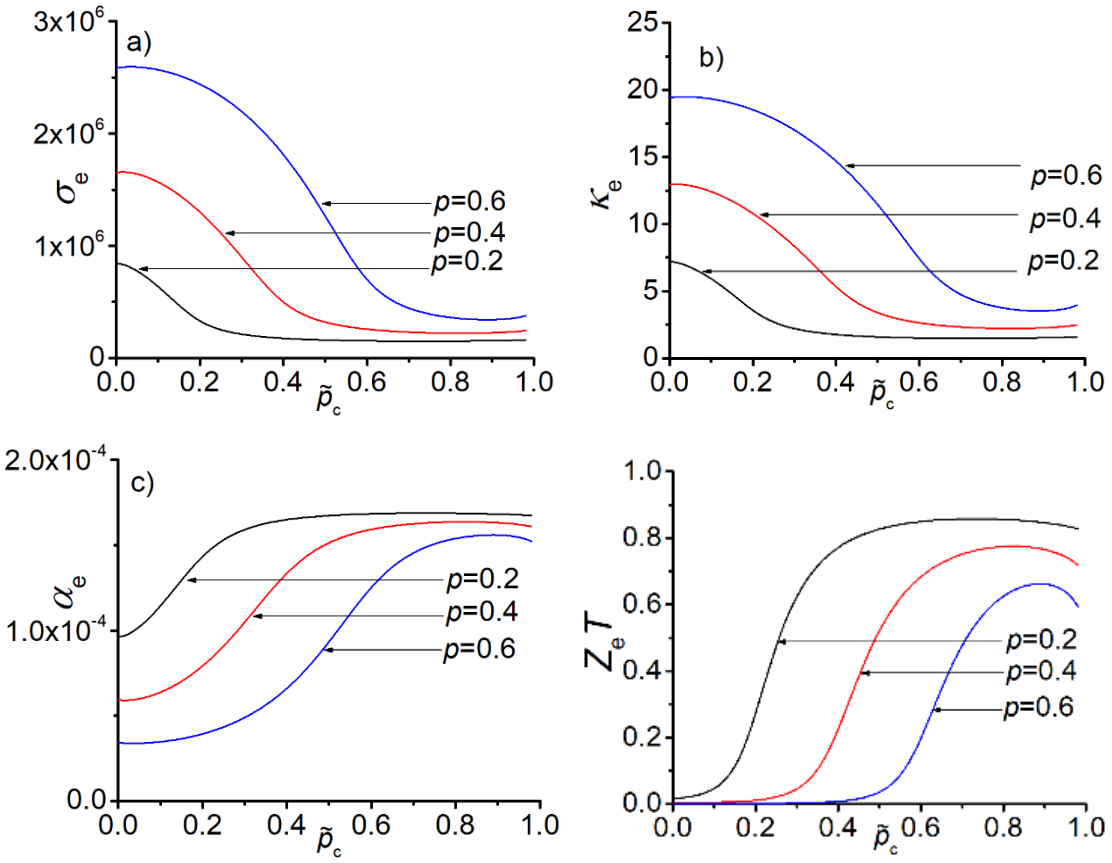

Fig. 2 Dependences of effective kinetic coefficients on the percolation threshold $\tilde{p}_c$ *at a given concentration p of the first phase. The values of coefficients in the phases were selected the same as in Fig. 1.*

Fig. 2 shows that the value of effective conductivity, at a given concentration, decreases with increasing the threshold $\tilde{p}_c$. The effective thermal conductivity behaves similarly. It is also noteworthy that, at a given concentration, with increasing the threshold $\tilde{p}_c$, the thermoelectric figure of merit (the Ioffe number) also increases, but at large $\tilde{p}_c$ the maximum is noticeable and the growth changes to a small drop. It would be interesting to verify the existence of such a maximum experimentally and to determine whether this maximum is an "artifact" of our modification.

Modification of the Bruggeman-Landauer approximation for thermoelectric phenomena in the "anomalous" case

Correction (3) introduced in the Bruggeman-Landauer approximation (2) suggests that the conductivity of the first phase is greater than the conductivity of the second phase $\sigma_1 > \sigma_2$. In this case, at $\tilde{p}_c$ given in (3), the percolation threshold that can be found when solving (2) will be equal to the preassigned $p_c = \tilde{p}_c$. Subject to the inverse inequality $\sigma_2 > \sigma_1$, correction (3) should be changed.

At $\alpha_1 = \alpha_{e2} = 0$, i.e. in the absence of thermoelectric phenomena, the effective medium approximations (13) or (14) are divided into two independent – one for electric conductivity, the other – for thermal conductivity. In the case when $\sigma_1 > \sigma_2$ and $\kappa_1 > \kappa_2$ these independent equations includes the same correction $c(p, \tilde{p}_c)$. However, in the opposite case, when $\sigma_1 > \sigma_2$, but $\kappa_1 > \kappa_2$, corrections for σ_e and κ_e

should be different. In the general case, when $\alpha_1 \neq \alpha_2$, this difference remains and modification (13) (14) assumes a more complex form.

$$\frac{\frac{\hat{\Omega}_e - \hat{\Omega}_1}{2\hat{\Omega}_e + \hat{\Omega}_1}}{1 + \hat{C}(p, \tilde{p}_c)\frac{\hat{\Omega}_e - \hat{\Omega}_1}{2\hat{\Omega}_e + \hat{\Omega}_1}} p + \frac{\frac{\hat{\Omega}_e - \hat{\Omega}_2}{2\hat{\Omega}_e + \hat{\Omega}_2}}{1 + \hat{C}(p, \tilde{p}_c)\frac{\hat{\Omega}_e - \hat{\Omega}_2}{2\hat{\Omega}_e + \hat{\Omega}_2}}(1-p) = 0, \tag{15}$$

where

$$\hat{C}(p, \tilde{p}_c) = \begin{pmatrix} c_\sigma(p, \tilde{p}_c) & 0 \\ 0 & c_\kappa(p, \tilde{p}_c) \end{pmatrix}, \tag{16}$$

and corrections $c_\sigma(p, \tilde{p}_c)$ and $c_\kappa(p, \tilde{p}_c)$ in (16), depending on the ratios σ_1 / σ_2 и κ_1 / κ_2 are of different form. In the case when $\sigma_1 > \sigma_2$ and $\kappa_1 < \kappa_2$ the correction $c_\sigma(p, \tilde{p}_c)$ remains the same – (3), and $c_\kappa(p, \tilde{p}_c)$ is given by

$$c_\kappa(p, \tilde{p}_c) = [1 - 3(1 - \tilde{p}_c)]\left(\frac{p}{\tilde{p}_c}\right)^{\tilde{p}_c}\left(\frac{1-p}{1-\tilde{p}_c}\right)^{1-\tilde{p}_c}. \tag{17}$$

Fig. 3 shows the concentration dependences of σ_e, κ_e, α_e, Z_eT for different values of percolation threshold.

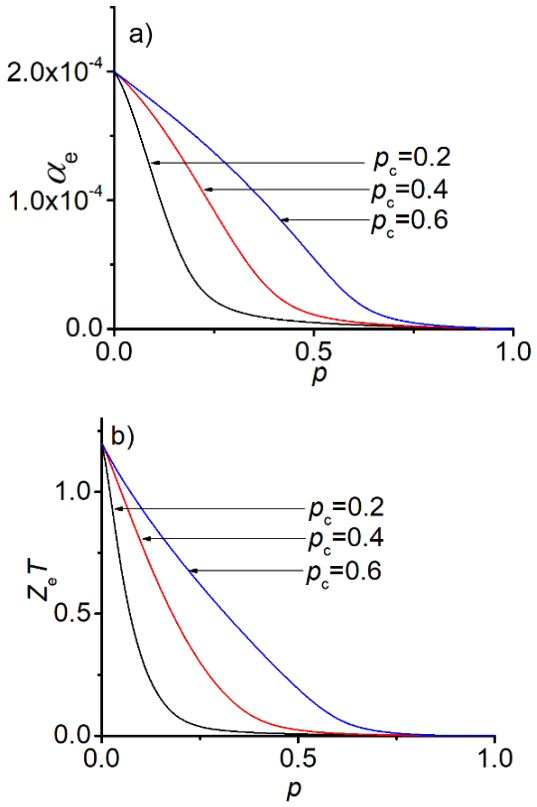

Fig. 3. Dependences of effective thermoEMF and figure of merit on the concentration p of the first phase at a given percolation threshold $\tilde{p}_c$. The values of coefficients in the phases were selected the same as in Fig. 1.

One of such materials for which the Wiedemann-Franz law – high conductivity, but low thermal conductivity - is violated significantly, is described in [16].
Fig.4 shows the dependences of effective properties on the value of percolation threshold.

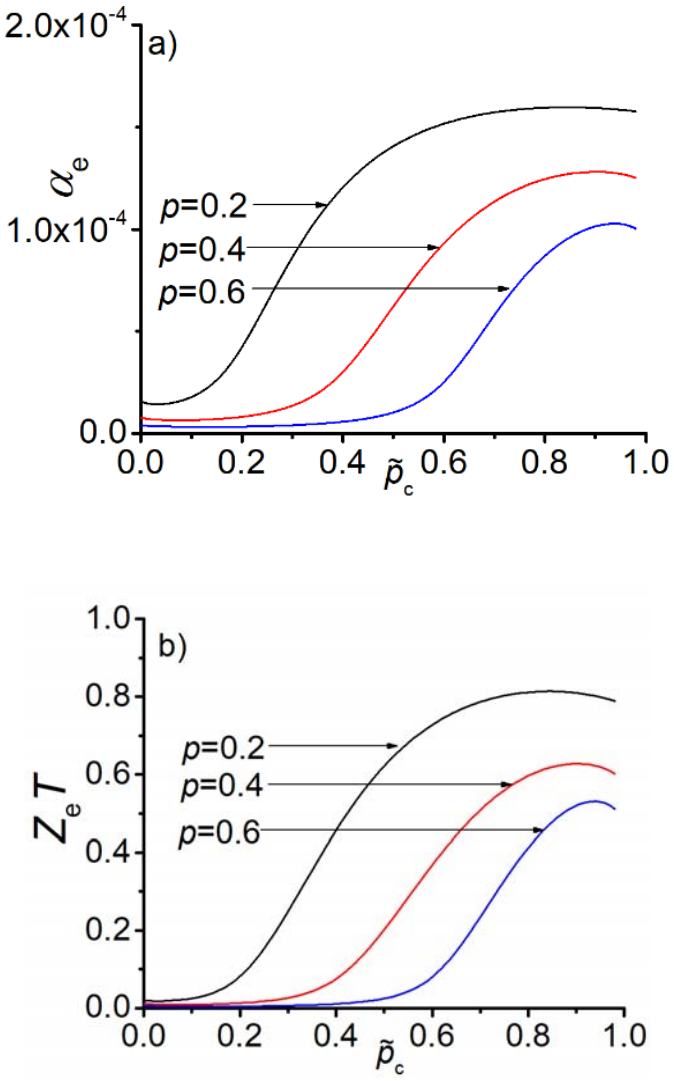

Fig. 4. Dependences of effective thermoEMF and figure of merit on the percolation threshold $\tilde{p}_c$ at a given concentration p of the first phase. The values of coefficients in the phases were elected the same as in Fig. 1.

Just as in the usual case, the effective figure of merit has a maximum.

Discussion

The figure below shows the dependences of effective conductivity and thermal conductivity on the concentration and percolation threshold in the "anomalous" case. It should be noted that effective conductivity has an unusual behavior: when a phase with good conductivity is added, effective conductivity first decreases, and then begins to grow. It seems interesting to experimentally verify whether this is a defect in the theory, or whether such conductivity is actually observed in real composites.

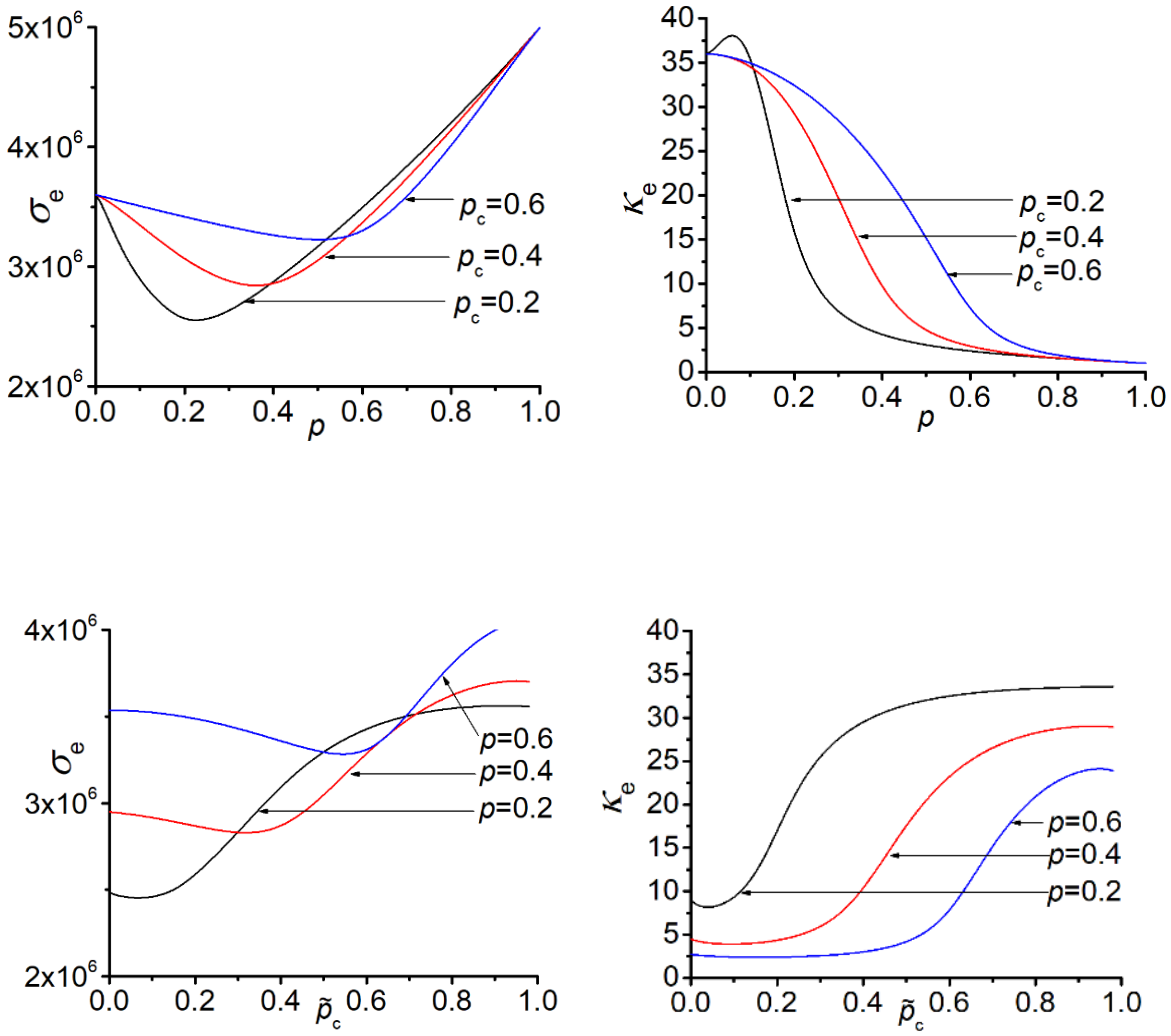

Fig. 5. Dependences of effective thermoEMF and figure of merit on the percolation threshold $\tilde{p}_c$ at a given concentration p of the first phase.

The values of coefficients in the phases were selected the same in Fig.1.

Conclusions

This paper considers a modification of effective medium theory (self-consistency method) for thermoelectric phenomena in the case of a preassigned percolation threshold. Such a modification was first proposed in [11] for the description of galvanomagnetic phenomena and was used for the description of a series of experimental results [9-11,17]. In [18], the modification was used in the proposed approach of "mobile percolation threshold" to describe the magnetodielectric effect and the peculiarities of magnetic permeability of magnetoelastomers, in [19,20], to describe a gigantic magnetoelastic effect.

A similar modification is proposed here for a system of equations describing thermoelectric phenomena in macroscopically inhomogeneous two-phase composites.

The results obtained can be used for the description of thermoelectric properties of composites with different structures corresponding to different percolation thresholds.

References

1. Torquato S. (2002). *Random heterogeneous materials. Microstructure and macroscopic properties.* New York: Springer Verlag. doi: 10.1115/1.1483342
2. Balagurov B.Ya. (2015). *Elektrofizicheskiie svoistva kompozitov [Electrophysical properties of composites]*. Moscow: Lenand [in Russian].
3. Choy T.C. (2016). *Effective medium theory: principles and applications. Oxford:* Oxford University Press. doi:10.1093/acprof:oso/9780198705093.001.0001
4. Andrianov I.V., Awrejcewicz J., Danishevskyy V.V. (2018). *Asymptotical mechanics of composites.* Cham, Germany: Springer. doi: 10.1007/978-3-319-65786-8
5. Andrianov I.V., Awrejcewicz J., Starushenko G.A. (2017). Asymptotic models and transport properties of densely packed, high-contrast fibre composites. Part I: Square lattice of circular inclusions. *Compos. Struct.*, *179*, 627. doi: 10.1016/j.compstruct.2017.07.070
6. Andrianov I.V., Awrejcewicz J., Starushenko G.A. (2017). Asymptotic models for transport properties of densely packed, high-contrast fibre composites. Part II: Square lattices of rhombic inclusions and hexagonal lattices of circular inclusions. *Compos. Struct.*,180, 359. doi: 10.1016/j.compstruct.2017.07.068
7. Snarskii A., Bezsudnov I.V., Sevryukov V.A., Morozovskiy A., Malinsky J. (2016). *Transport processes in macroscopically disordered media. From mean field theory to percolation.* New York: Springer Verlag. doi: 10.1007/978-1-4419-8291-9
8. Landau L. D., Lifshitz E. M. (1984). *Electrodynamics of continuous media. 2 ed*. Oxford: Butterworth-Heinemann.
9. Bruggeman V.D. (1935). Berechnung verschiedener physikalischer Konstanten von heterogenen Substanzen. I. Dielektrizitätskonstanten und Leitfähigkeiten der Mischkörper aus isotropen Substanzen. *Ann. Phys*. *(Leipzig)*, *416*, 664. doi: 10.1002/andp.19354160705
10. Landauer R. (1952). The electrical resistance of binary metallic mixtures. *J. Appl. Phys. 23*, 784. doi:10.1063/1.1702301
11. Sarychev A.K., Vinogradov A.P. (1983). Effective medium theory for the magnetoconductivity tensor of disordered material. *phys. stat. sol. (b)*, *117*, K113-K118. doi: 10.1002/pssb.2221170252
12. Samoilovich A.G. (2007). *Termoelektricheskiie i termodinamicheskiie metody prevrashcheniia energii [Thermoelectric and thermodynamic power conversion methods]*. Moscow: LKI (URSS) [in Russian].
13. Nye J.F. (964). Physical properties of crystals. Oxford: Clarendon Press.
14. Webmann I., Jortner J.,Cohen M. H. (1977). *Phys.Rev. B*, 16, 6, 2959.
15. Rowe D. M. (2006). *Thermoelectrics Handbook (Macro to Nano)*. Boca-Raton: Taylor Francis.
16. Lee S., Hippalgaonkar K., Yang F., Hong J., Ko C., Suh J., Liu K., Wang K., Urban J. J., Zhang X., Dames C., Hartnoll S. A., Delaire O., Wu J. (2017). *Science*, 355, 371.
17. Bergman D. J. (1978). The dielectric constant of a composite material—a problem in classical physics. *Phys. Rep.,* 43, 9, 407.
18. Snarskii A., Zorinets D., Shamonin M., Kalita V. (2019). Theoretical method for calculation of effective properties of composite materials with reconfigurable microstructure: electric and magnetic phenomena. *Phys. A: Stat. Mech. Appl. 535*, 122467. doi: 10.1016/j.physa.2019.122467
19. Snarskii A., Shamonin M., Yuskevich P. (2020). Colossal magnetoelastic effects in magnetoactive elastomers. arxiv: 2002.11762.
20. Snarskii A., Shamonin M., Yuskevich P. (2020). Effective medium theory for the elastic properties of composite materials with various percolation thresholds. *Materials,* 13, 1243.

Submitted 14.06.2019

А. Снарський *док. фіз.-мат. наук, професор*[1,2],
П. Юськевич[1]

[1]Національний технічний університет України
"Київський політехнічний інститут імені Ігоря Сікорського",
проспект Перемоги 37, 03056 Київ, Україна,
asnarskii@gmail.com
[2]Інститут проблем реєстрації інформації НАН України,
вул. Н. Шпака 2, 03113 Київ, Україна

ТЕОРІЯ СЕРЕДНЬОГО ПОЛЯ ДЛЯ ТЕРМОЕЛЕКТРИЧНИХ ВЛАСТИВОСТЕЙ КОМПОЗИТНИХ МАТЕРІАЛІВ З РІЗНИМИ ПОРОГАМИ ПРОТІКАННЯ

В роботі побудовано модифіковану теорію ефективного середовища для обчислень ефективних кінетичних коефіцієнтів термоелектричних композитів з різними значеннями порогів протікання. Показано, що навіть за концентрацій поза критичною областю величина порогу істотна для визначення ефективних властивостей. Розглянуто два принципово різних випадки набору локальних властивостей композиту. Один з них, коли провідність і теплопровідність однієї з фаз одночасно більша за провідність та теплопровідність другої фази. Другий, аномальний випадок, коли електропровідність першої фази (σ_1) більша від другої, але теплопровідність першої фази менша від другої, показує незвичайну концентраційну поведінку ефективної провідності, тобто при зростанні частки добре провідної фази ефективна провідність σ_e демонструє зменшення, а не зростання як у стандартному випадку,(див. рис.1а), яке при $p \approx \tilde{p}_c$ переходить в зростання. Бібл. 5, рис. 5.

Ключові слова: термоелектрика, теорія протікання, поріг протікання, композити, ефективні властивості.

А. Снарский *док. физ.-мат. наук, профессор*[1,2],
П. Юськевич[1]

[1]Национальный технический университет Украины
“Киевский политехнический институт имени Игоря Сикорского”,
проспект Победы 37, 03056 Киев, Украина,
asnarskii@gmail.com
[2]Институт проблем регистрации информации НАН Украины,
ул. Н. Шпака 2, 03113 Киев, Украина

ТЕОРИЯ СРЕДНЕГО ПОЛЯ ДЛЯ ТЕРМОЭЛЕКТРИЧЕСКИХ СВОЙСТВ КОМПОЗИТНЫХ МАТЕРИАЛОВ С РАЗЛИЧНЫМИ ПОРОГАМИ ПРОТЕКАНИЯ

В работе построена модифицированная теория эффективной среды для вычислений эффективных свойств термоэлектрических композитов с различными значениями порогов протекания. Показано, что даже при концентрациях вне критической области величина порога существенна для определения эффективных свойств. Рассмотрены два принципиально разных случая набора локальных свойств композита. Один из них, когда проводимость и теплопроводность одной из фаз одновременно больше проводимости и теплопроводности второй фазы. Второй, аномальный случай, когда электропроводность первой фазы (σ_1) больше второй, но теплопроводность первой фазы меньше второй, показывает необычные концентрационное поведение эффективной проводимости, т.е. при возрастании хорошо проводящей фазы эффективная проводимость α_e показывает падение (а не рост как в стандартном случаем, см. рис.1а), которое при $p \approx \tilde{p}_c$ переходит в рост. Библ. 5, рис. 5.

Ключевые слова: термоэлектричество, теория протекания, порог протекания, композиты, эффективные свойства.

References

1. Torquato S. (2002). *Random heterogeneous materials. Microstructure and macroscopic properties.* New York: Springer Verlag. doi: 10.1115/1.1483342
2. Balagurov B.Ya. (2015). *Elektrofizicheskiie svoistva kompozitov [Electrophysical properties of composites]*. Moscow: Lenand [in Russian].
3. Choy T.C. (2016). *Effective medium theory: principles and applications. Oxford:* Oxford University Press. doi:10.1093/acprof:oso/9780198705093.001.0001
4. Andrianov I.V., Awrejcewicz J., Danishevskyy V.V. (2018). *Asymptotical mechanics of composites.* Cham, Germany: Springer. doi: 10.1007/978-3-319-65786-8
5. Andrianov I.V., Awrejcewicz J., Starushenko G.A. (2017). Asymptotic models and transport properties of densely packed, high-contrast fibre composites. Part I: Square lattice of circular inclusions. *Compos. Struct.*, *179*, 627. doi: 10.1016/j.compstruct.2017.07.070
6. Andrianov I.V., Awrejcewicz J., Starushenko G.A. (2017). Asymptotic models for transport properties of densely packed, high-contrast fibre composites. Part II: Square lattices of rhombic inclusions and hexagonal lattices of circular inclusions. *Compos. Struct.*,180, 359. doi: 10.1016/j.compstruct.2017.07.068
7. Snarskii A., Bezsudnov I.V., Sevryukov V.A., Morozovskiy A., Malinsky J. (2016). *Transport processes in macroscopically disordered media. From mean field theory to percolation.* New York: Springer Verlag. doi: 10.1007/978-1-4419-8291-9
8. Landau L. D., Lifshitz E. M. (1984). *Electrodynamics of continuous media. 2 ed*. Oxford: Butterworth-Heinemann.
9. Bruggeman V.D. (1935). Berechnung verschiedener physikalischer Konstanten von heterogenen Substanzen. I. Dielektrizitätskonstanten und Leitfähigkeiten der Mischkörper aus isotropen Substanzen. *Ann. Phys*. *(Leipzig)*, *416*, 664. doi: 10.1002/andp.19354160705
10. Landauer R. (1952). The electrical resistance of binary metallic mixtures. *J. Appl. Phys. 23*, 784. doi:10.1063/1.1702301
11. Sarychev A.K., Vinogradov A.P. (1983). Effective medium theory for the magnetoconductivity tensor of disordered material. *phys. stat. sol. (b)*, *117*, K113-K118. doi: 10.1002/pssb.2221170252
12. Samoilovich A.G. (2007). *Termoelektricheskiie i termodinamicheskiie metody prevrashcheniia energii [Thermoelectric and thermodynamic power conversion methods]*. Moscow: LKI (URSS) [in Russian].
13. Nye J.F. (964). Physical properties of crystals. Oxford: Clarendon Press.
14. Webmann I., Jortner J.,Cohen M. H. (1977). *Phys.Rev. B*, 16, 6, 2959.
15. Rowe D. M. (2006). *Thermoelectrics Handbook (Macro to Nano).* Boca-Raton: Taylor Francis.

16. Lee S., Hippalgaonkar K., Yang F., Hong J., Ko C., Suh J., Liu K., Wang K., Urban J. J., Zhang X., Dames C., Hartnoll S. A., Delaire O., Wu J. (2017). *Science*, 355, 371.
17. Bergman D. J. (1978). The dielectric constant of a composite material—a problem in classical physics. *Phys. Rep.,* 43, 9, 407.
18. Snarskii A., Zorinets D., Shamonin M., Kalita V. (2019). Theoretical method for calculation of effective properties of composite materials with reconfigurable microstructure: electric and magnetic phenomena. *Phys. A: Stat. Mech. Appl. 535*, 122467. doi: 10.1016/j.physa.2019.122467
19. Snarskii A., Shamonin M., Yuskevich P. (2020). Colossal magnetoelastic effects in magnetoactive elastomers. arxiv: 2002.11762.
20. Snarskii A., Shamonin M., Yuskevich P. (2020). Effective medium theory for the elastic properties of composite materials with various percolation thresholds. *Materials,* 13, 1243.

Submitted 14.06.2019

A.V. Prybyla, *cand. phys. - math. sciences*[1,2]
A.M. Kibak[1,2]


A.V. Prybyla

[1]Institute of Thermoelectricity
of the NAS and MES of Ukraine,
e-mail: anatych@gmail.com
1, Nauky str., Chernivtsi, 58029, Ukraine;
[2]Yu.Fedkovych Chernivtsi National University,
2, Kotsiubynskyi str., Chernivtsi, 58000, Ukraine


A.M. Kibak

EXPERIMENTAL STUDY OF A THERMOELECTRIC COOLING MODULE FOR AN X-RAY DETECTOR

The paper presents the results of experimental studies of a thermoelectric multistage thermoelectric cooling module for X-ray detectors. A specialized bench was developed, a thermoelectric cooling module was manufactured, and a series of its studies was conducted under conditions simulating its operation as part of an X-ray detector. Bibl. 6, Fig. 3.
Key words: experimental study, thermoelectric cooling, X-ray detector.

Introduction

General characterization of the problem. Thermoelectric cooling is rather widely used to assure the necessary operating temperature of various radiation detectors [1 – 3]. The detector device, arranged on the heat-absorbing surface of thermoelectric cooling module, as a rule, is mounted into a sealed housing, the basis of which is in good thermal contact with the heat exchanger.

Single-stage thermoelectric modules are used for shallow cooling of radiation sensors to ~ 250 K. Two-stage thermoelectric coolers (TEC) are used to cool sensors to operating temperature 230 K, three-stage TEC – to temperature of 210 K, four-stage TEC – to temperature of 190 K [3]. Such converters offer a number of advantages, including small size, durability, high reliability, and up to 20 years of service life.

In [6], a computer-aided design of a four-stage thermoelectric cooling module was performed to provide the temperature and thermal conditions for the operation of an X-ray detector.

The purpose of this work is to experimentally verify the results of simulating a thermoelectric multistage cooler for an X-ray detector.

TEC design

As a result of computer design and optimization, the structure of thermoelectric cooler for an X-ray detector was developed (Fig.1) which comprises 4 stages with 6, 12, 27 and 65 pairs of legs (with dimensions 0.6 x 0.6 x 1.8 mm^3) of thermoelectric material based on n- and p-type bismuth telluride (Bi_2Te_3) with the overall dimensions 12 x 16 x 12 mm^3. The size of cooled area is 4 x 8 mm. Electric insulating plates are made of aluminum oxide (Al_2O_3) 0.5 mm thick, electric interconnects – of copper (Cu) with anti-diffusion nickel layer (Ni) 0.1 mm thick.

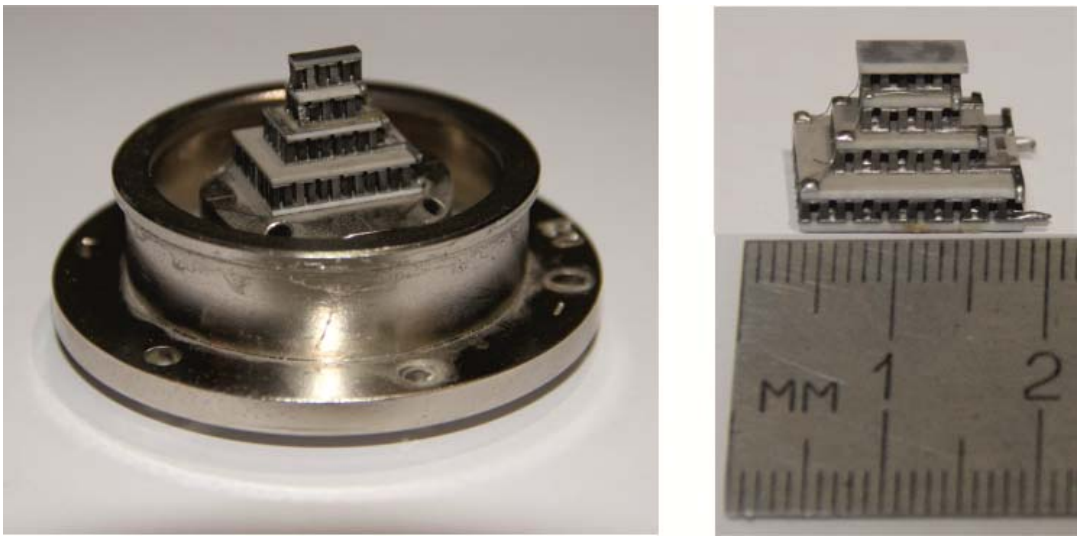

Fig. 1. Appearance of thermoelectric cooling module for an X-ray radiation detector

To conduct experimental studies of thermoelectric multi-stage cooler of X-ray detectors, special measuring bench was developed for maximum reproduction of its operating modes (Fig.2).

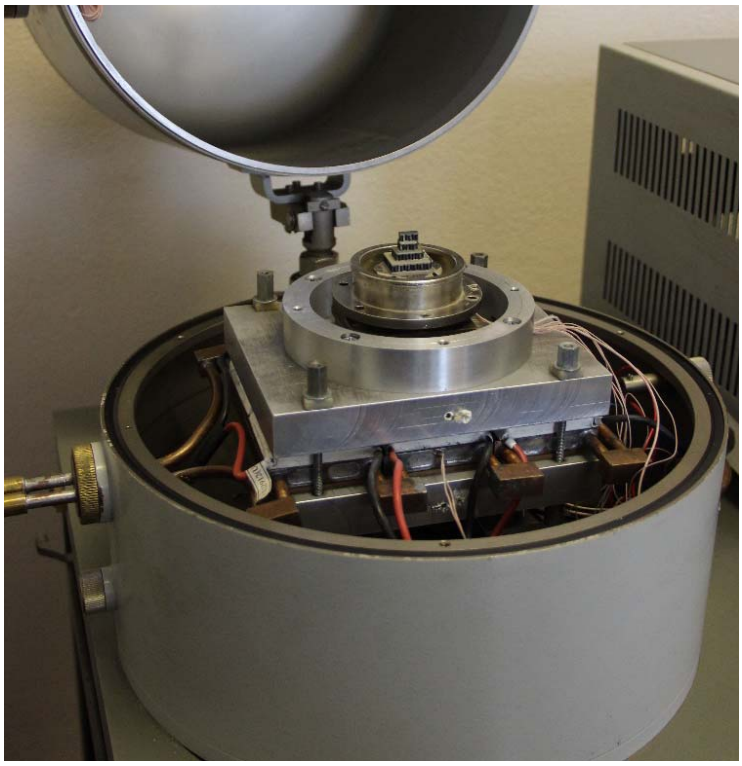

Fig. 2.Appearance of thermoelectric cooling module for an X-ray radiation detector

The bench consists of a vacuum post for reproduction of medium inside an X-ray detector, a thermoelectric multi-stage cooling module proper, a thermal load simulating furnace, a system for heat

removal and a set of measuring thermocouples.

Results of experimental studies

Measuring process took place in vacuum, electric power to thermoelectric module was supplied by means of special thermal leads. On the upper surface of the thermoelectric module (the cold side of the thermoelectric module on which the X-ray detector is located), a heat flow simulator furnace was placed. The measurements were carried out using special thermocouples (chromel-kopel thermocouples).

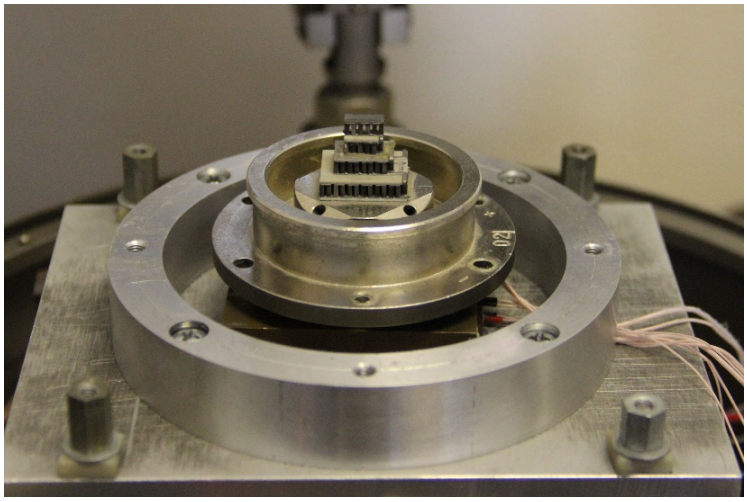

Fig. 3. Appearance of thermoelectric cooling module in measuring bench

During measurement, the main results of designing thermoelectric cooling module for an X-ray detector have been confirmed:

- maximum temperature difference ΔT_{max} = 102 K at detector base temperature T_c=-70 °C;
- electric power W=3 W;
- coefficient of performance ε ≈ 0.018.

The results obtained prove the possibilities of using thermoelectric coolers for assuring temperature and thermal conditions for X-ray radiation detectors and outperform the well-known world analogs.

Conclusions

1. A thermoelectric cooler of an X-ray detector was manufactured comprising 4 stages of Bi_2Te_3 thermoelectric material with overall dimensions 12 x 16 x 12 mm while assuring cooled area 4 x 8 mm.
2. A special bench was developed and a series of measurements of the parameters of thermoelectric cooling module for an X-ray detector was carried out.
3. The electric power of thermoelectric converter $W = 3$ W was measured, which at the coefficient of performance $\varepsilon = 0.018$ assures the detector base temperature $T_c^{(1)}$ = -70 °C and ΔT_{max} = 102 K.
4. The measurements in general repeat the results of computer-aided design of the thermoelectric cooling module for X-ray detectors and confirm that the developed TEC outperforms the well-known world analogs.

References

1. Rogalski A. (2012). Progress in focal plane arrays technologies. *Progress in Quantum Electronics*, 36, 342–473.
2. Piotrowski A., Piotrowski J., Gawron W., Pawluczyk J. and Pedzinska M. (2009). Extension of usable spectral range of Peltier cooled photodetectors. *ACTA Physica Polonica A*, 116, 52 – 55.
3. Anatychuk L.I., Vikhor L.N. (2013). The limits of thermoelectric cooling for photodetectors. *J. Thermoelectricity*, 5, 54-58.
4. Buhay O.M., Drozdenko M.O., Storizhko V.Yu. (2014). Microanalytical X-ray facility in IAP NASU. *Nanotechnology and Nanomaterials, Book of Abstracts*. Lviv.
5. Broerman E.C., Keyser R.M., Twomey T.R., Upp D.L. *A new cooler for HPGe detector systems*. ORTEC, PerkinElmer Instruments, Inc Oak Ridge TN 37831-0895 USA.
6. Anatychuk L.I., Prybyla A.V. (2019). Design of thermoelectric cooling module for X-ray radiation detector. *J.Thermoelectricity*, 2, 53 – 58.

Submitted 20.06.2019

Прибила А.В., *канд. фіз.-мат. наук*[1,2]
Кібак А.М.

[1]Інститут термоелектрики НАН і МОН України,
вул. Науки, 1, Чернівці, 58029, Україна;
e–mail: anatych@gmail.com;
[2]Чернівецький національний університет
ім. Юрія Федьковича, вул. Коцюбинського 2,
Чернівці, 58012, Україна

ЕКСПЕРИМЕНТАЛЬНЕ ДОСЛІДЖЕННЯ ТЕРМОЕЛЕКТРИЧНОГО МОДУЛЯ ОХОЛОДЖЕННЯ ДЕТЕКТОРА РЕНТГЕНІВСЬКОГО ВИПРОМІНЮВАННЯ

У роботі наведено результати експериментальних досліджень термоелектричного багатокаскадного термоелектричного модуля охолодження рентгенівських детекторів. Розроблено спеціалізований стенд, виготовлено термоелектричний модуль охолодження та проведено серію його досліджень в умовах, що імітують його роботу у складі детектора рентгенівського випромінювання. Бібл. 6, рис. 3 .

Ключові слова: експериментальне дослідження, термоелектричне охолодження, рентгенівський детектор.

Прибыла А.В., *канд. физ.-мат. наук*[1,2]
Кибак А.М.

[1]Институт термоэлектричества НАН и МОН Украины,
ул. Науки, 1, Черновцы, 58029, Украина, *e–mail: anatych@gmail.com;*
[2]Черновицкий национальный університет им. Юрия Федьковича,
ул. Коцюбинского, 2, Черновцы, 58012, Украина

ЭКСПЕРИМЕНТАЛЬНОЕ ИССЛЕДОВАНИЕ ТЕРМОЭЛЕКТРИЧЕСКОГО МОДУЛЯ ОХЛАЖДЕНИЯ ДЕТЕКТОРА РЕНТГЕНОВСКОГО ИЗЛУЧЕНИЯ

В работе приведены результаты экспериментальных исследований термоэлектрического многокаскадного термоэлектрического модуля охлаждения рентгеновских детекторов. Разработан специализированный стенд, изготовлен термоэлектрический модуль охлаждения и проведена серия его исследований в условиях, которые имитируют его роботу в составе детектора рентгеновского излучения. Библ. 6, рис. 3.

Ключевые слова: экспериментальное исследование, термоэлектрическое охлаждение, рентгеновский детектор.

References

1. Rogalski A. (2012). Progress in focal plane arrays technologies. *Progress in Quantum Electronics*, 36, 342–473.
2. Piotrowski A., Piotrowski J., Gawron W., Pawluczyk J. and Pedzinska M. (2009). Extension of usable spectral range of Peltier cooled photodetectors. *ACTA Physica Polonica A*, 116, 52 – 55.
3. Anatychuk L.I., Vikhor L.N. (2013). The limits of thermoelectric cooling for photodetectors. *J. Thermoelectricity*, 5, 54-58.
4. Buhay O.M., Drozdenko M.O., Storizhko V.Yu. (2014). Microanalytical X-ray facility in IAP NASU. *Nanotechnology and Nanomaterials, Book of Abstracts*. Lviv.
5. Broerman E.C., Keyser R.M., Twomey T.R., Upp D.L. *A new cooler for HPGe detector systems*. ORTEC, PerkinElmer Instruments, Inc Oak Ridge TN 37831-0895 USA.
6. Anatychuk L.I., Prybyla A.V. (2019). Design of thermoelectric cooling module for X-ray radiation detector. *J.Thermoelectricity*, 2, 53 – 58.

Submitted 20.06.2019

Cherkez R.G., *dok. phys.– mat. sciences, Acting professor*[1,2]
Pozhar E.V., Zhukova A.S., Khrykov V.K.

[1]Institute of Thermoelectricity of the NAS and MES of Ukraine,
1, Nauky str., Chernivtsi, 58029, Ukraine
[2]Yuriy Fedkovych Chernivtsi National University,
2, Kotsiubynsky str., Chernivtsi, 58012, Ukraine

INFLUENCE OF THE NUMBER OF CHANNELS ON THE EFFICIENCY OF PERMEABLE THERMOELEMENTS OF *Bi-Te-Se-Sb* BASED MATERIALS

The basic properties of thermoelectric materials are analyzed. For a permeable thermoelement of Bi-Te-Se-Sb based materials a physical model is presented and a mathematical description is given. Computer calculation of parameters for Bi-Te-Se-Sb based permeable thermoelements is made. The dependence of permeable thermoelement efficiency and its generated power W on the number of channels N_k is presented graphically. Bibl. 5, Fig. 2.

Key words: Thermoelectric materials, generator efficiency, design of permeable segmented thermoelement, thermoEMF

Introduction

Permeable thermoelectric elements are characterized by the presence in their structure of channels for pumping liquid or gaseous heat carrier through them. The presence of heat exchange in the bulk of the leg increases the intensity of heat transfer, leads to the redistribution of temperature fields, potentials and heat fluxes, thus affecting the energy characteristics of the thermoelement. By controlling the thermophysical parameters (heat carrier pumping rate, heat transfer rate, electric current density), it is possible to realize such working conditions whereby the energy efficiency of power conversion will be improved [1].

The first theoretical studies of permeable thermoelements for gas fluxes showed the prospect of their creation, predicting a 30-40% increase in the coefficient of performance while cooling the air and an increase in the efficiency of the generators by 20-30 % with the use of low-potential thermal energy of gases. The use of permeable structures in *Bi-Te* thermoelectric elements can improve energy conversion efficiency by 30 % [2]. However, such studies were conducted for the simplest model of permeable thermoelement in one-dimensional approximation without taking into account the temperature dependences of the material parameters, connecting heat spreaders.

Over the past decade, promising *Bi-Te-Se-Sb* based thermoelectric materials have been attracting increasing attention of researchers. They are environmentally safe and are characterized by high values of the Seebeck coefficient and electrical conductivity with maximum values of dimensionless thermoelectric figure of merit parameter *ZT* at the level of 1 - 1.1 in the temperature range 300-600 K.

Physical model and its mathematical description

A physical model of permeable thermoelement of materials based on *Bi-Te-Se-Sb* in electric energy generation mode is represented in Fig. 1.

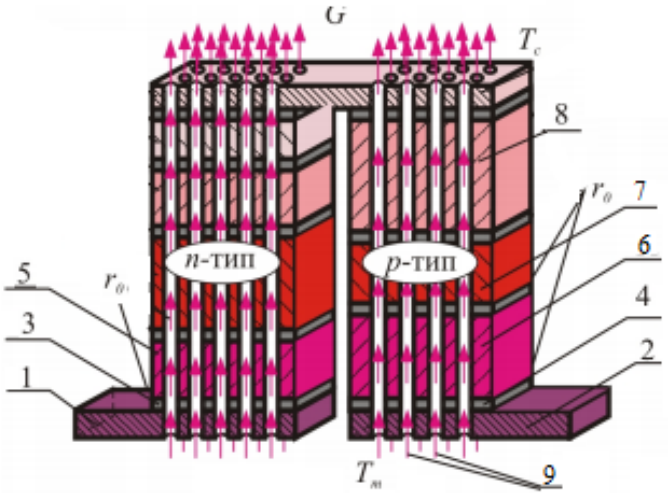

Fig. 1. Physical model of permeable segmented thermoelement
1, 2 – connecting plates; 3, 4 – connecting layers; 5 – segments (sections) of n-type leg; 6, 7, 8 – segments (sections) of p-type leg; 9 – heat carrier.

The thermoelement consists of *n*- and *p*-type legs whose physical properties are temperature-dependent. Heat input is realized by passing heat carrier along the legs through the channels (pores). Each leg comprises N_n and N_p segments, and the contact resistance of compound is r_0. The lateral surfaces of the legs are adiabatically isolated; heat carrier temperature at thermoelement inlet T_m is assigned. The temperature of cold junctions T_c is thermostated.

A system of differential equations describing the distribution of temperatures and heat fluxes in a steady-state one-dimensional case, in the infinitely small part *dx* of each *k*-th segment of *n*- and *p*-type legs, in the dimensionless coordinates is given by relations [2]:

$$\left.\begin{aligned}
&\frac{dT}{dx} = -\frac{\alpha_k j}{\kappa_k} T - \frac{j}{\kappa_k} q, \\
&\frac{dq}{dx} = \frac{\alpha_k^2 j}{\kappa_k} T + \frac{\alpha_k j}{\kappa_k} q + j\rho_k + \frac{\alpha_T \Pi_K^1 N_K l_K^2}{(S - S_K) j}(t - T), \\
&\frac{dt}{dx} = \frac{\alpha_T \Pi_K^1 N_K l_k}{G c_P}(t - T),
\end{aligned}\right\}_{n,p} \quad \begin{aligned} &k = 1, \ldots, N_{n,p} \\ &x_{k-1} \le x \le x_k \end{aligned}$$

where Π^l_K is channel perimeter; N_K is the number of channels; S_K is cross-sectional area of all the channels; S is a section of leg together with the channels; *G* is heat carrier consumption in the channels; C_p is specific heat of heat carrier; t is heat carrier temperature at point x; *T* is leg temperature at point *x*; αT is heat-transfer coefficient; α and κ are the Seebeck coefficient and thermal conductivity, and ρ is the resistivity of leg material.

Specific heat fluxes *q* and the reduced density of electric current *j* are determined through the expression:

$$q = \frac{Q}{I}, \qquad j = \frac{Il}{S},$$

where Q is power of heat flux passing through thermoelement leg, I is electric current, S is cross-sectional area of thermoelement legs.

The boundary conditions necessary for solving the equation with regard to the Joule-Lenz heat release due to contact resistance r_0 at points of connection of leg segments are formulated as:

$$T_{n,p}(0) = T_C, \qquad t_{n,p}(1) = T_m, \qquad q_{n,p}(1) = 0,$$
$$T_{n,p}(x_k^+) = T_{n,p}(x_k^-), \qquad q_{n,p}(x_k^+) = q_{n,p}(x_k^-) + \frac{r_0}{S_{n,p}} I,$$

where indices "-" and "+" denote the values of functions immediately to the left and right of the interface of segments x_k; $k = 1, \ldots, N$ is the index which determines leg segment number.

For seeking optimal concentrations of doping impurities which determine carrier concentrations in leg segments it is necessary to assign the dependences of material parameters α, κ, ρ on temperature and concentration of carriers (or impurities).

The main task in the design of permeable segmented generator thermoelement is to determine such matched parameters (reduced current density j in the legs, heat carrier consumption in channels G, concentration of doping impurities in materials of each segment) whereby the efficiency of the thermoelement reaches a maximum [3].

The efficiency will be determined through the relation of electric power P generated by the thermoelement to a change in heat carrier enthalpy:

$$\eta = \frac{P}{\sum_{n,p} Gc_p (T_m - T_C)},$$

and its maximum will be reduced to achievement of functional minimum:

$$J = \ln\left[\sum_{n,p}\left\{Gc_P (T_m - T_C)\right\}\right] - \ln\left[\sum_{n,p}\left\{Gc_P (T_m - t(0)) + q(0)\frac{j(S - S_K)}{l} - I\left(\frac{r_0}{S_n} + \frac{r_0}{S_p}\right)\right\}\right].$$

This problem was solved through use of the Pontryagin maximum principle, on which basis the relations yielding the necessary optimality conditions were obtained. Such a method as applied to thermoelectric power conversion is described in many works, for instance [4]. The same method was also used for creation of computer program and research on permeable thermoelement of *Bi-Te-Se-Sb* based thermoelectric materials [5].

Results of solving the problem

Calculations of permeable thermoelectric generator were performed with regard to losses of heat with exhaust gas and such input data as optimization of current density and heat carrier consumption, and optimization by equal concentration in leg sections with introduction of complex – G. $b_r := G \cdot C_p \cdot S_k \cdot N_k$.

The following input data was used. The inlet heat carrier temperature is 600 K, the temperature of thermoelement cold junctions is 300 K; the channel diameter is 0.01 cm; the channel perimeter (circle) is 0.031416 cm; the cross-sectional area of all N_k – channels is 0.0024 cm^2; the number of sections in one leg is 1 pcs; the height of legs is 20 cm; the cross-sectional area of leg material is 0.9976 cm^2.

The temperature dependences of α, σ, κ parameters of *Bi-Ti-Se-Sb* based materials were used for calculations [5]

It is seen that the efficiency of *Bi-Te-Se-Sb* based permeable thermoelement increases with increasing the number of channels. Maximum efficiency lies in the area from 25 to 80 channels per 1cm^2, and power – from 25 to 60. The specific electric power has a maximum in this case with 40 channels per 1 cm^2 and is P = 1.57 W. So, the rational number of channels per unit area will be within 25 – 60 pcs.

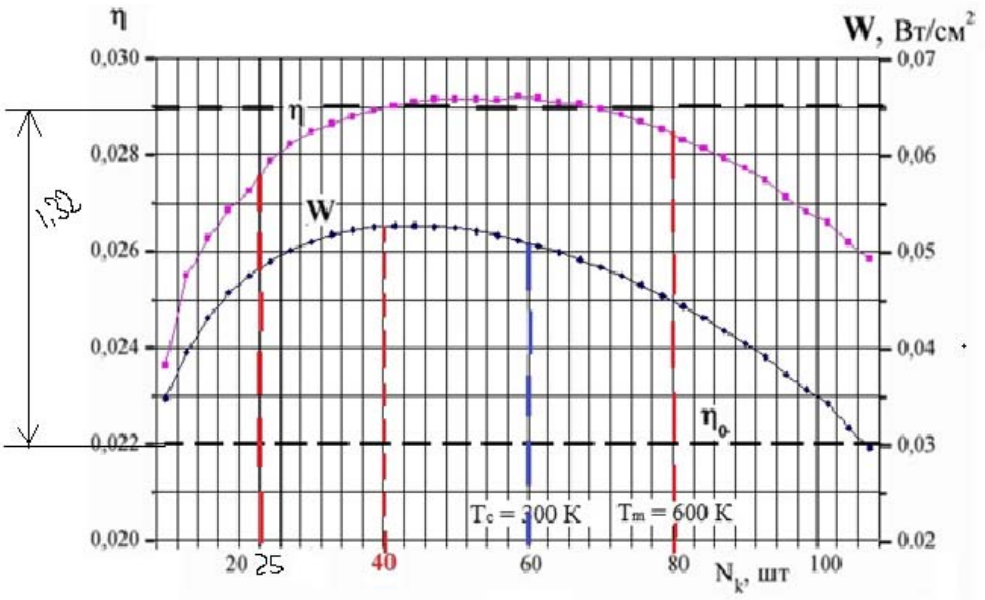

Fig. 2. Dependences of the efficiency and the generated power W of Bi-Te-Se-Sb based permeable thermoelement on the number of channels N_k

The data obtained testify that the efficiency increases with increasing the number of channels and reaches the highest value, just as in the two previous cases, at heat carrier temperature T_m = 600 K and is η = 6.8%. The increase in efficiency can reach 1.32 times as compared to conventional thermoelement.

Conclusions

Thus, for different operating conditions of a permeable generator thermoelement of *Bi-Te-Se-Sb* based materials it is necessary to determine its optimal design parameters (leg height, channel diameter and their number), whereby the maximum energy conversion efficiency and electric power will be obtained. The efficiency under optimal working conditions is higher than that of conventional thermoelement by a factor of 1.32. Comparison with η_0, the efficiency of conventional thermoelement operating under similar conditions, also indicates the possibility of about 32% increase in the efficiency of *Bi-Te-Se-Sb* based permeable thermoelement when converting energy.

References

1. Anatychuk L.I. (2003). *Termoelektrichestvo. Tom II. Termoelektricheskiie preobrazovateli energii [Thermoelectricity. Vol.II. Thermoelectric power converters]*. Chernivtsi: Bukrek [in Russian].
2. Anatychuk L.I., Cherkez R.G. (2010). Permeable segmented thermoelement in electric power generation mode. *J.Thermoelectricity*, 3, 5-12.
3. Cherkez R. G. (2012). Energy possibilities of permeable generator thermoelements based on segmented legs. AIP Conf. Proc. 1449, 443, pp. 439-442; doi:http://dx.doi.org/10.1063/1.4731590
4. Pontryagin L.S., Boltianskiy V.G., Gamkrelidze R.F., Mishchenko. (1976). *Matematicheskaia teoriia optimalnykh protsessov [Mathematical theory of optimal processes]*. Moscow: Nauka [in Russian].
5. Bublik V.T., Drabkin I.A., Karataiiev V.V., et al. (2012). Obiomnyi nanostrukturirovannyi termoelektricheskii material na osnove $(Bi,Sb)_2Te_3$, poluchennyi metodom iskrovogo plasmennogo spekaniia (SPS) [Bulk nanostructured thermoelectric material based on $(Bi,Sb)_2Te_3$ obtained by spark

plasma sintering method (SPS)]. *Proc. of XIII Interstate Workshop "Thermoelectrics and their Application" (Russia, Saint-Petersburg, 2012)* (pp.70–75).

Submitted 03.07.2019

Черкез Р.Г. *док. фіз.– мат. наук, в.о. професора*[1,2]
Пожар Е.В., Жукова А.С., Хриков В.К.

[1]Інститут термоелектрики НАН України та МОН України,
вул. Науки, 1, Чернівці, 58029, Україна,
e-mail: anatych@gmail.com;
[2]Чернівецький національний університет ім. Юрія Федьковича,
вул. Коцюбинського, 2, Чернівці, 58012, Україна

ВПЛИВ ЧИСЛА КАНАЛІВ НА ЕФЕКТИВНІСТЬ ПРОНИКНИХ ТЕРМОЕЛЕМЕНТІВ З МАТЕРІАЛІВ НА ОСНОВІ *Bi-Te-Se-Sb*

Проведено аналіз основних властивостей термоелектричних матеріалів. Для проникного термоелементу з матеріалів на основі Bi-Te-Se-Sb приведено фізичну модель та дано математичний опис. Зроблено комп'ютерний розрахунок параметрів для проникних термоелементів, що виготовлені на основі Bi-Te-Se-Sb. Представлено графічний вигляд залежності ККД і потужності проникного, яка генерується W від числа каналів N_k.
Ключові слова: Термоелектричні матеріали, ККД генератору, проектування проникного сегментного термоелемента, термо-ЕРС.

Черкез Р.Г, *док. физ.-мат. наук,и.о. профессора*[1,2]
Пожар Е.В., Жукова А.С., Хрыков В.К.

[1]Институт термоэлектричества НАН и МОН Украины,
ул. Науки, 1, Черновцы, 58029, Украина,
e–mail: anatych@gmail.com;
[2]Черновицкий национальный университет имени Юрия Федьковича,
ул. Коцюбинского, 2, Черновцы, 58012, Украина

ВЛИЯНИЕ ЧИСЛА КАНАЛОВ НА ЭФФЕКТИВНОСТЬ ПРОНИЦАЕМЫХ ТЕРМОЭЛЕМЕНТОВ ИЗ МАТЕРИАЛОВ НА ОСНОВЕ *Bi-Te-Se-Sb*

Проведен анализ основных свойств термоэлектрических материалов. для проницаемого термоэлемента из материалов на основе Bi-Te-Se-Sb, приведена физическая модель и дано ее математическое описание. Сделан компьютерный расчет параметров проницаемых термоэлементов, изготовленных на основе Bi-Te-Se-Sb. Представлены графически зависимости КПД и мощности, проницаемого генерируемого W вид числа каналов N_k.
Ключевые слова: термоэлектрические материалы, КПД генератора, проектирование проницаемого сегментного термоэлемента, термоЭДС.

References

1. Anatychuk L.I. (2003). *Termoelektrichestvo. Tom II. Termoelektricheskiie preobrazovateli energii [Thermoelectricity. Vol.II. Thermoelectric power converters]*. Chernivtsi: Bukrek [in Russian].
2. Anatychuk L.I., Cherkez R.G. (2010). Permeable segmented thermoelement in electric power generation mode. *J.Thermoelectricity*, 3, 5-12.
3. Cherkez R. G. (2012). Energy possibilities of permeable generator thermoelements based on segmented legs. AIP Conf. Proc. 1449, 443, pp. 439-442; doi:http://dx.doi.org/10.1063/1.4731590
4. Pontryagin L.S., Boltianskiy V.G., Gamkrelidze R.F., Mishchenko. (1976). *Matematicheskaia teoriia optimalnykh protsessov [Mathematical theory of optimal processes]*. Moscow: Nauka [in Russian].
5. Bublik V.T., Drabkin I.A., Karataiiev V.V., et al. (2012). Obiomnyi nanostrukturirovannyi termoelektricheskii material na osnove $(Bi,Sb)_2Te_3$, poluchennyi metodom iskrovogo plasmennogo spekaniia (SPS) [Bulk nanostructured thermoelectric material based on $(Bi,Sb)_2Te_3$ obtained by spark

Submitted 03.07.2019

L.I. Anatychuk *acad. National Academy of Sciences of Ukraine*[1,2],
N.V. Pasechnikova *doc. med. sciences, National Academy of medical sciences of Ukraine*[3],
V.O. Naumenko *doc. med. sciences*[3],
O.S. Zadorozhnyi *cand. med. sciences*[3],
Nazaretian P.E.[3], **Havryliuk M.V.**[1,2], **Tiumentsev V.A.**[1],
R.R. Kobylianskyi *cand. Phys.-math. sciences*[1,2],

[1]Institute of Thermoelectricity of the NAS and MES of Ukraine,
1, Nauky str., Chernivtsi, 58029, Ukraine;
[2]Yu.Fedkovych Chernivtsi National University,
2, Kotsiubynskyi str., Chernivtsi, 58012, Ukraine
[3]State Institution "The Filatov Institute of Eye Diseases and Tissue Therapy of the NAMS of Ukraine", Odesa, Ukraine

THERMOELECTRIC DEVICE FOR HYPOTHERMIA OF THE HUMAN EYE

The paper presents the results of the development of a thermoelectric device in the form of a monocular dressing for contact cooling of the human eye through the eyelids. The developed device allows controlled local contact cooling of the eye structures through the eyelids and is designed to treat the acute and chronic eye diseases, reduce intraocular pressure, and reduce pain and inflammatory processes of the eye. The design features of the device and its technical characteristics are presented. Bibl. 23, Fig. 2, table 1.
Key words: thermoelectric device, thermoelectric cooling, hypothermia of the human eye.

Introduction

Therapeutic hypothermia is a curative effect that involves reducing the patient's body temperature by forcing heat away from the surface of the body or internal organs to reduce the risk of ischemic tissue damage. Therapeutic hypothermia in medicine has been known for over 200 years as an effective and proven method of neuroprotection in patients with some critical conditions, which reduces the mortality of patients and reduces the amount of damage to brain tissue. Currently, therapeutic hypothermia is considered to be the most promising physical method of neuroprotective protection of the brain, since from the standpoint of evidence-based medicine there is no effective method of pharmacological neuroprotection in neuroresuscitation practice [1]. Therapeutic hypothermia is successfully used in various fields of medicine (cardiac surgery, neurosurgery, resuscitation, etc.) in order to increase the resistance of brain cells to ischemia [2-6].

It is known that cerebral metabolism changes with the temperature of the brain, on average by 6-8% when the temperature of the body changes by 1 °C [1]. Lowering the temperature of the neurons of the central nervous system causes the development of metabolic depression in them, which leads to a decrease in oxygen consumption, increased resistance to hypoxia, ischemia and reperfusion [7, 8]. In general, the following mechanisms of the neuroprotective action of therapeutic hypothermia are

currently distinguished: inhibition of destructive enzymatic reactions; inhibition of free radical reactions; plasticity protection of lipoproteins of cytoplasmic membranes; reduced oxygen consumption in areas of the brain with low blood flow; improving oxygen delivery to the ischemic zones of the brain and reducing intracranial pressure; inhibition of biosynthesis and production of exitotoxic neurotransmitters [9 12].

At the same time, it is known that general therapeutic hypothermia is accompanied by the risk of complications, so it can be applied only in specially equipped resuscitation units. In clinical conditions in an ophthalmic hospital, it is not justified due to the complexity of its implementation [3, 4]. In ophthalmology there is a prospect of using local therapeutic hypothermia, for example, to reduce intraocular pressure. According to some authors, this effect is achieved by reducing the production of intraocular fluid and improving the outflow of watery moisture.

In so doing, there is a decrease in pain syndrome [13 – 15]. There is evidence in the literature that local hypothermia of the eye can lead to a decrease in fibrin production, a decrease in bleeding volume, and a decrease in photodamage during surgery [16]. A number of authors demonstrate a decrease in choroidal blood flow and a decrease in damage to the hemato-retinal barrier in conditions of local hypothermia [17, 18]. There is evidence of the use of local hypothermia to reduce inflammatory reactions [19]. It is known that after local hypothermia significant hemodynamic changes occur in the eye that are characterized by a significant expansion of the vessels and a decrease in their peripheral resistance, leading to an increase in blood flow to the vascular tract, an increase in pulse volume and blood flow velocity [20].

There are various ways to cool the eyes. In the experiment, it was confirmed that with local contact hypothermia, a decrease in the temperature of the intraocular medium of the rabbit eye is possible, both by cooling directly the external surface of the cornea and when exposed to cold through closed eyelids [21]. To solve this problem, you can use, for example, a bubble with ice, laying it on the eyelids [14]. Another way to achieve local hypothermia is achieved by irrigating the outer surface of the eye with chilled solutions. During intraocular surgery, local hypothermia of the eye can be created by lowering the temperature of irrigation solutions [22]. With regard to modern technologies, the development of special thermoelectric devices for local contact eye cooling looks promising. This will allow more efficient and controlled use of the beneficial effects of therapeutic hypothermia for the treatment of ophthalmic diseases.

Therefore, *the purpose of this work* is to design and manufacture an experimental sample of thermoelectric device in the form of a monocular dressing for contact cooling of the human eye through the eyelids.

Device design and specifications

At the Institute of Thermoelectricity of the NAS and MES of Ukraine within cooperation agreement with the State Institution "The Filatov Institute of Eye Diseases and Tissue Therapy of the NAMS of Ukraine"a thermoelectric device was developed in the form of a monocular dressing for contact cooling of the human eye through the eyelids (Fig.1). The technical characteristics of the device are given in Table 1.

The device is designed to treat acute and chronic eye diseases, reduce intraocular pressure, reduce pain and inflammation of the human eye. The developed thermoelectric medical device allows controlled local cooling of eye structures through the eyelids and makes it possible to develop and introduce the technology of controlled local therapeutic hypothermia in ophthalmology. This device is original and has no world analogues.

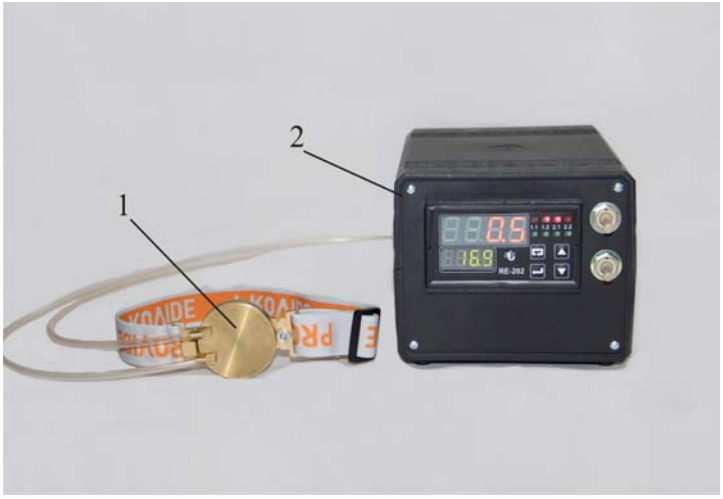

Fig.1. Experimental sample of a thermoelectric device in the form of a monocular dressing for contact cooling of human eyes through the eyelids: 1 – cooling plate, 2 – thermoelectric electronic cooling, control and power supply unit

Table

Device specifications

№	Device specifications	Parameter values
1.	Operating temperature range	(+5 ÷ +40) °C
2.	Temperature accuracy	± 0.2 ºC
3.	Discreteness of the measured and set temperature	± 0.1 ºC
4.	Temperature measurement error, not more	± 0.2 ºC
5.	Thermal load in the external circuit, not more	20 W
6.	Total power consumption, not more	120 W
7.	Supply voltage (AC 50 Hz)	220 ± 10 V
8.	Overall dimensions of cooling plate	(75×45×12) mm
9.	Dimensions of thermoelectric electronic cooling, control and power supply unit	(180×120×100) mm
10.	Pump performance	40 l/h
11.	Length of hoses with external temperature sensor	1 m
12.	Device weight	1.5 kg
13.	Device run-up time	10 min
14.	Device continuous work time	48 h

The device consists of two main functional units: cooling plate 1 and thermoelectric electronic cooling, control and power supply unit 2 (Fig. 1). The cooling plate 1 is a liquid heat exchanger made of a

highly conductive material - copper. The electronic unit 2 comprises a thermoelectric cooling unit, a power supply unit and an electronic control unit based on a programmable thermoregulator of the type RE-202. In turn, the thermoelectric cooling unit contains a Peltier thermoelectric module [23, 24], liquid heat exchangers and a circulation pump.

The Peltier thermoelectric module is designed to cool or heat the liquid circulating in the outer circuit. The hot side of this thermoelectric module is cooled by an internal liquid circuit connected to the water supply network. The circulation pump provides for the circulation of the liquid coolant in the outer circuit.

The power supply unit is designed to power the thermoelectric module from an alternating current network of 220 V. The temperature regulator RE-202 measures the temperature from internal and external thermoresistive sensors and generates control signals for the control circuit. In turn, the control circuit controls the thermoelectric module according to a predetermined program in order to maintain the operating temperature set by the operator.

On the front panel of the device there are toggle switches "ON", "HEATING / COOL" and a digital display of the temperature regulator RE-202. The rear panel of the device acommodates a “NETWORK” toggle switch, a socket for connecting to a 220 V network, sockets for connecting external temperature sensors “T1” and “T2”, “CIRCUIT INPUT”, “CIRCUIT OUTPUT”, “WATER INPUT”, “WATER OUTPUT” unions and a 5 A fuse.

A block-diagram of the thermoelectric device for contact cooling of the human eye is shown in Fig.2, where 1 is a 220V network switch, 2 is a RE-202 measuring thermoregulator, 3 is a power supply unit switch, 4 is a power supply unit, 5 is a tank with the liquid of heat exchanger circuit, 6 is a temperature sensor of the object, 7 is a temperature sensor of heat exchanger circuit, 8 is a job type switch, 9 is a circulation pump, 10 is a working heat exchanger of liquid circuit, 11 is an active heat exchanger of liquid circuit, 12 is a thermoelectric Peltier module, 13 is a power relay of thermoelectric Peltier module; 14 is a passive heat exchanger of liquid circuit, 15 is water mains.

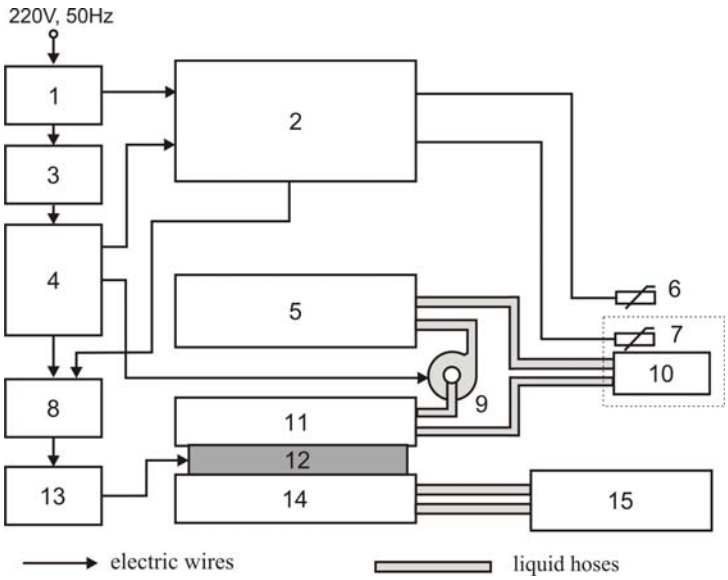

Fig. 2. Block-diagram of a thermoelectric device in the form of a monocular dressing for contact cooling of the human eye through the eyelids: 1 – 220 V mains switch, 2 - measuring thermoregulator RE-202 3 –power supply switch, 4 – power supply unit, 5 – tank with a liquid of heat exchanger circuit, 6 – object temperature sensor, 7 – temperature sensor of heat exchanger circuit, 8 – job type switch, 9 – circulation pump, 10 – working heat exchanger of liquid circuit, 11 – active heat exchanger of liquid circuit, 12 – thermoelectric Peltier module, 13 – power relay of thermoelectric Peltier module, 14 –passive heat exchanger of liquid circuit, 15 – water mains.

Operating principle of device

The operating principle of device is cooling or heating (thermal stabilization) of the human eye in order to treat acute and chronic diseases of the eye, reduce intraocular pressure, reduce pain and inflammatory processes.

The proposed device works as follows. After electrical power supply and selection of cooling or heating mode, the thermoelectric module maintains the temperature set by the thermoregulator by means of liquid circulating in the circuit. If the internal temperature sensor is selected as the feedback sensor, the preset temperature in the liquid circuit stabilizes. If an external sensor is selected as the feedback sensor and it is located in a thermostatically controlled object, then the temperature of the object is stabilized.

The specified device is simple, compact, portable and reliable in operation, which allows a doctor or a medical person to use it without special training, having read the instruction in advance. Thus, the technical advantages of this device include: the presence of a highly efficient thermoelectric Peltier module, the ability to measure and maintain a set temperature with a discreteness of ± 0.2 ° C, the safety of use of the device and the ability to monitor the temperature of the human eye surface in real time.

The introduction of such a device into medical practice will be of great social and economic importance as it will reduce the risk of ophthalmic complications, preserve the viability of patients' eye structures, and provide highly skilled care both in specialized medical establishments and in extreme conditions. This, in turn, will provide the right conditions for the preservation of human health, improve the efficiency and quality of health care delivery and make a significant contribution to the development of the newest domestic medical thermoelectric equipment.

It should be noted that in order to confirm the effectiveness of the device, the development of methods of treatment and clinical trials, the developed experimental model of the device for contact cooling of the human eye through the eyelids was submitted to the State Institution “The Filatov Institute of Eye Diseases and Tissue Therapy of the NAMS Ukraine” within cooperation agreement. The results of clinical trials of the device will be the subject of subsequent publications on this subject matter.

Conclusions

1. For the first time, a design was developed and an experimental sample was made of a thermoelectric device in the form of a monocular dressing for contact cooling of human eyes through the eyelids. The device is designed to treat the acute and chronic eye diseases, reduce intraocular pressure, and reduce pain and inflammation of the human eye. The proposed device has no world analogues.
2. The developed thermoelectric medical device makes it possible to carry out controlled contact cooling of human eye structures in the temperature range (+5 ÷ +40) °C and will further allow developing and introducing the technology of controlled local therapeutic hypothermia in ophthalmology.

References

1. Tsarev A.V. (2014). Tselevoi temperaturnyi menedzhment v klinicheskoi praktike intensivnoi terapii kriticheskikh sostoianii [Targeted temperature management in the clinical practice of

critical state intensive therapy]. *Meditsina neotlozhnykh sostoianii – Emergency Medicine*, 7, 186-191 [in Russian].

2. Alzaga A.G., Cerdan M., Varon J. (2006). Therapeutic hypothermia. *Resuscitation*, 70 (3), 369-380.
3. Polderman K.H., Herold I. (2009). Therapeutic hypothermia and controlled normothermia in the ICU: Practical considerations, side effects, and cooling methods. *Crit. Care Med*., 37, 1101-1120.
4. Saad H. , Aladawy M. (2013). Temperature management in cardiac surgery. *Glob. Cardiol. Sci. Pract.,* 1, 44-62.
5. The hypothermia after cardiac arrest group. Mild therapeutic hypothermia to improve the neurologic outcome after cardiac arrest. (2002). *N. Engl. J. Med*., 346, 549-556.
6. Yenari M.A., Han H.S. (2012). Neuroprotective mechanisms of hypothermia in brain ischaemia. *Nat. Rev. Neurosci*, 13, 267-278.
7. Bernard S., Buist M. (2003). Induced hypothermia in critical care medicine: A review. *Critical Care Medicine*, 31, 2041-2051.
8. Lampe J.W., Becker L.B. (2011). State of the art in therapeutic hypothermia. *Annu. Re. Med*., 11, 104-10.
9. Usenko L.V., Tsarev A.V. (2009). Iskusstvennaia hipotermiia v sovremennoi reanimatologii [Artificial hypothermia in modern resuscitation]. *Obshchaiia reanimatologiia – General Resuscitation*, 5(1), 21-23.
10. Mayer S.A., Sessler V.A. (2005). *Therapeutic hypothermia*. New York: Marcel Dekker.
11. Nunnally M.E., Jaeschke R., Bellingan G.J., et al. (2011). Targeted temperature management in critical care: A report and recommendations from five professional societies. *Critical Care Medicine*, 39, 1113-1125.
12. Safar P. (2002). *Cerebral resuscitation from temporary complete global brain ischemia. In: Cerebral blood flow: mechanisms of ischemia, diagnosis, and therapy*. Pinsky M.R.(Ed.) Berlin: Springer.
13. Chanchikov G.F., Zavolskaia Z.P., Bereznikova V.I. (1978). Vliianiie umerennoi lokalnoi hipotermii na ophtalmotonus, zritelnyie funktsii i gidrodinamiku glaz bolnykh glaukomoi [Influence of moderate local hypothermia on intralocular tension, visual functions and hydrodynamics of patients ill with glaucoma]. *Oftalmologicheskii Zhurnal - J. Ophthalmology*, 8, 594-597 [in Russian].
14. Shif L.V., Taratynova A.V., Neiman V.A., Angelova N.V. (1981). Primeneniie lokalnoi gipotermii pri ostrom pristupe glaukomy i glaukome v terminalnoi stadii, oslozhnivsheisia bolevym sindromom [The use of local hypothermia in an acute attack of glaucoma and glaucoma in the terminal stage, complicated by pain]. *Oftalmologicheskii Zhurnal - J. Ophthalmology,* 3, 187-188 [in Russian].
15. Tamai K., Majima A., Honda F. (1993). Experimental study on local cooling of the eyeball in ocular surgery. The local cooling effect on uveal blood circulation, intraocular pressure, and intravitreous pressure. *Nippon Ganka Gakkai Zasshi*, 97, 509–513.
16. Jabbour N.M., Schepens C.L., Buzney S.M. (1998). Local ocular hypothermia in experimental intraocular surgery. *Ophthalmology,* 95, 1685-1690.
17. Fujishima H., Yagi Y, Toda I., Shimazaki J., Tsuota K (1995). Increased comfort and decreased inflammation of the eye by cooling after cataract surgery. *Am. J. Ophthalmol*., 119, 301-306.

18. Tamai K., Toumoto E., Majima A. (1997). Local hypothermia protects the retina from ischaemic injury in vitrectomy. *Br J. Ophthalmol*., 81, 789-794.
19. Zolotareva M.M., Chvialeva K.I., Vasilevich A.I. (1978). *Gipotermiia pri glaznykh zabolevaniiakh [Hypothermia with eye diseases]*. Minsk [in Russian].
20. Lazarenko V.I., Chanchikov G.F., Kornilovskii I.M., Gaidabura V.G. (1976). Vliianiie umerennoi lokalnoi hipotermii na hemo- i hidrodinamicheskiie pokazateli zdorovykh glaz [Influence of moderate local hypothermia on the hemo-and hydrodynamic parameters of healthy eyes]. *Oftalmologicheskii Zhurnal - J. Ophthalmology*, 6, 419-422 [in Russian].
21. Zadorozhnyi O.S., Nazaretian R.E., Mirnenko V.V., Naumenko V.A., Pasechnikova N.V. (2018). *Eksperimentalnoie issledovaniie epibulbarnoi i intraokuliarnoi temperatury krolika v usloviiakh hipotermii [Experimental study of epibulbar and intraocular temperature of rabbit under hypothermia]*. *Oftalmologiia. Vostochnaia Evropa - Ophthalmology. Eastern Europe*, 1, 73-81.
22. Anatychuk L.I., Pasechnikova N.V., Naumenko V.A., Nazaretian R.E., Umanets N.N., Kobylianskyi R.R., Zadorozhnyi O.S. (2019). Dynamics of intraocular temperature in the process of vitreoretinal surgery using irrigational solutions of various temperature. *Oftalmologicheskii Zhurnal - J. Ophthalmology,* 1, 33-38 [in Russian].
23. Anatychuk L.I. (1979). *Termoelementy i termoelektricheskiie ustroistva. Spravochnik (Thermoelements and thermoelectric devices. Handbook)*. Kyiv: Naukova Dumka [in Russian].
Anatychuk L.I. (2003). *Termoelektrichestvo.T.2. Termoelektricheskiie preobrazovateli energii [Thermoelectricity. Vol.2. Thermoelectric power converters]*. Kyiv-Chernivtsi: Institute of Thermoelectricity [in Russian].

Submitted 10.07.2019

Анатичук Л.І. *акад. НАН України*,[1,2]
Пасєчнікова Н.В. *док. мед.– наук, НАМН України*,[3]
Кобилянський Р.Р. *канд. фіз.– мат. наук*[1,2],
Науменко В.О.[3], **Задорожний О.С.** *канд. мед.– наук* [3],
Гаврилюк М.В.[1,2], **Тюменцев В.А.**[1]

[1]Інститут термоелектрики НАН і МОН України,
вул. Науки, 1, Чернівці, 58029, Україна,
e-mail: anatych@gmail.com;
[2]Чернівецький національний університет імені Юрія Федьковича,
вул. Коцюбинського 2, Чернівці, 58012, Україна,
[3]ДУ «Інститут очних хвороб і тканинної терапії
ім. В.П. Філатова НАМН України», Французький
бульвар, 49/51, Одеса, 65061, Україна,
e-mail:zadoroleg2@gmail.com.

ТЕРМОЕЛЕКТРИЧНИЙ ПРИЛАД ДЛЯ ГІПОТЕРМІЇ ОКА ЛЮДИНИ

У роботі наведено результати розробки термоелектричного приладу у вигляді монокулярної пов'язки для контактного охолодження ока людини через повіки. Розроблений прилад дає можливість контрольованого локального контактного охолодження структур ока через повіки та призначений для лікування гострих і хронічних захворювань ока, зниження внутрішньоочного тиску, зменшення больового синдрому та запальних процесів ока. Наведено особливості конструкції приладу та його технічні характеристики. Бібл. 23, рис. 2, табл. 1.

Ключові слова: термоелектричний прилад, термоелектричне охолодження, гіпотермія ока людини.

Анатичук Л.І. *ак. НАН України*,[1,2]
Пасєчнікова Н.В. *доктор мед. наук, НАМН України*,[3]
Кобилянський Р.Р. *канд. фіз.-мат. наук*[1,2],
Науменко В.О.[3], **Задорожний О.С.** *канд. мед. наук* [3],
Гаврилюк М.В.[1,2], **Тюменцев В.А.**[1]

[1]Институт термоэлектричества НАН и МОН Украины, ул. Науки, 1, Черновцы, 58029, Украина, *e–mail: anatych@gmail.com;*
[2]Черновицкий национальный университет им. Юрия Федьковича, ул. Коцюбинского, 2, Черновцы, 58012, Украина
[3]ДУ «Институт глазных болезней і тканевой терапии им. В.П. Филатова НАМН Украины», Французький бульвар, 49/51, Одеса, 65061, Украина, *e-mail:zadoroleg2@gmail.com.*

ТЕРМОЭЛЕКТРИЧЕСКИЙ ПРИБОР ДЛЯ ГИПОТЕРМИИ ОКА ЧЕЛОВЕКА

В работе приведены результаты разработки термоэлектрического устройства в виде монокулярной повязки для контактной охлаждения глаза человека через века. Разработанный прибор дает возможность контролируемого локального контактного охлаждения структур глаза через века и предназначен для лечения острых и хронических заболеваний глаза, снижение внутриглазного давления, уменьшение болевого синдрома и воспалительных процессов глаза. Приведены особенности конструкции прибора и его технические характеристики. Библ. 23, рис. 2, табл. 1.

Ключевые слова: термоэлектрический прибор, термоэлектрическое охлаждение, гипотермия глаза человека.

References

1. Tsarev A.V. (2014). Tselevoi temperaturnyi menedzhment v klinicheskoi praktike intensivnoi terapii kriticheskikh sostoianii [Targeted temperature management in the clinical practice of

critical state intensive therapy]. *Meditsina neotlozhnykh sostoianii – Emergency Medicine*, 7, 186-191 [in Russian].

2. Alzaga A.G., Cerdan M., Varon J. (2006). Therapeutic hypothermia. *Resuscitation*, 70 (3), 369-380.
3. Polderman K.H., Herold I. (2009). Therapeutic hypothermia and controlled normothermia in the ICU: Practical considerations, side effects, and cooling methods. *Crit. Care Med*., 37, 1101-1120.
4. Saad H. , Aladawy M. (2013). Temperature management in cardiac surgery. *Glob. Cardiol. Sci. Pract.,* 1, 44-62.
5. The hypothermia after cardiac arrest group. Mild therapeutic hypothermia to improve the neurologic outcome after cardiac arrest. (2002). *N. Engl. J. Med*., 346, 549-556.
6. Yenari M.A., Han H.S. (2012). Neuroprotective mechanisms of hypothermia in brain ischaemia. *Nat. Rev. Neurosci*, 13, 267-278.
7. Bernard S., Buist M. (2003). Induced hypothermia in critical care medicine: A review. *Critical Care Medicine*, 31, 2041-2051.
8. Lampe J.W., Becker L.B. (2011). State of the art in therapeutic hypothermia. *Annu. Re. Med*., 11, 104-10.
9. Usenko L.V., Tsarev A.V. (2009). Iskusstvennaia hipotermiia v sovremennoi reanimatologii [Artificial hypothermia in modern resuscitation]. *Obshchaiia reanimatologiia – General Resuscitation*, 5(1), 21-23.
10. Mayer S.A., Sessler V.A. (2005). *Therapeutic hypothermia*. New York: Marcel Dekker.
11. Nunnally M.E., Jaeschke R., Bellingan G.J., et al. (2011). Targeted temperature management in critical care: A report and recommendations from five professional societies. *Critical Care Medicine*, 39, 1113-1125.
12. Safar P. (2002). *Cerebral resuscitation from temporary complete global brain ischemia. In: Cerebral blood flow: mechanisms of ischemia, diagnosis, and therapy*. Pinsky M.R.(Ed.) Berlin: Springer.
13. Chanchikov G.F., Zavolskaia Z.P., Bereznikova V.I. (1978). Vliianiie umerennoi lokalnoi hipotermii na ophtalmotonus, zritelnyie funktsii i gidrodinamiku glaz bolnykh glaukomoi [Influence of moderate local hypothermia on intralocular tension, visual functions and hydrodynamics of patients ill with glaucoma]. *Oftalmologicheskii Zhurnal - J. Ophthalmology*, 8, 594-597 [in Russian].
14. Shif L.V., Taratynova A.V., Neiman V.A., Angelova N.V. (1981). Primeneniie lokalnoi gipotermii pri ostrom pristupe glaukomy i glaukome v terminalnoi stadii, oslozhnivsheisia bolevym sindromom [The use of local hypothermia in an acute attack of glaucoma and glaucoma in the terminal stage, complicated by pain]. *Oftalmologicheskii Zhurnal - J. Ophthalmology,* 3, 187-188 [in Russian].
15. Tamai K., Majima A., Honda F. (1993). Experimental study on local cooling of the eyeball in ocular surgery. The local cooling effect on uveal blood circulation, intraocular pressure, and intravitreous pressure. *Nippon Ganka Gakkai Zasshi*, 97, 509–513.
16. Jabbour N.M., Schepens C.L., Buzney S.M. (1998). Local ocular hypothermia in experimental intraocular surgery. *Ophthalmology,* 95, 1685-1690.
17. Fujishima H., Yagi Y, Toda I., Shimazaki J., Tsuota K (1995). Increased comfort and decreased inflammation of the eye by cooling after cataract surgery. *Am. J. Ophthalmol*., 119, 301–306.
18. Tamai K., Toumoto E., Majima A. (1997). Local hypothermia protects the retina from

ischaemic injury in vitrectomy. *Br J. Ophthalmol*., 81, 789-794.

19. Zolotareva M.M., Chvialeva K.I., Vasilevich A.I. (1978). *Gipotermiia pri glaznykh zabolevaniiakh [Hypothermia with eye diseases]*. Minsk [in Russian].
20. Lazarenko V.I., Chanchikov G.F., Kornilovskii I.M., Gaidabura V.G. (1976). Vliianiie umerennoi lokalnoi hipotermii na hemo- i hidrodinamicheskiie pokazateli zdorovykh glaz [Influence of moderate local hypothermia on the hemo-and hydrodynamic parameters of healthy eyes]. *Oftalmologicheskii Zhurnal - J. Ophthalmology*, 6, 419-422 [in Russian].
21. Zadorozhnyi O.S., Nazaretian R.E., Mirnenko V.V., Naumenko V.A., Pasechnikova N.V. (2018). *Eksperimentalnoie issledovaniie epibulbarnoi i intraokuliarnoi temperatury krolika v usloviiakh hipotermii [Experimental study of epibulbar and intraocular temperature of rabbit under hypothermia]*. *Oftalmologiia. Vostochnaia Evropa - Ophthalmology. Eastern Europe*, 1, 73-81.
22. Anatychuk L.I., Pasechnikova N.V., Naumenko V.A., Nazaretian R.E., Umanets N.N., Kobylianskyi R.R., Zadorozhnyi O.S. (2019). Dynamics of intraocular temperature in the process of vitreoretinal surgery using irrigational solutions of various temperature. *Oftalmologicheskii Zhurnal - J. Ophthalmology,* 1, 33-38 [in Russian].
23. Anatychuk L.I. (1979). *Termoelementy i termoelektricheskiie ustroistva. Spravochnik (Thermoelements and thermoelectric devices. Handbook)*. Kyiv: Naukova Dumka [in Russian].
Anatychuk L.I. (2003). *Termoelektrichestvo.T.2. Termoelektricheskiie preobrazovateli energii [Thermoelectricity. Vol.2. Thermoelectric power converters]*. Kyiv-Chernivtsi: Institute of Thermoelectricity [in Russian].

Submitted 10.07.2019

P.D. Mykytiuk. *cand. phys. – math. science* [1,2]
O.Yu. Mykytiuk. *cand. phys. – math. science, dochentr*[3]


P.D. Mykytiuk

[1]Institute of Thermoelectricity of the NAS and MES of Ukraine, 1, Nauky str, Chernivtsi, 58029, Ukraine;
e-mail: anatych@gmail.com;
[2]Yuriy Fedkovych Chernivtsi National University, 2, Kotsiubynsky str., Chernivtsi, 58012, Ukraine;
[3]Higher State Educational Institution of Ukraine "Bukovinian State Medical University", 2, Theatre Square, Chernivtsi, 58002, Ukraine


O.Yu. Mykytiuk.

SOME OPTIONS FOR IMPROVING PARAMETERS OF THERMOELECTRIC CONVERTERS

The sensitivity of thermal converter as a function of mutual arrangement of its structural elements was investigated. The importance of optimally matching the resistances of thermocouple and heater for each specific application of thermal converter and the advisability of optimizing its structural elements were confirmed. Bibl. 6, Fig. 2, Tabl. 1.
Key words: thermoelectric converter, thermocouple, heater, sensitivity.

Introduction

The basic parameters of metrological-purpose thermal converters up to this time have been mainly improved by increasing the thermoelectric parameters of semiconductor materials used for the manufacture of thermocouples, one of the basic structural elements of thermal converters.

However, in [1] it was shown that the use of a thermoelectric material with maximum thermoelectric figure of merit (Z) is not always a decisive factor in improving parameters of thermal converter. For example, a significant increase in the sensitivity of thermal converter can be obtained by optimizing the thermal mode of its operation in order to increase the efficiency of using the heat generated by the heater, minimizing the influence of the thermocouple on the temperature distribution in the heater [2], optimizing the structural elements, and choosing the most effective operating mode for a specific thermal converter application, etc.

The purpose of this work is to study possible options for improving parameters of thermal converters based on the optimization of thermal converter structural elements and their operating mode.

Dependence of thermal converter sensitivity on the geometric dimensions of its housing

When designing thermal converter, it is necessary to keep in mind that thermal mode of thermal converter is determined not only by the geometric dimensions of thermocouple and heater, but also by the distance between them and thermal converter housing.

To optimize thermal converter by the geometric dimensions, a series of experimental studies was carried out to determine the sensitivity of thermal converter to the distance between the housing cover

and the plane in which thermocouple and heater are located. The studies were carried out in the media with different heat transfer conditions - in vacuum, xenon and air.

The results of the experiments are presented in Fig.1.

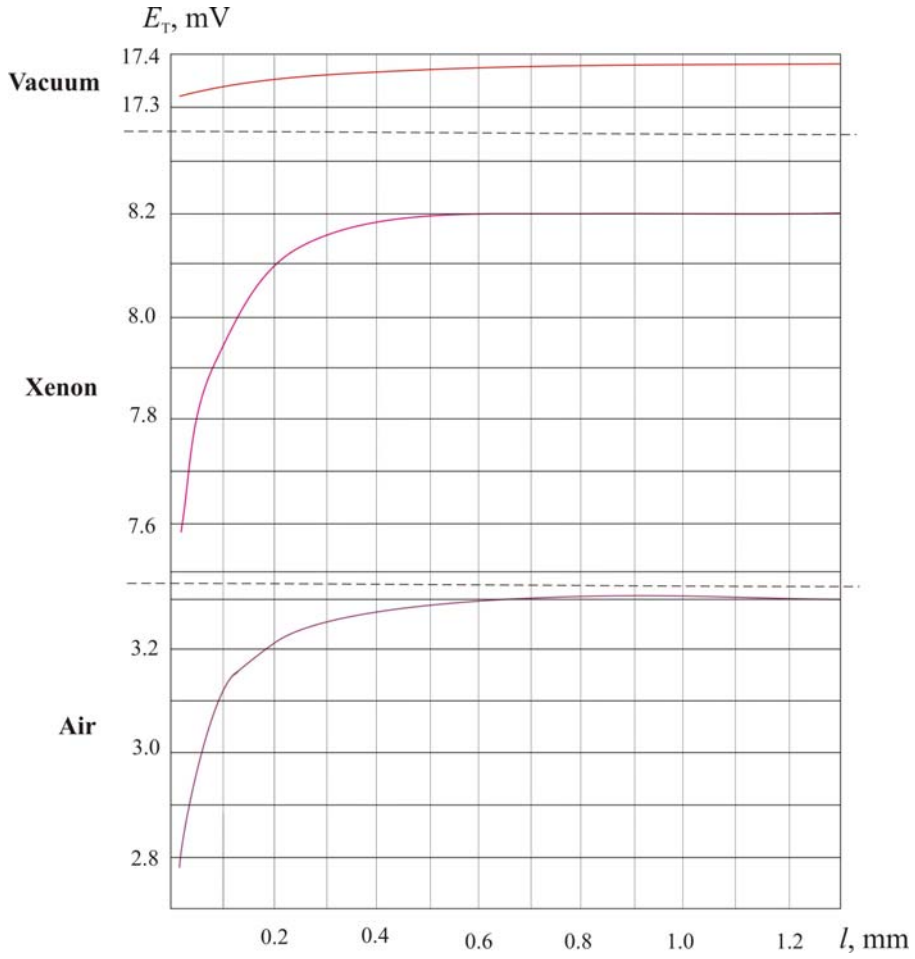

Fig.1. Dependence of output signal E_T of thermal converter on the height l of the housing cover above the thermocouple.

It can be seen from Fig. 1 that from a distance $l = 0.5 \div 0.6$ mm, further increase of L practically does not change the conditions of heat exchange between the structural elements of thermal converter and its housing.

The data obtained in xenon and vacuum confirm the theoretical calculations that the intensity of heat transfer in vacuum is much lower than the intensity of heat exchange in a gas environment.

The above studies were carried out for a type 4604 thermal converter with a rated current of 25mA and a thermocouple signal $E_T \geq 10$ mV. Such 4604 thermal converter is structurally manufactured in a housing of height of 5.5 mm and diameter of 4.9 mm. It should be noted that for thermal converters of other ratings mounted in a similar housing, the research data can be somewhat different. However, the purpose of the experimental studies was to establish the very fact of the influence of the thermal converter housing on the location of thermocouple and heater in it.

Matching of thermal converter thermocouple resistance with load resistance

The question of choosing the optimal operating mode for thermal converter has long been fully considered in [3]. However, thermal converter developers do not always take into account the

importance of matching thermocouple resistance with load resistance. Therefore, it makes sense to dwell on this issue once again.

The expression for the electric power P_{out}, which the thermocouple develops at load r, can be written as:

$$P_{out}=(E-I_T \cdot R_T) \cdot I_T=E_n \cdot I_T \quad (1)$$

where R_T, I_T are the resistance and rated current of the thermocouple, and E_n is the load voltage r.

Let us transform E_q. (1), expressing it through the resistance ratio of thermocouple R_T and load r.

$$P_{вих} = \frac{E_T^2}{R_T} \frac{1}{\left(m+2+\frac{1}{m}\right)} \quad (2)$$

where $m = \frac{r}{R_t}$ where $m=r/R_T$

Fig. 2 shows a plot of the maximum thermocouple power w versus m, where for convenience the values of E_T and R_T are taken to be 1.

As can be seen from Fig. 2, the maximum load power is observed at m = 1.

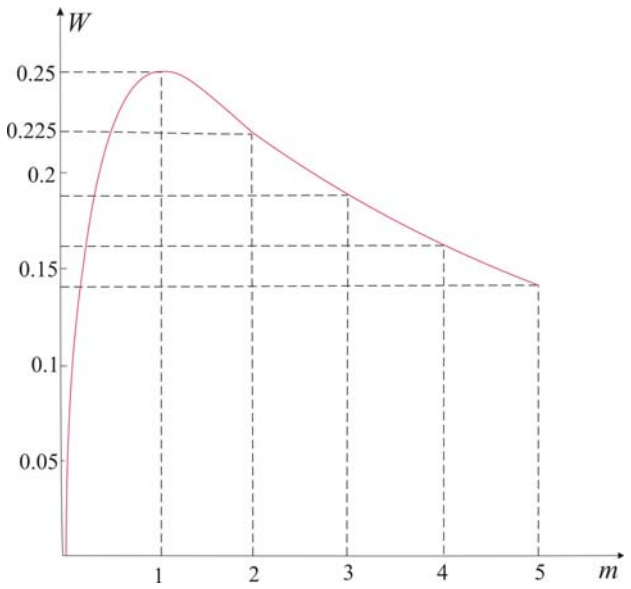

Fig. 2. The plot of w versus m

Optimization of heater and thermocouple

A significant increase in the volt-watt sensitivity of thermal converter can be achieved by improving the efficiency of using the heat generated by the heater. In [4], the option of using a heater with a variable resistance along the length was studied, with the aim of maximizing the concentration of heat at the point of contact between the heater and the thermocouple junction. According to estimates made in [4], this approach allows increasing the temperature at the point of contact between the thermocouple junction and the heater by almost a factor of two. Based on these research results, several thermal converter designs with heaters of variable cross section were created. Such thermal converters were studied in the air, in xenon, and in vacuum on a VUP-4A unit at a pressure of 10^4 mm Hg. The experimental results are shown in Table 1. For comparison, Table 1 presents the parameters of the product adopted as an analogue, namely thermal converter 2101.

Table

Parameters of thermal converter

Type or design of thermal converter	Average parameters of thermal converter							
	R_n, Ohm not more	R_T, Ohm not more	E_T in the air not less	S_w in the air V/W	E_T in xenon, mV	S_w in xenon, mV	E_T in vacuum, mV	S_w, in vacuum, mV
Thermal converter 2401 (АЮЖ 3.360.009 ТУ)	12	7	-	-	8	8	-	-
Thermal converter with a profile heater	16	10	3.0	7.5	5.2	13	7.2	18
Thermal converter with a prefabricated heater	16	10	2.8	7	4.4	11	6.4	16
Thermal converter with increased thermocouple resistance	16	20 40	3.2 3.6	8 9	6.0 7.2	15 12	8.8 12	22 90

Table shows that a significant increase in the volt-watt sensitivity of thermal converter can be achieved by evacuating its working volume. However, in this case, the problem is the availability of a vacuum-tight case for thermal converter. Nevertheless, creating such a case will not solve the problem. A number of studies will have to be carried out under vacuum conditions, which may require the development of new technology for the production of such material and methods for its investigation.

From the standpoint of practical applications, an interesting variant is the design of thermal converter with increased thermocouple resistance. As can be seen from Table 1, the sensitivity of such thermal converter at R_T = 40 Ohm reaches 30 V/W significantly exceeding the sensitivity of thermal converters, in which the thermocouple has R_T = 10 Ohm.

The problem with the widespread use of high-resistance thermal converters is the technological complexity of manufacturing microminiature thermocouples with a cross-section of legs at the level of 15 × 15 microns. Currently, the technology for manufacturing such products is mainly based on the use of manual labor.

Conclusion

1. The dependence of thermal converter sensitivity on the mutual arrangement of the heater thermocouple and housing for the thermal converter 46014 is established.
2. When matching the load and thermocouple resistances, high metrological parameters of thermal converter are achieved when their resistance ratio m is within $0.6 \leq m \leq 2$.

References

1. Mykytiuk P.D., Mykytiuk O.Yu. (2019). In reference to the choice of thermocouple material for metrological-purpose thermal converters. *J.Thermoelectricity*.

2. Mykytiuk P.D., Mykytiuk O.Yu. (2018). Impact of thermocouple on temperature distribution in the heater of measuring thermal converter. *J.Thermoelectricity*, 1, 64–59.
3. Anatychuk L.I. (1979). *Termoelementy i termoelektricheskiie ustroistva [Thermoelements and thermoelectric devices]*. Kyiv: Naukova dumka [in Russian].
4. Mykytiuk P.D., Mykytiuk O.Yu. (2018). Temperature distribution in a heater with a resistance variable along its length in thermoelectric converter. *J.Thermoelectricity*, 2, 79–74.

Submitted 18.07.19

Микитюк П.Д. *канд. фіз.-мат. наук*[1,2]
Микитюк О.Ю. *канд. фіз.- мат. наук, доцент*[3]

[1]Інститут термоелектрики НАН і МОН України,
вул. Науки, 1, Чернівці, 58029, Україна,
e-mail: anatych@gmail.com;
[2]Чернівецький національний університет
імені Юрія Федьковича, вул. Коцюбинського 2,
Чернівці, 58012, Україна,
[3]Вищий державний навчальний заклад України
«Буковинський державний медичний університет»,
Театральна площа, 2, Чернівці, 58012, Україна

ПРО ДЕЯКІ ВАРІАНТИ ПОКРАЩЕННЯ ПАРАМЕТРІВ ТЕРМОЕЛЕКТРИЧНИХ ПЕРЕТВОРЮВАЧІВ

Досліджено залежність чутливості термоперетворювача від взаємного розташування його конструктивних елементів. Підтверджено важливість оптимального узгодження опору термопари з опором нагрівника для кожного конкретного застосування термоперетворювача та доцільність оптимізації елементів його конструкції. Бібл. 4, рис. 2, табл. 1
Ключові слова: термоелектричний перетворювач, термопара, нагрівник, чутливість.

Микитюк П.Д. *канд. физ.-мат. наук*[1,2]
Микитюк О.Ю. *канд. физ.- мат. наук, доцент*[3]

[1]Институт термоэлектричества НАН и МОН Украины,
ул. Науки, 1, Черновцы, 58029, Украина, *e-mail: anatych@gmail.com*;
[2]Черновицкий национальный университет
имени Юрия Федьковича, ул. Коцюбинского 2,
Черновцы, 58012, Украина
[3]Высшее государственное учебное заведение Украины
«Буковинский государственный медицинский университет»,
Театральная площадь, 2, Черновцы, 58002, Украина

О НЕКОТОРЫХ ВАРИАНТАХ УЛУЧШЕНИЯ ПАРАМЕТРОВ ТЕРМОЭЛЕКТРИЧЕСКИХ ПРЕОБРАЗОВАТЕЛЕЙ

Исследована зависимость чувствительности термопреобразователя от взаимного расположения его конструктивных элементов. Подтверждена важность оптимального согласования сопротивления термопары с сопротивлением нагревателя для каждого конкретного применения термопреобразователя и целесообразность оптимизации элементов его конструкции. Библ. 4,Рис. 2, табл. 1.

.**Ключевые слова**: термоэлектрический преобразователь, термопара, нагреватель, чувствительность.

References

1. Mykytiuk P.D., Mykytiuk O.Yu. (2019). In reference to the choice of thermocouple material for metrological-purpose thermal converters. *J.Thermoelectricity*.
2. Mykytiuk P.D., Mykytiuk O.Yu. (2018). Impact of thermocouple on temperature distribution in the heater of measuring thermal converter. *J.Thermoelectricity*, 1, 64–59.
3. Anatychuk L.I. (1979). *Termoelementy i termoelektricheskiie ustroistva [Thermoelements and thermoelectric devices]*. Kyiv: Naukova dumka [in Russian].
4. Mykytiuk P.D., Mykytiuk O.Yu. (2018). Temperature distribution in a heater with a resistance variable along its length in thermoelectric converter. *J.Thermoelectricity*, 2, 79–74.

Submitted 18.07.19

Anatychuk L.I., *acad. National Academy of Sciences of Ukraine*[1,2]
Lysko V.V. *cand. phys.- math. sciences* [1,2]


Anatychuk L.I.

[1]Institute of Thermoelectricity of the NAS
and MES of Ukraine,
1, Nauky str., Chernivtsi, 58029, Ukraine;
[2]Yu.Fedkovych Chernivtsi National University,
2, Kotsiubynskyi str., Chernivtsi, 58000, Ukraine,
e-mail: anatych@gmail.com


Lysko V.V.

ON THE POSSIBILITY OF USING THERMOELECTRIC GENERATORS FOR HIGH-POWER TRANSPORT STARTING PRE-HEATERS

The main reasons for the complicated start-up of vehicles at low ambient temperatures are analyzed. The advantages and disadvantages of using pre-heating to improve engine start-up are identified. The principle of operation and design features of general-purpose pre-heaters and pre-heaters for armored vehicles are given. The rationality of using thermoelectric generators for the operation of such equipment is substantiated. The results of studies on the thermodynamic features of preheating systems for an internal combustion engine, in which the sources of electricity are thermoelectric generators, are presented. The physical schemes of the "pre-heater-thermogenerator" systems are considered and their energy characteristics are evaluated. The most effective applications of thermoelectric sources of electricity for engine start training for operation are determined. Bibl. 32, Fig. 3, Tabl. 1.
Key words: starting pre-heater, thermoelectric generator, physical model, efficiency.

Introduction

To overcome the difficulties associated with operating cars at low temperatures, various means of thermal pre-training of internal combustion engines (ICE) are increasingly used [1, 2]. The most effective of these are starting pre-heaters, namely flame sources of heat that run on the fuel of cars and heat the engine coolant. To overcome the difficulties associated with the operation of automobiles at low temperatures, various means of thermal pre-training of internal combustion engines (ICE) are increasingly used [1, 2]. The most effective among such means are starting pre-heaters, namely flame heat sources that run on automobile fuel and carry out heating of the engine coolant. In addition to a reliable start of the internal combustion engine, the use of starting pre-heaters creates conditions for saving on average about 90-150 liters of fuel per season, reduces the toxicity of exhaust gases during engine warming up to 5 times and allows increasing engine life by 200-300 km per start when heated from temperature (-20 ÷ -30) ° C [3, 4].

Pre-heating of the engine is also important for large-size equipment, including that of military purpose. The main reasons that make it difficult to start armored vehicles at low ambient temperatures are:

1. Increasing the viscosity of engine oil on the parts of connecting rod and piston group of an internal combustion engine (ICE).

2. Lubricant viscosity increase in transmission units.

3. Freezing of fuel in fuel lines, fuel filter and other parts of the fuel system.

4. Deterioration of fuel ignition conditions in engine cylinders, which is associated with a decrease in its volatility and low temperatures of air entering the internal combustion engine cylinders from the environment.

5. Freezing of heat carrier in the engine cooling system.

6. Decrease in the power of starter generator due to the reduced capacity of the batteries.

7. The excessive consumption of fuel during the cold start of the internal combustion engine, which is not always available in the places of military operations.

The influence of these factors at low temperatures is manifested simultaneously, which leads to a reduction in engine life and premature failure of combat armored vehicles. This significantly increases the likelihood of sudden violations and failures in the operation of the equipment.

The determining factor limiting the possibility of mass use of starting pre-heaters is the discharge of the battery during operation of the pre-heat equipment [5].

One of the promising methods for solving the problem of battery discharge during thermal preparation of vehicle engines for launch is the use of thermoelectric generators as sources of electric energy for starting pre-heaters [6 - 12]. This idea is the basis of research pursued at the Institute of Thermoelectricity, aimed at creating thermoelectric pre-heat sources for engines of passenger cars [13 – 16]. As a result of the research, an experimental sample of a thermoelectric diesel engine pre-heater with a thermal power of 3 kW was developed for pre-heating of internal combustion engines up to 4 liters. The heater contains a thermoelectric generator with an electric power of 80 - 100 W, which operates from the heat of the starting pre-heater and provides power to its components. In addition, the excess electric energy of the thermogenerator can be used to recharge the car battery, which was confirmed by experimental tests of the heater in bench conditions [17].

The purpose of this work is to analyze the feasibility of using thermoelectric generators for high-power transport starting pre-heaters, in particular for armored vehicles and to select the most efficient physical scheme for creating such generators.

Brief description of high-power heaters

Modern starting pre-heaters with a thermal power from 15 kWfor diesel engines are presented in Table 1. The leading companies in this direction are Webasto and Eberspächer (Germany), Teplostar and Shardrinsk Automotive Components Plant (Russian Federation), PROHEAT (Canada) [18-31].

Company Webasto (Germany) produces starting pre-heaters with a thermal power up to 35 kW [18, 19]. The electric energy consumption of such heaters is 90-170 W without regard to the power of circulation pump. In so doing, the electric power of recommended circulation pumps of the type U 4814 is 104 W, of the type U 4851 – 209 W. Therefore, total electric energy consumption of starting pre-heaters from Webasto with a thermal power 16 - 35 kW is from 194 to 379 W.

Table 1

Starting pre-heaters with a thermal power from 15 kW for diesel engines

Manufacturer	Model	Output thermal power, kW	Electric power consumption, W	Fuel consumption, l/h
Webasto (Germany)	DBW 160	16	90*	2.3

continuation of table

	DBW 230	23.3	110*	3.0
	DBW 300	30	130*	4.0
	DBW 350	35	170*	4.4
	* - without circulation pump (electric power consumption of recommended circulation pumps of the type *U* 4814 – 104 Вт, *U* 4851 – 209 W)			
Eberspächer (Germany)	Hydronic L 16	16	60**	2
	Hydronic L 24	24	80**	2.9
	Hydronic L 30	30	105**	3.7
	Hydronic L 35	35	120**	4.2
	** - without circulation pump (electric power consumption of recommended circulation pumps of the type Flowtronic 5000 – 104 W, Flowtronic 6000 SC – 210 W)			
Teplostar (RF)	14 ТС-10	15	132	2
	20 ТС-Д38	20	200	2.5
	АПЖ – 30Д-24	30	336	3.7
JSC “Shadrinsk Automotive Components Plant” (RF)	ПЖД24Б	24	170	3.8
	ПЖД30	30	340	5
	ПЖД30Г	30	340	5
	ПЖД30Е	30	340	5
	ПЖД30Л	30	340	5
	ПЖД30М	30	340	5
	ОЖД30.8106010	30	140	3.8
	ПЖД44Ш	37	340	8.5
	ПЖД600	58	490	11.4
PROHEAT (Canada)	M50 12V	15	114***	1.8
	M50 24V	15	125***	1.8
	M80 12V	23	102***	3
	M80 24V	23	125***	3
	M90 24V	26	125***	3.1
	M105 24V	31	228***	4
	M125 24V	37	228***	4.2
	*** - without circulation pump			

Company Eberspächer (Germany) produces *L*-series starting pre-heaters with a thermal power of 16 to 35 kW [20, 21]. The consumed electric power of such heaters is 60-120 W, without regard to the power of the circulation pump.

Hydronic *L* heaters are the most powerful liquid heaters from Eberspächer. Designed for installation on vehicles with large engine displacement and large interior, Hydronic *L* 30 / 35kW are available with both spaced and compact version with integrated components: water pump, fuel filter, which saves time on installation. The heater is capable of operating both on diesel fuel and on fuel oil.

The electric power of the recommended circulation pumps: type Flowtronic 5000 - 104 W, Flowtronic 6000 SC - 210 W. Thus, the total energy consumption of the Eberspächer Hydronic *L* Series Pre-Heater is from 164 to 330 watts.

The Russian company Teplostar produces three models of starting pre-heaters with thermal power from 15 to 30 kW - 14TS-10, 20 TS-D38, АПЖ - 30Д-24 [22-24]. The electric power consumption of such heaters is 132-336 watts.

Shadrinsk Automotive Components Plant (RF) produces starting pre-heaters with thermal power up to 58 kW [25-29]. The electric power consumption of heaters with thermal power from 24 to 58 kW is 170-490 W.

Company PROHEAT (Canada) produces starting pre-heaters of M-series with thermal power from 15 to 37 kW [30]. The electric power consumption of such pre-heaters is 114 - 128 W without taking into account the power of circulation pump.

Thus, up to 500 W of electrical energy is required to operate starting pre-heaters shown in Table 1.

Starting pre-heater in armored vehicles is used to heat the coolant in the cooling system and the oil in the circulation tank before starting the engine [31]. It is installed in the fighting compartment of the tank and consists of a boiler and mechanisms for supplying and burning fuel (fuel pump, fan, nozzle, glow plug), a water pump and gearbox with manual and electric drives.

The boiler is a cylindrical heater, all-welded stainless steel construction, consisting of a body, a flame tube and a coil box.

The boiler body and the flame tube have double cylindrical walls between which internal cavities are formed, filled with coolant (boiler water space). The internal cavities of the body and the flame tube are interconnected by four tubes.

The inner front part of the boiler body together with the conical cover forms the boiler furnace, and the rear part forms the gas chamber. An exhaust pipe is welded from below to the boiler body, which discharges combustion products through an opening in the tank bottom to the outside. A box is welded on top of the body, which contains a coil for heating the fuel. The heated liquid enters from the boiler body into the coil box through an opening located in the upper part of the body.

The pump assembly of the heater includes a water pump; fan, fuel pump and gearbox with manual and electric actuators. This whole assembly is mounted in a common crankcase.

The centrifugal type water pump is used for forced circulation if the coolant in the heating system. A centrifugal fan delivers the air necessary for the combustion of fuel in the boiler furnace. The plunger type fuel pump delivers fuel to the nozzles of the heater. The control of the pumping unit can be carried out mechanically using a manual drive and electrically from an electric motor.

The centrifugal heater nozzle is designed to spray fuel in the furnace of the boiler, which is ignited by the spark plug. The spark plug is powered by a 24V battery. In the event of a spark plug failure, the fuel can be ignited by a torch through the upper right hole of the cone, which is closed by a plug.

To disconnect the heater from the cooling system (for the summer period of operation of the tank), a heater shut-off valve is installed.

During the operation of the heater, the coolant under the action of the water pump of the heater is fed through the pipeline and branched into four parallel streams.

The first flow passes through the engine, heats the cylinder heads and blocks and returns to the heater through the water pump.

The second flow passes through the pipeline into the coil of the circulating oil tank, heats the oil in the circulation tank and returns to the heater boiler through the housing of the intake oil pipeline.

The third flow passes through the water radiator through the water pump of the engine and by the pipeline returns to the boiler of the heater.

The fourth flow passes from the discharge pipe of the heater through the pipe into the cavity of the oil pump. From the pump, the liquid enters the casing of the intake pipe of the pump and then into the boiler of the heater. In the boiler, the liquid is heated and circulated again through the above flows.

Thus, in comparison with the pre-heater for traditional vehicles, the nozzle tank pre-heater has a number of design and functional differences, which makes it more reliable and efficient.

Such and improved nozzle starting pre-heaters with a thermal power of 30-70 kW are installed on many tanks developed by the former USSR - T-55, T-64, T-64A, T-72, etc. [32].

In modern armored personnel carriers, starting pre-heaters are installed, which are also used for other civilian vehicles - trucks, buses and special equipment with a liquid cooling system.

Since electric energy is needed to power the main functional components of starting liquid pre-heaters, its source is the battery of an armored vehicle. At low temperatures (-20 ÷ -40 ° C), the battery capacity decreases by 2 to 3 times, which creates problems in providing electric energy to both starting pre-heaters and other equipment that should work when the engine is not running. This situation creates risks when starting armored vehicles, so in practice it often becomes necessary to warm up engines without using starting pre-heaters - blowtorches, hot water, tank stoves, etc. In combat conditions, this creates significant problems in the operation of armored vehicles. Therefore, despite the advantages in the use of liquid starting pre-heaters, consisting, in particular, in increasing the engine life and saving fuel when starting it, the use of heaters still remains problematic due to their non-autonomous operation.

Some time ago, there were attempts to solve the problem of non-autonomous operation of starting pre-heaters by using a gas turbine internal combustion engine in combination with a dynamo, which is used to power the battery during start pre-heating. However, the main disadvantage of such a system is the increased noise level and high temperatures of the combustion products, which is an unmasking factor in the conditions of military operations.

To overcome this problem, it is promising to use thermoelectric sources of heat and electricity, which, in addition to pre-heating, supply the functional components of the heaters. Therefore, they do not need battery power to power them.

To use such sources of heat and electricity in order to improve the operational capabilities of armored military equipment, the electric power of the thermal generator 300-500 watts is necessary. Such thermoelectric devices have a high service life, are reliable and resistant to mechanical loads and meet the requirements for their use in military equipment.

In 1958-1969, works on the creation of a tank heater with a thermoelectric generator were carried out at VNII-100 [32]. The work was carried out jointly with the Institute of Semiconductors of the USSR Academy of Sciences and the Kalinin LPI. The TEG was supposed to provide an electrical power of approximately 500 watts, which would allow the tank crew to maintain the machine in standby mode, heat the living compartment, heat the batteries and spend some of the electricity on recharging the batteries or for running the radio station without starting the main engine. The heater had a thermal power of about 72 kW and an electrical power of 340 watts. Work on the improvement of TEG in the USSR lasted until the mid-1980's.

Physical schemes of starting pre-heaters and their analysis

Fig. 1 shows a physical model of system for start heating of engines that comprises liquid starting pre-heater and thermoelectric generator heat supply to which is carried out individually with the use of separate heat sources.

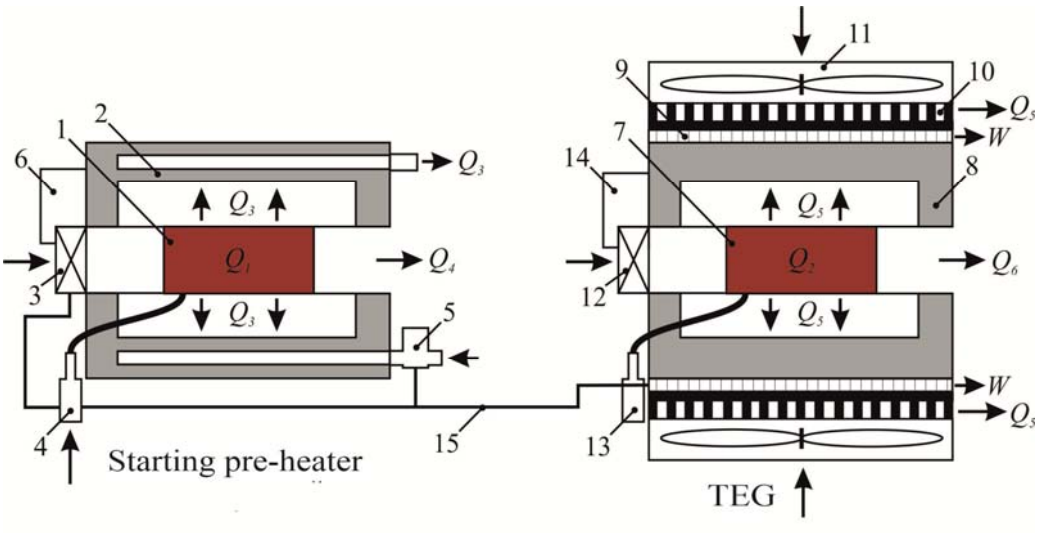

Fig. 1. Physical model of "staring pre-heater—thermoelectric generator" system with individual heat sources : 1 –starting pre-heater burner; 2 – heat exchanger; 3 – starting pre-heater air fan; 4 – starting pre-heater fuel pump; 5 – circulation pump; 6 – starting pre-heater electronic unit; 7 – thermogenerator burner; 8 –hot heat exchanger; 9 –thermopile; 10 – air radiator; 11 – fan for heat removal; 12 – thermogenerator air fan; 3 – thermogenerator fuel pump; 14 – thermogenerator electronic unit; 15 – electric connection means.

Liquid starting pre-heater is composed of heat source 1 which is in the internal volume of heat exchanger 2. As a heat source, a flame burner was used, air and fuel to which are supplied by a fan 3 and a pump 4.

In the heat exchanger of the heater, channels are made in which the heat carrier is heated, following which, by pumping with the circulation pump 5, it enters the car engine. Starting and controlling the operation of starting pre-heater components (air fan, fuel pump, circulation pump) is carried out by the electronic unit 6.

The thermoelectric generator contains an individual flame burner 7, a hot heat exchanger 8 for supplying heat to the thermopile 9 and a heat removal system, which consists of air radiators 10 and fans 11. The fuel and air are supplied to the heat source of the heat generator by the fan 12 and the fuel pump 13. To stabilize the output voltage of the thermogenerator and control its operation, an electronic unit 14 is provided in the TEG model.

The thermoelectric generator operates as follows. The thermal energy resulting from the combustion of fuel heats the hot heat exchanger, passes through the thermopile and is discharged into the environment. Due to the temperature difference between the hot and cold sides of the thermopile, an electric current is generated to power the pre-heater.

Thus, the system under consideration provides the starting pre-heater with the necessary electric energy, practically without using a battery. However, such a system can also perform additional functions, in particular, a thermogenerator can be used as an auxiliary source of electrical energy. This energy can be employed, if necessary, to charge the battery or other energy supply needs, for example, to power various additional electrical devices.

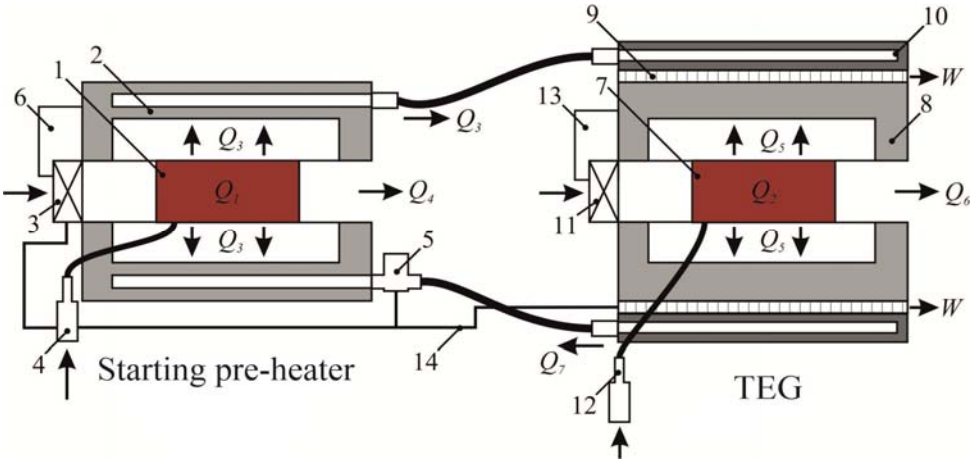

Fig. 2. Physical model of "starting pre-heater-thermoelectric generator" system with individual heat sources and a joint hydraulic circuit:
1 – starting pre-heater burner; 2 – heat exchanger; 3 – starting pre-heater air fan;
4 – staring pre-heater fuel pump; 5 – circulation pump;
6 – starting pre-heater electronic unit; 7 – thermogenerator burner;
8 – hot heat exchanger; 9 – thermopile; 10 – cold liquid heat exchanger;
11 – thermogenerator air fan; 12 –thermogenerator fuel pump;
13 –thermogenerator electronic unit; 14 – electric connection means.

Fig. 2 shows a diagram of the "pre-heater-thermoelectric generator" system, which combines the pre-heater and thermoelectric generator with a single hydraulic circuit. In this regard, in the cooling system of the thermogenerator, the air radiators and fans for removing heat from the thermopile are replaced by liquid heat exchangers 10 in which the heat carrier circulates.

Since the heat flux Q7, removed from the thermopile, is expended for heating the heat carrier, this system allows the engine to be preheated both with a starting pre-heater and using a thermoelectric generator.

The physical model of the system (Fig. 3) with a joint heat source comprises a hot heat exchanger 1, the internal volume of which accommodates a burner 2. Fuel and air delivery to the burner is realized by fan 3 and fuel pump 4. On the external surface of the hot heat exchanger there is a thermopile 5, the heat from which is removed by heating liquid circulating in the cold heat exchangers 6 by pumping with liquid pump 7. The start and control of the heater is carried out by the electronic unit 8.

Thus, in the above system, the thermoelectric generator and the pre-heater are combined in a single design, which allows you to obtain electric energy and heat the engine with one heat flow Q. In this case, part of the heat Q_1 is carried by the combustion products into the environment, and heat Q_2, in the form of heat Q_3 , and electric W power, is used to warm the engine and power the heater components, and, if necessary, to recharge the battery during preheating.

The highest values of efficiency are characterized by "thermoelectric generator-starting pre-heater" system with a joint source of heat and a system in which the starting pre-heater and TEG are combined by a hydraulic circuit. Obviously, a system with a joint heat source is cheaper, which makes it more efficient to use. At the same time, a system with a single hydraulic circuit can be more versatile. As a thermoelectric generator for such a case, a separate thermoelectric pre-heater of low thermal power can be used, the electric output power of which is enough to power the main pre-heater. Such a heater can be installed separately, in an accessible place of an armored vehicle, which makes its implementation easier.

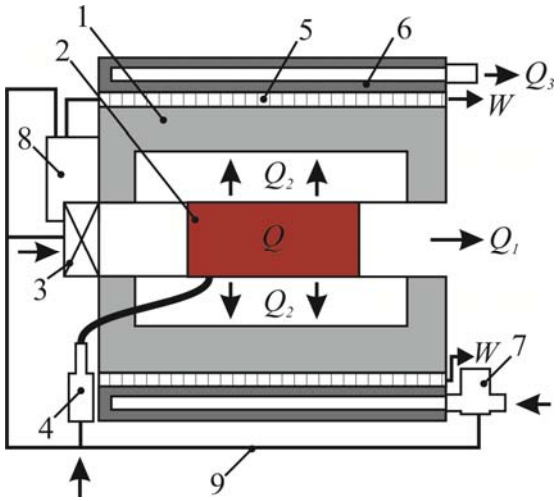

Fig. 3. Physical model of "starting pre-heater –thermoelectric generator" system with a joint heat source: 1 – starting pre-heater burner; 2 – hot heat exchanger; 3 – starting pre-heater air fan; 4 – starting pre-heater fuel pump; 5 –thermopile; 6 – cold liquid heat exchanger; 7 – starting pre-heater circulation pump; 8 – electronic unit; 9 – electric connection means.

Conclusions

1. The design features of general-purpose starting pre-heaters and high-power starting pre-heaters are considered. The possibility of using thermoelectric generators for the operation of such equipment is justified. The necessary electric power of such generators is determined – up to 500 W.
2. Physical schemes of starting pre-heaters with thermoelectric sources of electricity are considered. The most rational for start heating of internal combustion engines is "starting pre-heater-thermoelectric generator" system with a joint heat source and a system that combines starting pre-heater and thermogenerator with one hydraulic circuit.

References

1. Kuznetsov E.S., Boldin A.P., Vlasov V.M., et al. (2001). *Tekhnicheskaia eksplustatsiia avtomobilei. Uchebnik dlia vuzov. 4 izdaniie, pererabotannoie i dopolnennoie [Technical operation of cars. College textbook. 4th ed., revised and enlarged]*. Moscow: Nauka [in Russian].
2. Reznik L.G., Romalis G.M., Charkov S.T. (1989*). Effektivnost ispolzovaniia avtomobilei v razlichnykh usloviiakh ekspluatatsii [Efficiency of using cars in various operating conditions]*. Moscow: Transport [in Russian].
3. Matiukhin L.M. (2009). *Teplotekhnicheskiie ustroistva avtomobilei: uchebnoie posobiie [Thermotechnical devices of cars: Manual]*. Moscow: MADI [in Russian].
4. Naiman V.S. (2007). Vse o predpuskovykh obogrevateliakh i opotiteliakh [All about starting pre-heaters]. Moscow: ACT [in Russian].
5. Mykhailovsky V.Ya., Maksimuk M.V. (2015). Automobile operating conditions at low temperatures. The necessity of applying heaters and the rationality of using thermal generators for their work]. *J. of Thermoelectricity*, 3, 20–31.

6. *Patent of Ukraine № 102303* (2013). Anatychuk L.I., Mykhailovsky V.Ya. Thermoelectric power supply for automobile [in Ukrainian].
7. *Patent of Ukraine №72304* (2012). Anatychuk L.I., Mykhaolovsky V.Ya. Automobile heater with a thermoelectric power supply [in Ukrainian].
8. *Patent of Ukraine №124999* (2018). Maksimuk M.V. Automobile heater with a thermoelectric power supply [in Ukrainian].
9. *Pat. US6527548B1* (2003). Kushch Aleksandr S., Allen Daniel. Self-powered electric generating space heater.
10. *Pat. US2010/0115968A1*. Budde John, Baade Jeans, Stelter Michael. Heating apparatus comprising a thermoelectric device.
11. *Patent (RU) 2268393C1* (2006). Prilepo Yu.P. Device for facilitating internal combustion engine start [in Russian].
12. Mykhailovsky V.Ya., Maksimuk M.V. (2015). Rational powers of thermal generators for starting pre-heaters of vehicles. *J.Thermoelectricity*, 4, 65-74.
13. Maksimuk M.V. (2017). On the optimization of thermoelectric modules of automobile starting pre-heater. *J.Thermoelectricity*, 1, 57–67.
14. Maksimuk M.V. (2017). Design of automobile starting pre-heater with a thermoelectric generator. Diesel version. *J.Thermoelectricity*, 2, 32-43.
15. Maksimuk M.V. (2017). Design of automobile starting pre-heater with a thermoelectric generator. *Visnyk NTUU KPI. Series INSTRUMENTATION*, 54(2), 53-60.
16. Maksimuk M.V. (2018). Bench tests of thermoelectric starting pre-heater for cars. *J.Thermoelectricity,* 1, СТОР?
17. Webasto.WEB-site: https://www.webasto.com.
18. Liquid heater DBW 160/230/300/350. Assembly instruction.
19. Eberspächer. WEB-site: https://www.eberspacher.com.
20. Autonomous heating devices HYDRONIC L-II. Technical description, assembly, operation and maintenance instruction.
21. "TEPLOSTAR" Ltd. WEB-site: https://teplostar.inni.info.
22. Diesel starting pre-heater 14ТС – 10 – М5. Operation instruction АДВР.036.00.00.000 РЭ.
23. Diesel starting pre-heater 20ТС-Д38. Operation instruction АДВР.038.00.00.000 РЭ.
24. Automated liquid pre-heater АПЖ – 30Д-24. Operation instruction АДВР.056.00.00.000 РЭ.
25. JSC "Shandrinsk Automotive Components Factory". WEB-site: http://shaaz.biz.
26. Diesel pre-heaters ПЖД24Б. Operation instruction ПЖД24Б - 1015006 - 30 РЭ.
27. Diesel liquid pre-heater ПЖД30. Operation instruction ПЖД30-1015006 РЭ.
28. Autonomous liquid heater ОЖД30.8106010. Operation instruction ОЖД30.8106010 РЭ.
29. Liquid pre-heater of the type ПЖД600, ПЖД44Ш. Operation instruction ПЖД600-1015008 РЭ.
30. PROHEAT. WEB-site: http://www.proheat.com.
31. Rukovodstvo po materialnoi chasti i ekspluatatsii tanka T-54 [Guidance on the material part and operation of tank T-54]. Moscow: Military Publ. of the USSR Defense Ministry, 1969 (in Russian).
32. Pavlov M.V. (2009). *Otechestvennyie bronirovannyie mashiny 1945-1965 (XVII) [Home armoured machines1945–1965 (XVII)]. Tekhnika i vooruzheniie. Vchera, segodnia, zavtra… - Equipment and Weapons. Yesterday, today, tomorrow…"* 11, 2009[in Russian].

Submitted 05.06.2019

Анатичук Л.І. *акад. НАН України*,[1,2]
Лисько В.В. *канд. фіз. – мат. наук*[1,2]

[1]Інститут термоелектрики НАН і МОН України,
вул. Науки, 1, Чернівці, 58029, Україна;
[2]Чернівецький національний університет
ім. Юрія Федьковича, вул. Коцюбинського 2,
Чернівці, 58000, Україна,
e-mail: anatych@gmail.com

ПРО МОЖЛИВІСТЬ ВИКОРИСТАННЯ ТЕРМОЕЛЕКТРИЧНИХ ГЕНЕРАТОРІВ ДЛЯ ТРАНСПОРТНИХ ПЕРЕДПУСКОВИХ НАГРІВАЧІВ ВЕЛИКИХ ПОТУЖНОСТЕЙ

Проаналізовано основні причини ускладненого запуску транспортних засобів за понижених температур навколишнього середовища. Визначено переваги та недоліки в застосуванні передпускового підігріву для покращення запуску двигуна автомобілів. Наведено принцип роботи та особливості конструкції передпускових нагрівачів загального використання та передпускових нагрівачів для бронетехніки. Обґрунтовано раціональність використання термоелектричних генераторів для роботи такого обладнання. Наведено результати досліджень термодинамічних особливостей систем передпускового розігріву двигуна внутрішнього згорання, в яких джерелами електричної енергії є термоелектричні генератори. Розглянуто фізичні схеми систем «передпусковий нагрівник –термогенератор» та проведено оцінку їхніх енергетичних характеристик. Визначено найефективніші варіанти застосування термоелектричних джерел електрики для передпускової підготовки двигунів транспортних засобів до експлуатації. Бібл. 32, рис. 3, табл. 1.

Ключові слова: передпусковий нагрівник, термоелектричний генератор, фізична модель, ефективність.

Анатычук Л.И. *акад. НАН Украины*, [1,2]
Лысько В.В. *канд физ. – мат. наук*[1,2]

[1]Институт термоэлектричества НАН и МОН Украины,
ул. Науки, 1, Черновцы, 58029, Украина;
anatych@gmail.com
[2]Черновицкий национальный университет
им. Юрия Федьковича, ул. Коцюбинского 2,
Черновцы, 58000, Украина, e-mail:

О ВОЗМОЖНОСТИ ИСПОЛЬЗОВАНИЯ ТЕРМОЭЛЕКТРИЧЕСКИХ ГЕНЕРАТОРОВ ДЛЯ ТРАНСПОРТНЫХ ПРЕДПУСКОВЫХ НАГРЕВАТЕЛЕЙ БОЛЬШОЙ МОЩНОСТИ

Проанализированы основные причины осложненного запуска транспортных средств по пониженных температур окружающей среды. Определены преимущества и недостатки в применении предпускового подогрева для улучшения запуска двигателя автомобилей. Приведены принцип работы и особенности конструкции предпусковых нагревателей общего пользования и предпусковых нагревателей для бронетехники. Обоснованно рациональность использования термоэлектрических генераторов для работы такого оборудования. Приведены результаты исследования термодинамических особенностей систем предпускового разогрева двигателя внутреннего сгорания, в которых источниками электроэнергии являются термоэлектрические генераторы. Рассмотрены физические схемы систем «предпусковой отопитель - термогенератор» и проведена оценка их энергетических характеристик. Определены наиболее эффективные варианты применения термоэлектрических источников электричества для предпусковой подготовки двигателей транспортных средств к эксплуатации. Библ. 32, рис. 3, табл. 1.

Ключевые слова: предпусковой отопитель, термоэлектрический генератор, физическая модель, эффективность.

References

1. Kuznetsov E.S., Boldin A.P., Vlasov V.M., et al. (2001). *Tekhnicheskaia eksplustatsiia avtomobilei. Uchebnik dlia vuzov. 4 izdaniie, pererabotannoie i dopolnennoie [Technical operation of cars. College textbook. 4th ed., revised and enlarged]*. Moscow: Nauka [in Russian].
2. Reznik L.G., Romalis G.M., Charkov S.T. (1989*). Effektivnost ispolzovaniia avtomobilei v razlichnykh usloviiakh ekspluatatsii [Efficiency of using cars in various operating conditions]*. Moscow: Transport [in Russian].
3. Matiukhin L.M. (2009). *Teplotekhnicheskiie ustroistva avtomobilei: uchebnoie posobiie [Thermotechnical devices of cars: Manual]*. Moscow: MADI [in Russian].
4. Naiman V.S. (2007). Vse o predpuskovykh obogrevateliakh i opotiteliakh [All about starting pre-heaters]. Moscow: ACT [in Russian].
5. Mykhailovsky V.Ya., Maksimuk M.V. (2015). Automobile operating conditions at low temperatures. The necessity of applying heaters and the rationality of using thermal generators for their work]. *J. of Thermoelectricity*, 3, 20–31.
6. *Patent of Ukraine № 102303* (2013). Anatychuk L.I., Mykhailovsky V.Ya. Thermoelectric power supply for automobile [in Ukrainian].
7. *Patent of Ukraine №72304* (2012). Anatychuk L.I., Mykhaolovsky V.Ya. Automobile heater with a thermoelectric power supply [in Ukrainian].
8. *Patent of Ukraine №124999* (2018). Maksimuk M.V. Automobile heater with a thermoelectric power supply [in Ukrainian].
9. *Pat. US6527548B1* (2003). Kushch Aleksandr S., Allen Daniel. Self-powered electric generating space heater.
10. *Pat. US2010/0115968A1*. Budde John, Baade Jeans, Stelter Michael. Heating apparatus comprising a thermoelectric device.
11. *Patent (RU) 2268393C1* (2006). Prilepo Yu.P. Device for facilitating internal combustion engine start [in Russian].
12. Mykhailovsky V.Ya., Maksimuk M.V. (2015). Rational powers of thermal generators for starting pre-heaters of vehicles. *J.Thermoelectricity*, 4, 65-74.
13. Maksimuk M.V. (2017). On the optimization of thermoelectric modules of automobile starting pre-heater. *J.Thermoelectricity*, 1, 57–67.

14. Maksimuk M.V. (2017). Design of automobile starting pre-heater with a thermoelectric generator. Diesel version. *J.Thermoelectricity*, 2, 32-43.
15. Maksimuk M.V. (2017). Design of automobile starting pre-heater with a thermoelectric generator. *Visnyk NTUU KPI. Series INSTRUMENTATION*, 54(2), 53-60.
16. Maksimuk M.V. (2018). Bench tests of thermoelectric starting pre-heater for cars. *J.Thermoelectricity,* 1.
17. Webasto.WEB-site: https://www.webasto.com.
18. Liquid heater DBW 160/230/300/350. Assembly instruction.
19. Eberspächer. WEB-site: https://www.eberspacher.com.
20. Autonomous heating devices HYDRONIC L-II. Technical description, assembly, operation and maintenance instruction.
21. "TEPLOSTAR" Ltd. WEB-site: https://teplostar.inni.info.
22. Diesel starting pre-heater 14ТС – 10 – М5. Operation instruction АДВР.036.00.00.000 РЭ.
23. Diesel starting pre-heater 20ТС-Д38. Operation instruction АДВР.038.00.00.000 РЭ.
24. Automated liquid pre-heater АПЖ – 30Д-24. Operation instruction АДВР.056.00.00.000 РЭ.
25. JSC "Shandrinsk Automotive Components Factory". WEB-site: http://shaaz.biz.
26. Diesel pre-heaters ПЖД24Б. Operation instruction ПЖД24Б - 1015006 - 30 РЭ.
27. Diesel liquid pre-heater ПЖД30. Operation instruction ПЖД30-1015006 РЭ.
28. Autonomous liquid heater ОЖД30.8106010. Operation instruction ОЖД30.8106010 РЭ.
29. Liquid pre-heater of the type ПЖД600, ПЖД44Ш. Operation instruction ПЖД600-1015008 РЭ.
30. PROHEAT. WEB-site: http://www.proheat.com.
31. Rukovodstvo po materialnoi chasti i ekspluatatsii tanka T-54 [Guidance on the material part and operation of tank T-54]. Moscow: Military Publ. of the USSR Defense Ministry, 1969 (in Russian).
32. Pavlov M.V. (2009). *Otechestvennyie bronirovannyie mashiny 1945-1965 (XVII) [Home armoured machines1945–1965 (XVII)]. Tekhnika i vooruzheniie. Vchera, segodnia, zavtra… - Equipment and Weapons. Yesterday, today, tomorrow…"* 11, 2009[in Russian].

Submitted 05.06.2019

ARTICLE SUBMISSION GUIDELINES

For publication in a specialized journal, scientific works are accepted that have never been printed before. The article should be written on an actual topic, contain the results of an in-depth scientific study, the novelty and justification of scientific conclusions for the purpose of the article (the task in view).

The materials published in the journal are subject to internal and external review which is carried out by members of the editorial board and international editorial board of the journal or experts of the relevant field. Reviewing is done on the basis of confidentiality. In the event of a negative review or substantial remarks, the article may be rejected or returned to the author(s) for revision. In the case when the author(s) disagrees with the opinion of the reviewer, an additional independent review may be done by the editorial board. After the author makes changes in accordance with the comments of the reviewer, the article is signed to print.

The editorial board has the right to refuse to publish manuscripts containing previously published data, as well as materials that do not fit the profile of the journal or materials of research pursued in violation of ethical norms (for instance, conflicts between authors or between authors and organization, plagiarism, etc.). The editorial board of the journal reserves the right to edit and reduce the manuscripts without violating the author's content. Rejected manuscripts are not returned to the authors.

Submission of manuscript to the journal

The manuscript is submitted to the editorial office of the journal in paper form in duplicate and in electronic form on an electronic medium (disc, memory stick). The electronic version of the article shall fully correspond to the paper version. The manuscript must be signed by all co-authors or a responsible representative.

In some cases it is allowed to send an article by e-mail instead of an electronic medium (disc, memory stick).

English-speaking authors submit their manuscripts in English. Russian-speaking and Ukrainian-speaking authors submit their manuscripts in English and in Russian or Ukrainian, respectively. Page format is A4. The number of pages shall not exceed 15 (together with References and extended abstracts). By agreement with the editorial board, the number of pages can be increased.

To the manuscript is added:

1. Official recommendation letter, signed by the head of the institution where the work was carried out.

2. License agreement on the transfer of copyright (the form of the agreement can be obtained from the editorial office of the journal or downloaded from the journal website – Dohovir.pdf). The license agreement comes into force after the acceptance of the article for publication. Signing of the license agreement by the author(s) means that they are acquainted and agree with the terms of the agreement.

3. Information about each of the authors – full name, position, place of work, academic title, academic degree, contact information (phone number, e-mail address), ORCID code (if available). Information about the authors is submitted as follows:

authors from Ukraine - in three languages, namely Ukrainian, Russian and English;

authors from the CIS countries - in two languages, namely Russian and English;

authors from foreign countries – in English.

4. Medium with the text of the article, figures, tables, information about the authors in electronic form.

5. Colored photo of the author(s). Black-and-white photos are not accepted by the editorial staff. With the number of authors more than two, their photos are not shown.

Requirements for article design

The article should be structured according to the following sections:

- *Introduction*. Contains the problem statement, relevance of the chosen topic, analysis of recent research and publications, purpose and objectives.
- *Presentation of the main research material* and the results obtained.
- *Conclusions* summing up the work and the prospects for further research in this direction.
- *References*.

The first page of the article contains information:

1) in the upper left corner – UDC identifier (for authors from Ukraine and the CIS countries);

2) surname(s) and initials, academic degree and scientific title of the author(s);

3) the name of the institution where the author(s) work, the postal address, telephone number, e-mail address of the author(s);

4) article title;

5) abstract to the article – not more than 1 800 characters. The abstract should reflect the consistent logic of describing the results and describe the main objectives of the study, summarize the most significant results;

6) key words – not more than 8 words.

The text of the article is printed in Times New Roman, font size 11 pt, line spacing 1.2 on A4 size paper, justified alignment. There should be no hyphenation in the article.

Page setup: "mirror margins" – top margin – 2.5 cm, bottom margin – 2.0 cm, inside – 2.0 cm, outside – 3.0 cm, from the edge to page header and page footer – 1.27 cm.

Graphic materials, pictures shall be submitted in color or, as an exception, black and white, in .opj or .cdr formats, .jpg or .tif formats being also permissible. According to author's choice, the tables and partially the text can be also in color.

Figures are printed on separate pages. The text in the figures must be in the font size 10 pt. On the charts, the units of measure are separated by commas. Figures are numbered in the order of their arrangement in the text, parts of the figures are numbered with letters – a, b, .. On the back of the figure, the title of the article, the author (authors) and the figure number are written in pencil. Scanned images and graphs are not allowed to be inserted.

Tables are provided on separate pages and must be executed using the MSWord table editor. Using pseudo-graph characters to design tables is inadmissible.

Formulae shall be typed in Equation or MatType formula editors. Articles with formulae written by hand are not accepted for printing. It is necessary to give definitions of quantities that are first used in the text, and then use the appropriate term.

Captions to figures and tables are printed in the manuscript after the references.

Reference list shall appear at the end of the article. References are numbered consecutively in the order in which they are quoted in the text of the article. References to unpublished and unfinished works are inadmissible.

Attention! In connection with the inclusion of the journal in the international bibliographic abstract database, the reference list should consist of two blocks: CITED LITERATURE and REFERENCES (this requirement also applies to English articles):

CITED LITERATURE – sources in the original language, executed in accordance with the

Ukrainian standard of bibliographic description DSTU 8302:2015. With the aid of VAK.in.ua (http://vak.in.ua) you can automatically, quickly and easily execute your "Cited literature" list in conformity with the requirements of State Certification Commission of Ukraine and prepare references to scientific sources in Ukraine in understandable and unified manner. This portal facilitates the processing of scientific sources when writing your publications, dissertations and other scientific papers.

REFERENCES – the same cited literature list transliterated in Roman alphabet (recommendations according to international bibliographic standard APA-2010, guidelines for drawing up a transliterated reference list "References" are on the site http//www.dse.org.ua, section for authors).

To speed up the publication of the article, please adhere to the following rules:

- in the upper left corner of the first page of the article – the UDC identifier;
- family name and initials of the author(s);
- academic degree, scientific title;

begin a new line, Times New Roman font, size 12 pt, line spacing 1.2, center alignment;

- name of organization, address (street, city, zip code, country), e-mail of the author(s);

begin a new line 1 cm below the name and initials of the author(s), Times New Roman font, size 11 pt, line spacing 1.2, center alignment;

- the title of the article is arranged 1 cm below the name of organization, in capital letters, semi-bold, font Times New Roman, size 12 pt, line spacing 1.2, center alignment. The title of the article shall be concrete and possibly concise;
- the abstract is arranged 1 cm below the title of the article, font Times New Roman, size 10 pt, in italics, line spacing 1.2, justified alignment in Ukrainian or Russian (for Ukrainian-speaking and Russian-speaking authors, respectively);
- key words are arranged below the abstract, font Times New Roman, size 10 pt, line spacing 1.2, justified alignment. The language of the key words corresponds to that of the abstract. Heading "Key words" - font Times New Roman, size 10 pt, semi-bold;
- the main text of the article is arranged 1 cm below the abstract, indent 1 cm, font Times New Roman, size 11 pt, line space spacing 1.2, justified alignment;
- formulae are typed in formula editor, fonts Symbol, Times New Roman. Font size is "normal" – 12 pt, "large index" – 7 pt, "small index" – 5 pt, "large symbol" – 18 pt, "small symbol" – 12 pt. The formula is arranged in the text, center aligned and shall not occupy more than 5/6 of the line width, formulae are numbered in parentheses on the right;
- dimensions of all quantities used in the article are represented in the International System of Units (SI) with the explication of the symbols employed;
- figures are arranged in the text. The figures and pictures shall be clear and contrast; the plot axes – parallel to sheet edges, thus eliminating possible displacement of angles in scaling; figures are submitted in color, black-and-white figures are not accepted by the editorial staff of the journal;
- tables are arranged in the text. The width of the table shall be 1 cm less than the line width. Above the table its ordinary number is indicated, right alignment. Continuous table numbering throughout the text. The title of the table is arranged below its number, center alignment;

• references should appear at the end of the article. References within the text should be enclosed in square brackets behind the text. References should be numbered in order of first appearance in the text. Examples of various reference types are given below.

Examples of LITERATURE CITED

Journal articles

Anatychuk L.I., Mykhailovsky V.Ya., Maksymuk M.V., Andrusiak I.S. Experimental research on thermoelectric automobile starting pre-heater operated with diesel fuel. *J.Thermoelectricity*. 2016. №4. P.84–94.

Books

Anatychuk L.I. *Thermoelements and thermoelectric devices. Handbook.* Kyiv, Naukova dumka, 1979. 768 p.

Patents

Patent of Ukraine № 85293. Anatychuk L.I., Luste O.J., Nitsovych O.V. Thermoelement.

Conference proceedings

Lysko V.V. *State of the art and expected progress in metrology of thermoelectric materials.* Proceedings of the XVII International Forum on Thermoelectricity (May 14-18, 2017, Belfast). Chernivtsi, 2017. 64 p.

Authors' abstracts

Kobylianskyi R.R. *Thermoelectric devices for treatment of skin diseases*: extended abstract of candidate's thesis. Chernivtsi, 2011. 20 p.

Examples of REFERENCES

Journal articles

Gorskiy P.V. (2015). Ob usloviakh vysokoi dobrotnosti i metodikakh poiska perspektivnykh sverhreshetochnykh termoelektricheskikh materialov [On the conditions of high figure of merit and methods of search for promising superlattice thermoelectric materials]. *Termoelektrichestvo - J.Thermoelectricity,* 3, 5 – 14 [in Russian].

Books

Anatychuk L.I. (2003). *Thermoelectricity. Vol.2. Thermoelectric power converters*. Kyiv, Chernivtsi: Institute of Thermoelectricity.

Patents

Patent of Ukraine № 85293. Anatychuk L. I., Luste O.Ya., Nitsovych O.V. Thermoelements [In Ukrainian].

Conference proceedings

Rifert V.G. Intensification of heat exchange at condensation and evaporation of liquid in 5 flowing-down films. In: *Proc. of the 9th International Conference Heat Transfer.* May 20-25, 1990, Israel.

Authors'abstracts

Mashukov A.O. *Efficiency hospital state of rehabilitation of patients with color carcer.* PhD (Med.) Odesa, 2011 [In Ukrainian].